İSTANBUL TECHNICAL UNIVERSITY ★ INSTITUTE OF SCIENCE AND TECHNOLOGY

VIBRATION ANALYSIS AND SHAPE CONTROL OF A BEAM WITH PIEZOELECTRIC PATCHES

M.Sc. Thesis by
Habibe Tuğba TAN

Department : **Aeronautics and Astronautics Engineering**

Programme : **Aeronautics and Astronautics Engineering**

JUNE 2011

İSTANBUL TECHNICAL UNIVERSITY ★ INSTITUTE OF SCIENCE AND TECHNOLOGY

VIBRATION ANALYSIS AND SHAPE CONTROL OF A BEAM WITH PIEZOELECTRIC PATCHES

M.Sc. Thesis by
Habibe Tuğba TAN
511071144

Date of submission : **06 May 2011**
Date of defence examination: **08 June 2011**

Supervisor (Chairman) : **Prof. Dr. Metin Orhan KAYA (ITU)**
Members of the Examining Committee : **Prof. Dr. İbrahim ÖZKOL (ITU)**
Assoc. Prof. Erol UZAL (IU)

JUNE 2011

İSTANBUL TEKNİK ÜNİVERSİTESİ ★ FEN BİLİMLERİ ENSTİTÜSÜ

PİEZOELEKTRİK YAMALI BİR KİRİŞİN TİTREŞİM ANALİZİ VE ŞEKİL KONTROLÜ

YÜKSEK LİSANS TEZİ
Habibe Tuğba TAN
511071144

Tezin Enstitüye Verildiği Tarih : 06 Mayıs 2011
Tezin Savunulduğu Tarih : 08 Haziran 2011

Tez Danışmanı : Prof. Dr. Metin Orhan KAYA (İTÜ)
Diğer Jüri Üyeleri : Prof. Dr. İbrahim ÖZKOL (İTÜ)
Doç. Dr. Erol UZAL (İÜ)

HAZİRAN 2011

FOREWORD

I would like to express my deepest appreciation and thanks to my supervisor Prof. Dr. Metin Orhan KAYA for his support and guidance all along my thesis.

I also want to extend my grateful thanks to ITU Institute of Science and Technology for giving me the opportunity to do research and for the support in the scholarship that has permitted me the development of my research work.

During the long period to complete this thesis, I would sincerely like to thank Gizem Özek, Didem Bölek, Işıl Şakraker, my brother and my parents, and all friends no matter in İstanbul or in Paris, their love and support propel and strengthen me forever.

Also, I want to thank Aslı Tatar, and my other colleagues from Onur Air Technic, whose ideas, helps and friendships support me to finish my study.

I would also like to express my heartfelt thanks to Institut Polytechnique des Sciences Avancées and Monsieur Léo Maïni for giving me gorgeous days in Paris.

May 2011

H. Tuğba Tan

Physics Engineer

TABLE OF CONTENTS

Page

ABBREVIATIONS

EBT	**:** Euler-Bernoulli Beam Theory
TBT	**:** Timoshenko Beam Theory
ADP	**:** Ammonium Dihydrogen Phosphate
DKT	**:** Dipotassium Tartrate
EDT	**:** Ethylene Diamine Tartrate
DRFB	**:** Direct Rate Feedback
PZT	**:** Lead Zirconate Titanate
PVDF	**:** Polyvinylidene Fluride
MIT	**:** Massachusetts Institute of Technology
IMSC	**:** Independent Modal Space Control
MIMSC	**:** Modified Independent Modal Space Control
FLC	**:** Fuzzy Logic Controller
LQG	**:** Linear Quadratic Gauss
ER	**:** Electrorheological
MR	**:** Magnetorheological
SMA	**:** Shape Memory Alloys
MST	**:** Micro Systems Technology
MEMS	**:** Micro Electro Mechanical Systems
SAW	**:** Surface Acoustic Wave
IEEE	**:** The Institute of Electrical and Electronics Engineers

LIST OF TABLES

Page

LIST OF FIGURES

Page

VIBRATION ANALYSIS AND SHAPE CONTROL OF A BEAM WITH PIEZOELECTRIC PATCHES

SUMMARY

Piezoelectric materials have been affirmative subjects to be investigated and very popular in engineering applications in the latest researches. Piezoelectric structures are commonly less rigid, so they are more sensitive to enormous vibration problems and that is why they are increasingly needed for aerospace applications, likewise they provide new important capabilities in military and civilian aerospace applications. In particular, there are plenteous studies, which are aimed to estimate to control the vibration characteristics of structures with piezoelectrics. In this thesis, first of all, shape analysis and control of a beam with piezoelectric patches are examined with considering both Euler Bernoulli Beam Theory (EBT) and Timoshenko Beam Theory (TBT). In the determination of structural models, all solutions are performed analytically to a beam subjected to different boundary conditions. Moreover, the effects of not only different voltage but also piezoelectric patch position on frequency and on shape functions of beam are interrogated. With a view to control the shape of beam in a good manner and obtaining better results, the errors are minimized. Furthermore, how the piezoelectric patches can impose the shape of a beam is shown by the obtained solutions. In addition to all, equations of motion and natural frequencies of beams with piezoelectric patches are achieved by means of Euler Bernoulli Beam Theory (EBT).

PİEZOELEKTRİK YAMALI BİR KİRİŞİN TİTREŞİM ANALİZİ VE ŞEKİL KONTROLÜ

ÖZET

Günümüzde kullanım alanları oldukça genişleyen piezoelektrik malzemeler, araştırma ve geliştirme için uygun konu olarak algılayıcı, kumanda elemanı ve akıllı yapıların kullanımında sıklıkla karşımıza çıkmaktadırlar. Piezoelektrik malzemeler elektriksel alana maruz kaldıklarında boyutlarında değişiklikler olmakta ve tersi durumda boyutsal şekil değişikliklere zorlandıklarında da elektrik sinyalleri üretmektedirler. Mekanik gerilmeye maruz kaldıklarında elektrik alan oluşturan piezoelektrik malzemeler, yüksek elastisite modülleri sayesinde ana yapının katılık ve kütle matrislerine ihmal edilebilir boyutta bir artış sağladığından ana yapıda çok sayıda kullanılıp titreşim ve şekil kontrolünün sağlanması işlevini görmektedirler. Yan sistemlerin desteğini almaksızın sağladıkları bu özellikleri ile piezoelektrik malzemeler havacılık ve uzay sanayinde aktif titreşim kontrolünde yaygın olarak tercih edilmektedirler. Bu çalışmada, piezoelektrik yamalı bir kirişin farklı sınır koşulları ve farklı yükler altında titreşim analizinin yapılması amaçlanmaktadır. Buna bağlı, piezoelektik yamalı bir kirişin Euler-Bernoulli Kiriş Teorisi ve Timoshenko Kiriş Teorisi göz önünde bulundurularak şekil fonksiyonu ve şekil kontrol analizleri yapılmıştır. Farklı sınır koşulları için kiriş davranışının inceleneceği teorik çalışmada, piezoelektrik yama yer değişimi etkisi ve farklı voltaj uygulamalarının sonuçları araştırılmıştır. Piezoelektrik yama içeren, farklı sınır koşullarına maruz kalmış bir kirişin hareket denklemleri çıkartılmış ve doğal frekans hesapları yapılmıştır. Teorinin literatür çalışmaları ile doğrulanmasının amaçlandığı bu çalışma ile ülkemizde piezoelektrik malzeme teknolojisinin geliştirilmesi; bu sayede bilim ve mühendislik alanlarında kullanımının daha da yaygın hale gelmesi sağlanacaktır.

1. INTRODUCTION

1.1 Background to the Study

From the beginning of the world, materials technology has had such a exhaustive effect on the evolution of human civilization that the name of time periods have been defined by the materials such as the Stone Age, the Bronze Age, etc. Moreover today, with the huge advancement of different material technologies which can be called as bio technology, biomimetics, nanotechnology, and information technology, can be declared as the Smart Materials Age. [1]

Smart Materials, which can be described as materials that can significantly change their shape, stiffness, viscosity and some other mechanical properties, or their thermal, optical, or electromagnetic properties, to give the predictable and controllable feedback to their environments. Materials that perform sensing and actuating functions, including piezoelectrics, electrostrictors, magnetostrictors, and shape-memory alloys.

The function of smart structures for future aircrafts and space systems is expected to implement new and creative methods in military and civilian aerospace applications. Piezoelectric materials which can be counted as one of the most important smart materials has been increasingly needed for aerospace applications because of being light and less rigid, more sensitive to enormous vibration problems. In particular, there are plenteous studies which is aimed to estimate to control the vibration characteristics of structures with piezoelectrics.

1.2 Contents and Scope of This Study

The goal of this research is to do vibration analysis and shape control of a beam with piezoelectric patches, which are exposed to different boundary conditions.

Chapter 2 gives a detailed literature survey contains two parts. The first part explains historical development of piezoelectricity briefly and the second part includes researches about structural modeling of piezoelectric materials, use of piezoelectric materials, and recent developments.

Chapter 3 investigates the trends in the application of the smart structures including with both different smart materials and piezoelectric actuators. The theory of piezoelectricity, classification of piezoelectric materials and the characteristics of piezoelectric materials such as physical, dielectric properties and thermal considerations are discussed. Moreover, classification, properties and the applications of modern composite materials are explained in this section.

In chapter 4, first of all, Euler Bernoulli Beam Theory (EBT) and Timoshenko Beam Theory (TBT) are explained in detail. And then, relationships between EBT and TBT with considering related examples. Furhermore, dynamic analysis of a beam with piezoelectric patches is presented. Firstly, equation of motion is obtained and then solved. Natural frequencies are calculated.

Chaper 5 performs that shape analysis and control of a beam with piezoelectric patches are examined with considering both Euler Bernoulli Beam Theory (EBT) and Timoshenko Beam Theory (TBT). In the determination of structural models, all solutions are performed analytically to a beam subjected to different boundary conditions. Additionaly, the numerical analysis of natural frequencies of a beam with piezoelectric patches and shape analysis of beams with piezoelectric patches with using both EBT and TBT are demonstrated.

2. LITERATURE SURVEY

2.1 Historical Development of Piezoelectricity

Historical details about piezoelectricity can be easily found in literature, meanwhile the word piezoelectricity derives its name from the Greek language piezo or piezin, which means to squeeze or press, and the literal translation of piezoelectricity is pressure electricity with this prefix piezo-. In science, it exactly shows the certain materials and substances which have the special characteristics of generating a charge or voltage when they are exposed to pressure. And oppositely, when an electrical field is applied to these materials, there occurs some specific changes on their shapes.

In the mid-18th century Carl Linnaeus and Franz Aepinus studied the pyroelectric effect which means if a temperature change occurs in a material, then in response, an electric potential is generated. Due to this knowledge, René Just Haüy and Antoine César Becquerel postulated a correlation between mechanical stress and electric charge; aside from the experiments which were found inconclusive by both scientists.

Furthermore, The brothers Pierre Curie and Jacques Curie presented the first demonstration of the direct piezoelectric effect was in 1880. Comparing and understanding the pyroelectricity and crystal structures, they got the ability for predicting crystal behavior, and demonstrated the effect using crystals of tourmaline, quartz, topaz, cane sugar, and Rochelle salt (sodium potassium tartrate tetrahydrate) in which the piezoelectricy is exhibit most in Quartz and Rochelle salt.

However, the converse piezoelectric effect was not predicted by The Curies, Gabriel Lippmann mathematically deduced from fundamental thermodynamic principles in 1881. And immediately the existence of the converse effect was confirmed by The Curie Brothers, and they obtained quantitative proof of the complete reversibility of electro-elasto-mechanical deformations in piezoelectric crystals.

From its discovery until early in the twentieth century, piezoelectricity was predominatelya scientific curiosity. [2]During World War I, sonar which was the first practical application for piezoelectric devices first developed. In France in 1916, Paul Langevin and his friends developed an ultrasonic submarine detector which is the first engineering use of piezoelectricity. While the device was quite cheap and simple, it was the prototype to the sonar devices in widespread use today.

The success of using piezoelectricity in sonar created great interest of development in piezoelectric devices. Over the next few decades, new piezoelectric materials and new applications for those materials were investigated and developed. The microphone and the crystal phonograph pickup were improved during the 1930's and in the mid-1930's, The crystal ADP (ammonium-dihydrogen-phosphate) was developed which has the strong piezoelectric characteristics of Rochelle salt. EDT (ethylene diamine tartrate) , DKT (dipotassium tartrate) ,BaTiO3(), and ADP are the significant materials among the many piezoelectric crystals to be discovered during the period of time from the 1930's through the 1950's. [2]

From the invention of piezoelectricity to nowadays, countless complex theories have been suggested about piezoelectricity which is very popular subject among scientists. First researches about piezoelectricity in literature are on finite and infinite various geometries such as thin beams, plates, disks and circular or cylindrical shells. Likewise, there are numerous studies on static or dynamic analysis of both whole piezoelectric materials and beams or plates which have piezoelectric layers or patches. With all these researches, a wide range of piezoelectric devices have been developed and applied multifarious usage areas.

2.2 Structural Modeling of Piezoelectric Materials

Since Pierre Curie first discovered the piezoelectric effect in 1880, nowadays the piezoelectricity finds wide application areas in the electrical, mechanical and aerospace engineering. Moreover, a number of piezoelectric devices which have been researched with huge involvement by scientists, have been generated and a great deal of complicated theories about piezoelectricity has been suggested.

First studies about piezoelectric effects have been about finite and infinite different geometrical structures such as thin beams, plates, disks and circular cylindrical shells. Also, there are plenty of researches about static or dynamic analysis of both whole piezoelectric materials and some structures which contain piezoelectric materials as bonding layers or adhesive patches.

In 1987, Crawley and Louis presented a study, which is the initiator of both analytic, and experimental searches about beams contain piezoelectric actuators. [3] They proposed a viable concept covers analytical solution for various actuator geometries on the purpose of vibration suppression. It is important cause of including investigation about not only isotropic but also composite beams and the derived static models are compared at each case.

There are numerous studies for the use of piezoelectric materials on beams in aerospace. Especially, to examine the vibration analysis of beams, which have piezoelectric actuators/sensors, appears in literature. Abramovich and Livshits studied the dynamic behavior of composite beams, which have uniform piezoelectric layers. They considered a First-order Timoshenko type analysis and presented numerical results for a variety of parameters of laminated beams with piezoelectric layers. [4]

In later years, Waisman and Abramovich suggest an active stiffening strategy. In the model, they studied the influence of the induced strains generated by piezoelectric patches on the dynamic behavior of a laminated composite beam, mode-shapes are numerically obtained and the results are compared with finite element analysis code. [5] And more, Abramovich et al developed different studies to realize the effects of piezoelectric usage which are about investigating the static behavior of piezoelectric actuated beams, explaining natural frequencies of beams contains piezoelectric patches, damping composite beams with piezoelectric layers and controlling the deflection of laminated composite beams with piezoceramics. [6] Also, Fridman and Abramovich researched the structural behavior of laminated composite beams consist of piezoelectric layers under axial compression using both analytically and numerically. [10]

Nir and Abramovich suggested a new design concept for smart wing. They used an airfoil skin made of passive composite materials combined with active layers of piezoceramic material in their design. The airfoil twists and its aerodynamic characteristics changes when an electric field is applied on the piezoelectric layers. These help to develop the optimization of design and to get high actuation twist angles and to be rigid enough to take on aerodynamics loads with minimum deflection. [11]

The active control of panel flutter including linearized potential flow aerodynamics is investigated by using direct rate feedback (DRFB) control scheme. This is implemented by using a piezoelectric transducer simultaneously as a sensor and actuator. [12]

In the work of Lim et al, examination of the vibration controllability of structures, which feature piezoelectric sensors and actuators with finite element analysis in the frequency domain, is displayed. [13]

Tzou and Ye examined not only pyroelectric but also thermal strain effects of pvdf and pzt devices using a new 3D thin piezothermoelastic solid finite element on a piezoelectric laminated square plate. Their analyses suggest that the pyroelectric effect of PVDF sensors is much more prominent than the thermal strain effect, on the other hand the PZT sensors exhibit the opposite phenomena. [14]

Brennan et al worked on strategies for the active control of flexural vibration on a beam. In their study, a model of the secondary source array is developed and coupled into the beam dynamics by using the wave approach to explain the behavior of the beam when three active control strategies are applied. [15]

In 1995, Hall and Prechtl designed a servoflap which has a piezoelectric bender to deflect a training edge flap use on a helicopter rotor blade which is an improvement of a study developed previously at MIT. [16] Furthermore, the paper about shape and placement of piezoelectric sensors for panel flutter limit-cycle suppression is presented in 1995. A method to design sensors (position and rate sensor) for panel flutter suppression is implied and the shape and location of sensors are depended on the control feedback gain. By using the shaped sensors designed with this recent approach, numerical simulation is illustrated for panel flutter suppression. [17]

Zhang and Kirpitchenko, in 2000, clarified a new model for understanding dynamics of passive structural control of a continuous structure with piezoelectric patches by means of suppression analysis of cantilevered beam subjected to an existing force. [18]

Lee and Elliott studied on active position control of a beam with piezoceramic actuators bonded on either side using control strategy that is based on internal model control architecture in 2000. [19] Another different study shows a new model for robust design of flexible structures by the use of piezoelectric actuators to do structural control with finite element analysis via using Hamilton's principle. [20]

A year after in 2001, Yaman et al presented a study about an active vibration control technique applied to a smart beam with surface bonded piezoelectric (PZT) patches. They implied the effects of element selection of the finite element modeling by using

ANSYS package program. An active vibration controller, which effectively suppresses the vibrations of the smart beam due to its first two flexural, is designed and H_∞ controllers' application achieved the vibration suppression. [21]

Sloss et al illustrated an integral equation approach for piezoelectric patch control in 2001. In their research, it is shown that there is an equivalence between the Eigen solutions of the differential equation formulation of the problem and the Eigen solutions of a certain integral equation. [22] Also, Li et al formulated a new optimal design methodology for the placement of piezoelectric actuator and the feedback gains in vibration suppression of flexible structure and the procedure that they developed leads to solutions that are independent of initial conditions of the flexible structure. [23]

Wang observed the ability of controlling vibration of beam structures with piezoelectric actuators and asserted that the optimal placement of piezoelectric actuators can be determined with his new method. [24]

In 2002, Park studied on the modeling of the resonant shunting damper that includes the additional damping mechanism generated by the shunt damping effect. The problem is solved using Hamilton's principle and the theoretical model is verified experimentally. As a result, it is achieved that resonant shunting damper obtains an effective means for vibration control. [25]

Singh et al introduced some new strategies for active control of vibrations and they compared their theory with the other methods of modal space control which are the independent modal space control (IMSC) and modified independent modal space control (MIMSC)in 2002. [26] At the same year, Wang and Quek presented the use of a pair of piezoelectric layers in increasing the flutter and buckling capacity of a column subjected to a follower force with considering a string at the end of the beam which has piezoelectric patches. [27]

One year after in 2003, Moon and Kim demonstrated a new optimal active/passive hybrid control design with piezoceramic actuators to achieve suppression of nonlinear panel flutter using finite element methods. [28] Numerical and experimental results of active compensation of thermal deformation of a composite beam using piezoelectric ceramic actuators is studied by Song et al, in 2003, and they considered a beam which has two film heaters are bonded to only one side, with the aim of introducing thermal distortion using thermally conductive materials.[29]

According to Tsai, structural vibration suppression via piezoelectric shunted network is less temperature dependent compared with mechanical passive damping and additionally he examined general modeling of a resonant shunting damper which has been made from piezoelectric materials. [30]

Another interesting paper is presented in 2003 by Dadfarnia et al. [31] They proposed a control strategy which is observed based and modeled as a flexible cantilever beam with translational base support for modeling the problem of a Cartesian robot arm.

In 2004, Lin and Nien investigated the modeling and vibration control of a smart beam using piezoelectric damping-modal actuators/sensors. [32] And Suleiman and Costa searched the active aero elastic control using piezoelectric actuators to full aircraft configurations and the application of piezoelectric shunts. [33]

Han et all involved active flutter suppression of a sweptback cantilevered lifting surface using piezoelectric actuation by finite element method, panel aerodynamic method, and the minimum state–space realization in 2005. [34]

Shih et al, in 2005, presented the general opto-piezothermoelastic equations for simulating multifield-coupled behavior of photostrictive optical actuators. By the help of these models, the capability to estimate the response of the structural member to a command illumination applied to the patched photostrictive actuator is obtained. [35]

Besides in 2005, Kapuira and Alam developed the coupled efficient layer wise (zigzag) theory and they analyzed the dynamic analysis of hybrid piezoelectric beams of an one-dimensional beam finite element with electric degrees of freedom. [36] And also, Moon and Hwang presented a study to improve a model to suppress the flutter of a supersonic composite panel using piezoelectric actuators [37]

In 2006, Lin and Liu illustrated a study to minimize structural vibration using collocated piezoelectric actuator/sensor pairs with the help of a novel resonant fuzzy logic controller (FLC) and enhance the performance of a flexible structure with resonant response.[38]

As well in 2006, Nyugen and Pietrzko explained a simulation of adaptive structures with shunt circuits using Finite Element Analysis with an experiment which consists in an aluminum cantilever beam actuated by a PZT patch. [39] More, Moon contemplated an active control law which depended on finite element modal analysis and have direct output feedback, with the aim of analyzing the for flutter suppression of the composite plates with piezoelectric layers exposed to not only aerodynamic but also thermal loads by aerodynamic heating. [40]

Raja et al illustrated a paper about flutter control of a smart plate with multilayered piezoelectric actuators based on the theory of Linear Qaudratic Gaussian output controller in 2006.[41]

Maurini et al, in 2006, investigated different numerical methods for modal analysis of a stepped piezoelectric beams modeled by Euler-Bernoulli Beam Theory and the numerical results are validated with experimental data. [42]

In 2007, Bhadbhade et al. [43] investigated a new type of vibrating mass gyroscope consists of a vibrating mass, which is driven in a primary direction, and attached to a rotating base. In their new model, there are piezoelectric actuators placed on the surface of the beam that induce the flexural vibration.

Kıral et al presented a study on active control the residual vibrations of a clamped-free beam subjected to a moving load. They considered both experimental and numerical methods by using finite element analysis package ANSYS in 2007. [44]

With the aim of modeling the axial and transverse response caused by the piezoelectric actuator and the characteristics of the voltage-generated piezoelectric forces, a different approach to exciting a one-dimensional structure with discontinuities using a piezoelectric actuator is examined. [45]

Qui and et al studied the design of an acceleration sensor based active vibration control for a cantilever beam with bonded piezoelectric patches. Suppression of the vibrations of a flexible beam by using a non-collocated acceleration sensor and discrete PZT patch sensor/actuator is aimed in this workout. Moreover, they presented acceleration sensor based control methods and compared with both experimental results and commercial finite element code ANSYS. [46]

Mahieddine and Ouali developed a model of finite elements for beams with piezoelectric sensors and actuators found on first order Kirchoff theory with considering lateral strains in 2008. [47]

Another effective method for suppressing the vibration of flexible structures with the sensors/actuators is based on the Linear Quadratic Gauss (LQG) optimal control method in 2010. [48]

In addition to all above, researching into shape control of beams with piezoelectric materials is the needed answer for a lot of analytical problems and important for the design and analysis of such a piezoelectric smart structure. In 1996, Donthireddy and

Chandrashekhara developed a layerwise theory for laminated composite beams with piezoelectric actuators and demonstrated the influence of various parametric studies such as boundary conditions, ply orientation, etc., on the change in shapes of beams with piezoelectric materials. [49] Moreover, Wang et al, in 1999, figured out the shape control of laminated beams with piezoelectric actuators with a formulation adopted the first order shear deformation beam theory of Timoshenko (1921). [50]

Subsequently, Yang and Ngoi presented analytical solutions of the deflection of a beam induced by not only piezoelectric actuators but also external forces, and they gave the detailed local shape information activated by piezoelectric materials for different boundary conditions. [51]

3. PIEZOELECTRIC MATERIALS

3.1 Smart Structures with Different Smart Materials

Recent years, as a result of increasing space activities, the use of lightweight and flexible structures is becoming more efficient to lessen the high cost of lifting the mass into orbit. , the vibrations once submitted to grow to large amplitudes owing to the flexibility in the system. Adding external passive damping to the system is not productive and desirable because of having more weight. This makes studies orientate to search the active and passive control.

Shen [52] gives the definition of “adaptive structures” or “smart structures” as the types of structures that are lighter, stronger, more durable and can be applied to a number of flight vehicles ranging from helicopters to interplanetary spacecraft, plus which are able to sense, to respond, and to control their own characteristics and states, so as to achieve much higher levels of operational performance to meet mission requirements.

Smart Materials can be defined as the materials that have one or more properties that can be significantly altered in a controlled fashion by external stimuli; such has electrical fields, magnetic fields, stress, moisture etc. Smart Materials convert one form of energy to another, so it can be said that they are a kind of transducers. Piezoelectric materials, Shape Memory Alloys, Electrostrictive Materials, Magnetostrictive Materials, Electrorheological (ER) Fluids, Magnetorheological (MR) Fluids, and Fiber Optic Sensors are the main smart material types.

• **Shape memory alloys (SMA):** These materials are a special class of metallic alloys that exhibit a shape transformation when temperature changes. If a shape memory alloy is inclined in its low temperature condition and the stresses are removed, it reaches again its original shape by phase transformation to its high temperature condition when exposed to heat. In addition, the process is repeatable with great accuracy.

In addition, some materials such as copper, nickel, titanium and zinc alloys along with others can exhibit the shape recovery effect. Shape memory alloys are used almost merely used as an actuator material, the most popular SMA material is Nickel Titanium Alloy, or Nitinol, which is useable in the form of wires and films. [53]

SMAs can be plastically deformed at relatively low temperature and their ability can provide a low mass and power structure.

• **Electrostrictive materials:** These materials behave like piezoelectric materials

but they differ from piezoelectrics in their response to the electric field and they are not poled. Although they have better strain capability and exhibit quicker response time than piezoelectric materials, the Electrostrictive materials shows more sensitivity to temperature variaton. Electrostrictive materials strain proportionally to the square of the applied voltage of the applied electric field. One of the most common materials is Lead-Magnesium-Niobate or PMN. [53]

• **Magnetostrictive materials :** Magnetostriction can be defined as the material property that causes a material to change its dimensions when it is exposed to an electro-magnetic field. Nominately, Magnetostrictive materials produce mechanical stress when subjected to magnetic field or vice versa.

Due to characteristics of magneto strictive materials they can be executed as actuators by applying a magnetic field, or sensors by measuring the magnetic field that they produce that is why they can be used as both actuators and sensors. The main advantage of these materials is the high force capability while its brittleness, heavy weight and high hysteresis in their response to the applied magnetic field are the some disadvantages of them.

One of the most popular Magnetostrictive materials is Terfenol-D, which produces relatively low strains, moderate forces over a wide frequency range, and has giant magnetostriction at room temperatures. [54]

• **Electrorheological (ER) fluids :**These fluids are a special fluids that has phase change characteristic transforming to solid when they exposed to an electric field. They give response to electricity in their viscosity, elasticity, and plasticity behavior. Besides, they have has a very fast response characteristic to the electric field and hence wide control bandwidth. They appear in research activities in the development of various engineering applications including shock absorbers, engine mount and smart structures. [55]

Electrorheological fluids behave like Newtonian fluids under no electric field conditions, but with the implementation of an electric field, these fluids behave similarly to Bingham plastics which behave as a rigid body at low stress but flow as viscous fluid at high stress.

• **Magnetorheological (MR) fluids :** These fluids are similar to Electrorheological fluids, when they subjected to a magnetic field, their apparent viscosity greatly increases to become a viscoeleastic solid. Magnetorheological Fluids have extremely higher densities and lower voltage requirements than Electrorheological fluids. [55]

• **Fiber optic sensors:** Fiber Optics are special type of sensors that transmit a light signal through the fiber and measure the return signal with the change of the signal properties determining the effects at the site of the sensor. Based on the light intensity, phase, frequency or the polarization, there are four types optical fiber sensors that are referred as intensiometric, interferometric, polarimetric and modalmetric sensors. [54]

3.2 Piezoelectricity

3.2.1 Theory of piezoelectricity

The piezoelectric effect can be defined as the linear electromechanical interaction between the mechanical and the electrical state in crystalline materials. To understand well, A piezoelectric ceramic can be considered which is a mass of perovskite crystals. In the piezoelectric ceramic each crystal is composed of a small, tetravalent metal ion placed inside a lattice of larger divalent metal ions and O2, as shown in Figure 1. At section (a), The unit cell has cubic geometry above the Curie temperature is shown and at section (b), the unit cell structure is tetragonal with Ba^{2+} and Ti^{4+} ions displaced relative to the O^{2-} below the Curie temperature is demonstareted. [56]

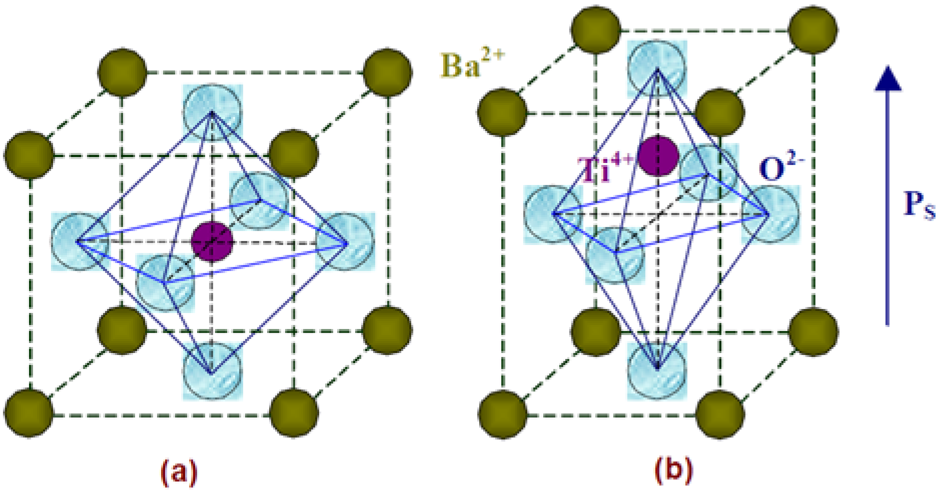

Figure 3.1: The crystal structure of perovskite barium titanate before and after polarization [56]

Fine powders of the component metal oxides are mixed in specific proportions and then this mixture is heated to form a uniform powder to prepare a piezoelectric ceramic. An organic binder is mixed with the powder and is formed into certain shapes such as discs, rods, plates. After, these elements are exposed to heat for a specific time, this process gives that the powder particles sinter and the material forms a dense crystalline structure. The elements are then cooled and, if needed, trimmed into specific shapes. Finally, electrodes are applied to the appropriate surfaces of the structure. [57]

Curie temperature which can be defined as the temperature at which spontaneous polarization is lost on heating is the critical point for piezoelectric crystals. Above this critical temperature each perovskite crystal in the heated ceramic element exhibits a simple cubic symmetry with no dipole moment, as demonstrated in Figure 3.2 on left. As it seen in the 3.2 on right, each crystal has tetragonal symmetry and eventually a dipole moment at temperatures below the Curie temperature which means that this compliance gives a net dipole moment and a net polarization.

As represented in Figure 3.2 (a) there is a random directional of polarization among neighboring domains and the ceramic element has no overall polarization.

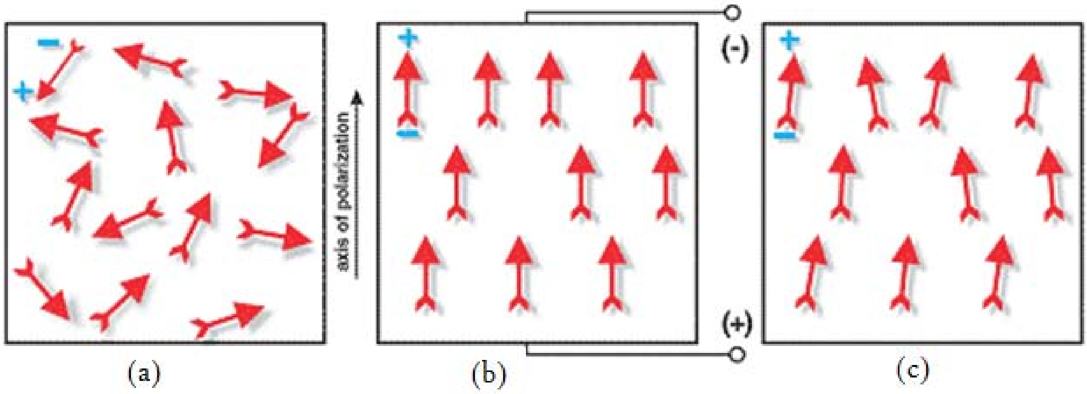

Figure 3.2: The polarization process of piezoelectric structure [56]

When a strong, DC electric field is exposed to the element, the domains in a ceramic element are aligned as shown at Figure 3.2 (b) at a temperature slightly below the Curie temperature. This is called the poling process and after the poling treatment, domains most nearly aligned with the electric field expand at the expense of domains that are not aligned with the field, and the element expands in the direction of the field.

Finally, Figure 3.2 (c) demonstrates the behavior of poles after the electric field is removed. Most of the dipoles are locked into a configuration of near alignment. Now, it seems that a permanent polarization occurs and the increase in the length of the element, however, is very small, usually within the micrometer range.

If piezoelectric material is subjected to a force, surface charge is induced by the dielectric displacement, hence an electric field is occurred. As it appears in Figure 3.3, on applied electrodes this field can be distributed as electrical voltage or like Figure 3.4, if the electrodes are shorted, the surface charge balance out by a current. This effect explains exactly the direct piezoelectric effect.

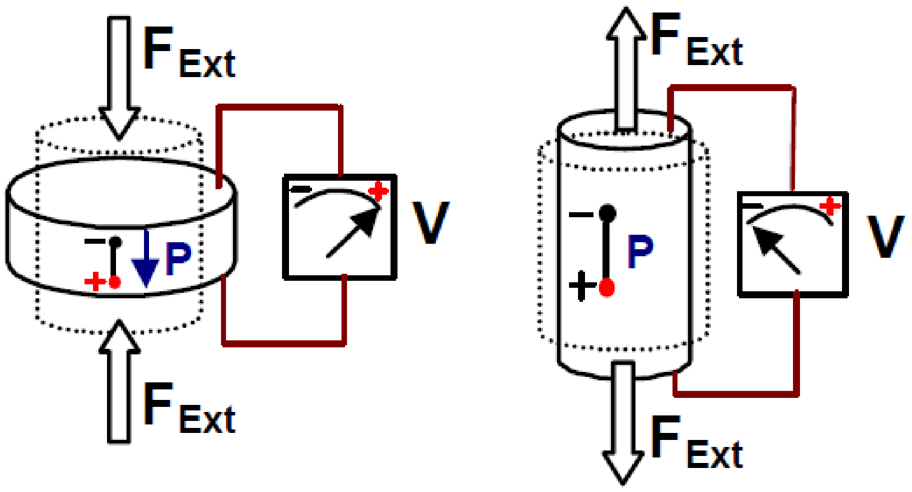

Figure 3.3: The direct effect with the piezoelectric material in open circuit. [56]

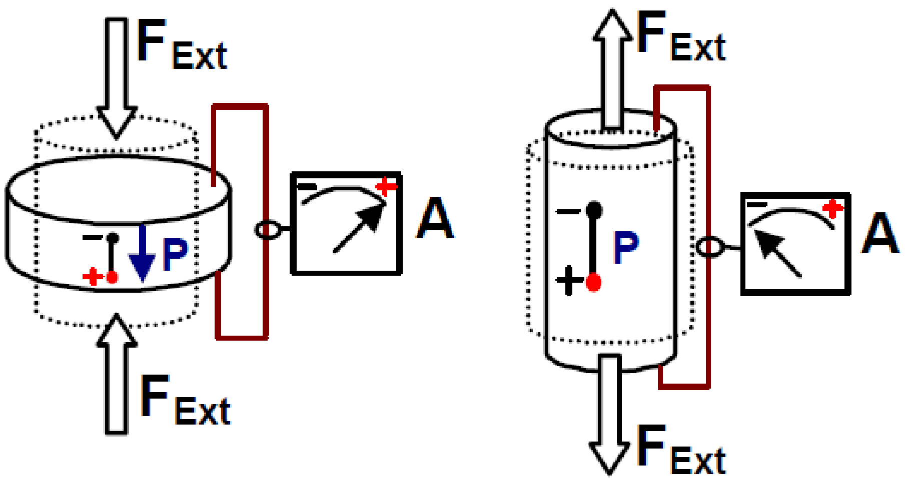

Figure 3.4: The direct effect with the piezoelectric material shorted. [56]

The mechanical behavior of a piezoelectric ceramic element and the properties of being poled are shown in Figure 3.5. Giving mechanical tension or compression to the piezoelectric element makes change into the dipole moment, creates voltage. If the material is subjected to compression along the polarization direction, or tension perpendicular to the polarization direction, it creates voltage of the same polarity as the poling voltage as seen in the Figure 3.5 (b).

On the other hand, as it clearly seems in the Figure 3.5 (c) that having tension along the direction of polarization, or compression perpendicular to that direction,

generates a voltage with polarity opposite to that of the poling voltage. This phenomenon explains how the device is being used as a sensor, , the ceramic element transforms the mechanical energy of compression or tension into electrical energy.
If the ceramic element is being applied a voltage of the same polarity as the poling voltage, as demonstrated in the Figure 3.5 (d), it will lengthen and so its diameter will become smaller Besides, if a voltage of polarity opposite to that of the poling voltage is applied, the element will become shorter and broader Figure 3.5 (e).

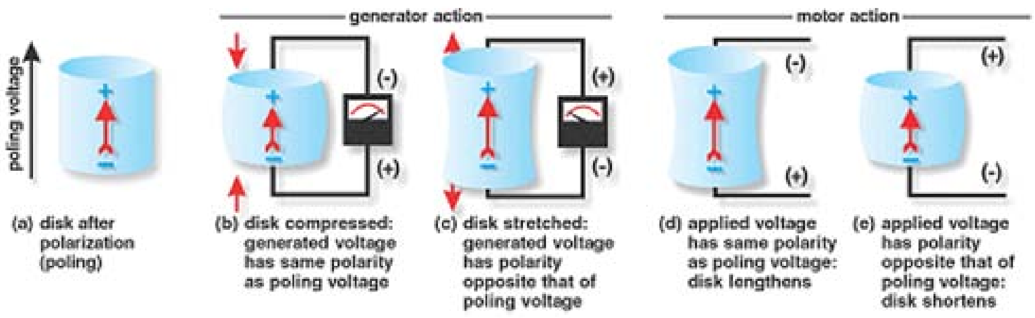

Figure 3.5: The reaction of a poled piezoelectric element. [56]

3.2.2 Classification of piezoelectric materials

Nowadays with the help of high technology, a variety of piezoelectric materials are being synthesized and optimized. As a consequence piezoelectric-based devices are undergoing a revolutionary development, specially for medicine and aerospace applications. There are several types of applications in piezoelectric materials usage areas which can be asserted as piezoelectric ceramics, piezoelectric single crystals, piezoelectric thin films, piezoelectric polymers , piezoelectric composites and piezoelectric coatings.
Variations of lead zirconate titanate and Barium titanate are the most commonly used piezoceramic materials in structural control and sensing and acoustics applications. The properties of these materials vary significantly due to small alterations in the constituent materials. A huge number of piezoceramic materials have been produced by small variations and additions to the constituent material over the past 50 years . They can be behaved like not only piezoelectric sensors, but also piezoelectric actuators.

Direct piezoelectric effect which can be simply described as w a piezoelectric transducer is mechanically stressed, it generates a voltage makes piezoelectric transducers suitable for sensing applications. Piezoelectric sensors which are compact, easy to embed and require moderate signal conditioning circuitry also suitable for applications that involve measuring low strain levels. They can be described as devices that use the piezoelectric effect to measure pressure, acceleration, strain or force by converting them to an electrical signal.

Meanwhile, piezoelectric actuators convert electrical energy into a mechanical displacement or stress using a piezoelectric effect. Various types of piezoelectric actuators utilizing the piezoelectric effect of piezoelectric elements have been developed in recent years by the mean of good responsiveness and conversion efficiency of piezoelectric elements. They have the advantage of a high actuating precision and a fast reaction.

3.2.2.1 Piezoelectic ceramics

It can be said that from the lead zirconate titanate (PZT) family comprises the usage of most of the piezoelectric materials, because of their excellent piezoelectric parameters, thermal stability, and dielectric properties. Additionally the properties of this family can be modified by changing the zirconium to titanium ratio or by addition of both metallic and non-metallic elements. Furthermore, piezoelectric ceramics can be divided two types depending on the by different formulations; which are soft and hard piezoceramics. Soft ceramics are characterized by large electromechanical coupling factors, large piezoelectric constants, high permittivity, large dielectric constants, high dielectric losses, low mechanical quality factors, and poor linearity. Moreover, soft ceramics produce larger displacements and wider signal band widths, relative to hard ceramics, but they exhibit greater hysteresis, and are more susceptible to depolarization or other deterioration. Lower Curie points which is generally below 300°C, dictate that soft ceramics be used at lower temperatures, large values for permittivity and dielectric dissipation factor restrict or eliminate soft ceramics from applications requiring combinations of high frequency inputs and high electric fields. Consequently, soft ceramics are used primarily in sensing applications, rather than in power applications.

Hard ceramics which have characteristics generally opposite soft ceramics, including Curie points above 300°C, small piezoelectric charge constants, large electromechanical coupling factors, and large mechanical quality factors are difficult to polarize or depolarize. Hard piezoceramics cannot produce the same large displacements in spite of generally being more stable than soft piezoceramics. Hard ceramics are capable of withstanding high mechanical stress and high electrical excitation levels. These materials are well suited for application of high voltage, or as high power generators and transducers. These materials generally have low loss factors and high mechanical quality.

Table 3.1: The properties of soft ceramics and hard ceramics.

Characteristic	Soft Ceramic	Hard Ceramic
Piezoelectric Constants	Larger	Smaller
Permittivity	Higher	Lower
Dielectric Constants	Larger	Smaller
Dielectric Losses	Higher	Lower
Electromechanical Coupling Factors	Larger	Smaller
Electrical Resistance	Very High	Lower
Mechanical Quality Factors	Low	High
Coercive Fields	Low	Higher
Linearity	Poor	Better
Polarization/Depolarization	Easier	More difficult

In addition to all above, ternary ceramic materials, lead metaniobate, as well as, barium and modified lead titanates are popular piezoceramic materials.

Some characteristics of piezoceramic materials can be seen in Table 3.2**,** where Qm is the mechanical quality factor, Tc is the Curie point, d_{31} is the the transverse charge coefficient, and k_p, k_t and k_{31} are the electromechanical coupling factors for planar, thickness, and transversal mode respectively.

Table 3.2: The selective parameters for piezoceramic materials. [67]

Material Property	PZT modified	Lead metaniobate	PSZNT 31/40/29	PZT, x=0.5	PSN-PLT
Q_m	350	40	222	74	41
T_c (^oC)	290	462		369	152
d_{31} ($\times 10^{-12}$ C/N)					-79
k_p	0.5		60		30.7
k_t		0.32		0.438	-
k_{31}		0.21		0.263	17.9

Additionally, the latest development in piezoceramic fibers is the modification of the viscous-suspension-spinning process (VSSP) for the production of continuos piezoelectric ceramic fibers for smart materials and active control devices, such as transducers, sensor/actuators and structural-control devices.

Synthesis of reactive PZT precursor powder by the oxalate coprecipitation technique has also been developed. The precursor transforms to phase pure PZT at or above 850 °C the PZT obtained by this technique showed a Curie temperature of 355 °C. The advantages of the coprecipitation technique are the lack of moisture sensitive and special handling precursors.

Although new materials have been investigated with the purpose of create replacements for ceramics, there has been a great improvement in their properties and, current research is focused in the development of new techniques for both synthesis and processing.

3.2.2.2 Piezoelectric single crystals

Berlinite, Cane sugar, Quartz, Rochelle salt, Topaz and Tourmaline-group minerals are Naturally-occurring crystals which helped the discover the piezoelectric effect and they also have been proves of piezoelectricity in early years.

Meanwhile, there are other numerous natural materials such as dry bone, exhibit some piezoelectric properties Tendon, Silk, Wood due to piezoelectric texture, Enamel, Dentin and some man-made crystals, quartz analogic crystals such as Gallium orthophosphate ($GaPO_4$) and Langasite ($La_3Ga_5SiO_{14}$). Also the fast development of the electronic technology necessitate new piezoelectric crystals with a high thermal stability and large electromechanical coupling factors.

While the piezoceramics dominate the single crystal materials in usage, single crystals piezoelectrics continue to make important contributions both in price-conscious consumer market and in performance - driven defense applications. Areas such as frequency stabilized oscillators, surface acoustic wave devices and filters with a wide pass band, are still dominated by single crystals.

3.2.2.3 Piezoelectric thin films

In recent days, deposition of piezoelectric thin films have had huge interest, within Micro Systems Technology (MST) or MEMS (Microelectromechanical systems) devices applications; while the aim is to investigate sensors and actuators based on PZT films with Si semiconductor-based signal processing; and for surface acoustic wave (SAW) devices. The main goal is to achieve higher electromechanical coupling coeffcient and temperature stability. The development of suitable measurement facilities to characterise the materials functional properties is complicated by the fact that the film is often attached to a substrate which acts to clamp the film thus affecting the system performance.

3.2.2.4 Piezoelectric polymers

In 1969, Kawai et al observed the strong piezoelectricity of polyvinylidene fluoride (PVDF) and this invention of piezoelectricity in polymeric materials was considered as an indication of a renaissance in piezoelectricity. PVDF is a highly non-reactive and pure thermoplastic fluoropolymer and it is stated that the piezoelectric coefficient of poled thin films of the material 10 times larger than that observed in any other polymer. [59]

PVDF exhibits piezoelectricity several times compared to quartz. When an electric field is applied, it behaves unlike ceramics, where the crystal structure of the material creates the piezoelectric effect, in polymers the intertwined long-chain molecules attract and repel each other.

It is stated that the degree of crystallinity and the morphology of the crystalline material have profound effects on the mechanical behavior of polymers. Additionally, in order to induce a piezoelectric response in amorphous systems the polymer is poled by application of a strong electric field at elevated temperature suffcient to allow mobility of the molecular dipoles in the polymer. Recent approaches have been focused in the development of cyano-containing polymers, due to the fact that cyano polymers could have many dipoles which can be aligned in the same direction. [58]

3.2.1.5 Piezoelectric composites

Piezocomposites have been accomplished by the combination of piezoelectric ceramics and polymers, the concluding material posses both the high piezoelectric properties of ceramics and the processability of polymers. Different type of piezocomposites have found wide applications as medical and industrial ultrasonic transducers. Polishing and poling are the following steps in order to achieve the final thickness and properties.

Additionaly, piezoelectric composites specify the advantage of wider bandwidth and reduction or elimination of unwanted modes of vibration in low frequency transducers. These dispositions are particularly advantageous in applications where low aspect ratios are a necessity due to the contrast requirements of beam angle and operating frequency. The piezoelectric composites were determined for underwater hydrophone applications in the low-frequency range, where the dimensions of the sample are much smaller than the acoustic wavelength.

It has been highlighted that certain composite hydrophone materials are two to three orders of magnitude more sensitive than single phase PZT ceramics, while assuring other requirements. [60]

The usage of composite materials has been enlarged to other applications, such as ultrasonic transducers for acoustic imaging, thermistors with both negative and positive temperature coefficients of resistance, and active sound absorbers.

3.2.1.6 Piezoelectric coatings

It is demonstrated that lots of potential applications correspond which require film thickness of 1 to 30 μm. Also there are some certain examples of these macroscopic devices involving ultrasonic high frequency transducers, fiber optic modulators and for self controlled vibrational damping systems. ZnO and PZT have been benefited for piezoelectric fiber optic phase modulators fabrication. Plus, sol-gel technique for thick PZT films and Piezoelectric polymer coatings for high-frequency fiber-optic modulators have been also developed. [58]

3.3 Characteristics of Piezoelectric Materials

3.3.1 Linear theory of piezoelectricity

The behavior of piezoelectric materials in the linear range can be justified by the linear theory of piezoelectricity which is illuminated in this section. the linear theory of piezoelectricity is very accurate in the case of non-ferroelectric materials, like quartz. However, in the case of ferroelectric materials, it is necessary to take into account the limitations of the application which is discussed later. The application of linear theory of piezoelectricity is limited for the resonance of the materials, their depolarization and for other non-linear effects such as hysteresis as a general rule.

3.3.1.1 Conventional assignment

IEEE Standard on Piezoelectricity which contains many equations based upon the analysis of vibrations in piezoelectric materials having simple geometrical shapes and all the material constants listed in the data sheets are standard values determined on defined bodies corresponding to the IEEE Standard on Piezoelectricity 1978, [61]. In accordance with this convention, orthogonal X,Y and Z (also 1,2,3) axes are customarily used as a basis for identifying the elasto-piezo-dielectric coefficients of a material. The Z direction is determined as the polarization direction. The numbers 4, 5 and 6 describe the mechanical shear stress which acts tangentially to the areas defining the co-ordinate system. As represented in the Figure 3.6, they can be understood as rotations around each axis.

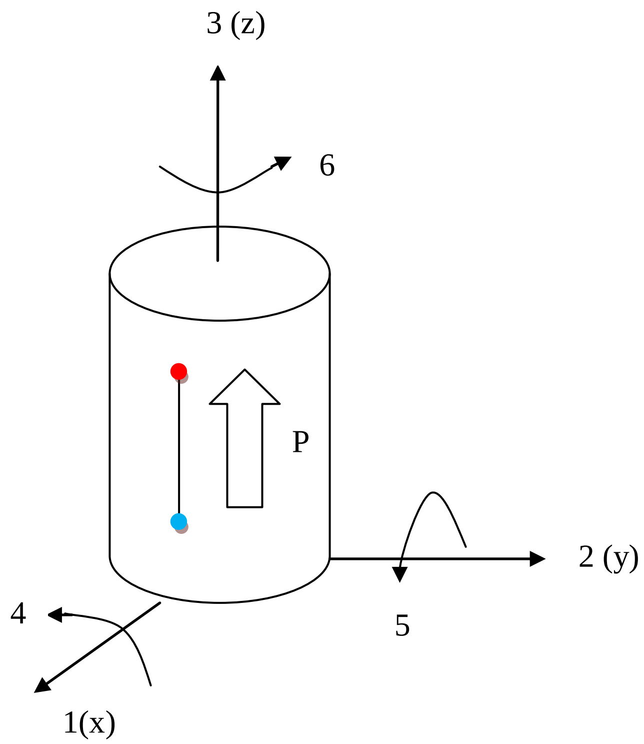

Figure 3.6: The conventions for axes

3.3.1.2 Basic equations

In general, the Direct Piezoelectric Effect (so-called Sensor effect) in a single crystal can be described by a matrix which explains the polarization developed by the crystal when an external stress (normal, T_1 to T_3 , and shear, T_4 to T_6) is applied onto the piezoelectric material.

A particular case of the direct piezoelectric effect is when the measure of the polarization is made at external electric field E=0 (shorted). In this case, the polarization developed is equal to the free charge q appeared in the electrodes, as given by equation (3.1)

$$P_i = q_i = d_{ij} \times T_j \qquad \textbf{(3.1)}$$

In equation (3.1), qi represents the linear free charge developed at the normal surface to the i direction. Equation (3.1) can also be expressed as:

$$\begin{Bmatrix} q_1 \\ q_2 \\ q_3 \end{Bmatrix} = \begin{bmatrix} d_{11} & d_{12} & d_{13} & d_{14} & d_{15} & d_{16} \\ d_{21} & d_{22} & d_{23} & d_{24} & d_{25} & d_{26} \\ d_{31} & d_{32} & d_{33} & d_{34} & d_{35} & d_{36} \end{bmatrix} \cdot \begin{Bmatrix} T_1 \\ T_2 \\ T_3 \\ T_4 \\ T_5 \\ T_6 \end{Bmatrix} \qquad \textbf{(3.2)}$$

In equations (3.1) and (3.2), the polarization vector is equal to the free charge in the electrodes due to the hypothesis of external electric field zero or piezoelectric shorted.

Previous equation (3.1) is completely true in single crystals and, in such a case, it represents the polarization generated in the material when a mechanical stress is applied. The piezoelectric coefficients, d_{ij}, will indicate the intensity of polarization in each direction.

When a ferroelectric material is used, a change in the spontaneous polarization (PS)i replaces P_i. If the consideration of linear range is taking into account, the equivalent expression for ferroelectric materials is given by

$$(PTOTAL)_I = (PS)_i + d_{ij} \times T_j \qquad \textbf{(3.3)}$$

In practice PS is considered only in the poling direction because in the transversal directions is negligible. Thus $(PS)_i = P_3$.

The Converse Piezoelectric Effect (so-called Actuator effect) described the strain generated in a piezoelectric material when it is subjected to an external electric field E_i. In particular if the material is not clamped (free-displacement condition, T_{ij}=0), the converse effect can be expressed as:

$$S_i = d_{ij}^{\theta T} . E_j \qquad \textbf{(3.4)}$$

Or more explicitly:

$$\begin{Bmatrix} S_1 \\ S_2 \\ S_3 \\ S_4 \\ S_5 \\ S_6 \end{Bmatrix} = \begin{bmatrix} d_{11}^{\theta T} & d_{12}^{\theta T} & d_{13}^{\theta T} \\ d_{21}^{\theta T} & d_{22}^{\theta T} & d_{23}^{\theta T} \\ d_{31}^{\theta T} & d_{32}^{\theta T} & d_{33}^{\theta T} \\ d_{41}^{\theta T} & d_{42}^{\theta T} & d_{43}^{\theta T} \\ d_{51}^{\theta T} & d_{52}^{\theta T} & d_{53}^{\theta T} \\ d_{61}^{\theta T} & d_{62}^{\theta T} & d_{63}^{\theta T} \end{bmatrix} . \begin{Bmatrix} E_1 \\ E_2 \\ E_3 \end{Bmatrix} \qquad \textbf{(3.5)}$$

In the previous equations (3.4) and (3.5), the coefficient ,T d_{ij} q is called, the charge piezoelectric coefficient. This coefficient indicates the intensity of the deformation in the i-direction, S_i, when a electric field is applied in the direction j, E_j. Its dimension is: [m/V] The superscript indexes are used to indicate the quantities that are kept constant or zero. The piezoelectric coefficient d_{ij} are identical to those for the direct effect.

3.3.1.3 Constitutive equations

In general, a linear dielectric can withstand at the same time external conditions of temperature, mechanical stress and electric field. In this case, it is possible to analyse the mechanical and the electrical behavior of the material and later coupling both results. In addition, piezoelectric effect highly depends on directions as discussed above sections.

Mechanical behavior of a piezoelectric material

Piezoelectric materails have specailty about developing an electric charge when they ar exposed to mechanical stress and in constrat they producemechanical extension when they are subjected to electric charge. An applied electric field generates in these materials a linearly proportional strain.

With the aim of understanding the mechanical behavior of a piezoelectric material, it can be started with their equations of motion in matrix form. The strain S describes the mechanical linear behavior (Hooke law approximation) of a piezoelectric material subjected to an electric field E, a stress T and a thermal variation D.

This is shown in the next matrix as:

$$\begin{Bmatrix} S_1 \\ S_2 \\ S_3 \\ S_4 \\ S_5 \\ S_6 \end{Bmatrix} = \begin{bmatrix} d_{11}^{\theta T} & d_{12}^{\theta T} & d_{13}^{\theta T} \\ d_{21}^{\theta T} & d_{22}^{\theta T} & d_{23}^{\theta T} \\ d_{31}^{\theta T} & d_{32}^{\theta T} & d_{33}^{\theta T} \\ d_{41}^{\theta T} & d_{42}^{\theta T} & d_{43}^{\theta T} \\ d_{51}^{\theta T} & d_{52}^{\theta T} & d_{53}^{\theta T} \\ d_{61}^{\theta T} & d_{62}^{\theta T} & d_{63}^{\theta T} \end{bmatrix} . \begin{Bmatrix} E_1 \\ E_2 \\ E_3 \end{Bmatrix} + \begin{bmatrix} s_{11}^{E,\theta} & s_{12}^{E,\theta} & s_{13}^{E,\theta} & s_{14}^{E,\theta} & s_{15}^{E,\theta} & s_{16}^{E,\theta} \\ s_{21}^{E,\theta} & s_{22}^{E,\theta} & s_{23}^{E,\theta} & s_{24}^{E,\theta} & s_{25}^{E,\theta} & s_{26}^{E,\theta} \\ s_{31}^{E,\theta} & s_{32}^{E,\theta} & s_{33}^{E,\theta} & s_{34}^{E,\theta} & s_{35}^{E,\theta} & s_{36}^{E,\theta} \\ s_{41}^{E,\theta} & s_{42}^{E,\theta} & s_{43}^{E,\theta} & s_{44}^{E,\theta} & s_{45}^{E,\theta} & s_{46}^{E,\theta} \\ s_{51}^{E,\theta} & s_{52}^{E,\theta} & s_{53}^{E,\theta} & s_{54}^{E,\theta} & s_{55}^{E,\theta} & s_{56}^{E,\theta} \\ s_{61}^{E,\theta} & s_{62}^{E,\theta} & s_{63}^{E,\theta} & s_{64}^{E,\theta} & s_{65}^{E,\theta} & s_{66}^{E,\theta} \end{bmatrix} . \begin{Bmatrix} T_1 \\ T_2 \\ T_3 \\ T_4 \\ T_5 \\ T_6 \end{Bmatrix} + \begin{Bmatrix} \alpha_1^{E,T} \\ \alpha_2^{E,T} \\ \alpha_3^{E,T} \\ \alpha_4^{E,T} \\ \alpha_5^{E,T} \\ \alpha_6^{E,T} \end{Bmatrix} . \Delta\theta \qquad \textbf{(3.6)}$$

The coefficient is the thermal expansion coefficient, defined as:

$$\alpha_i^{E,T} = \left[\frac{\partial S_i}{\partial \theta}\right]_{E,T=const} = \left[\frac{1}{{}^oK}\right] \qquad \textbf{(3.7)}$$

Electric behavior of a piezoelectric material

Similarly, the electric response of the material is described by the linear polarization P generated in the material due to mechanical, electrical or thermal deformation, and is given by equation (3.8) :

$$\begin{Bmatrix} D_1 \\ D_2 \\ D_3 \end{Bmatrix} = \begin{bmatrix} d_{11}^{E,\theta} & d_{12}^{E,\theta} & d_{13}^{E,\theta} & d_{14}^{E,\theta} & d_{15}^{E,\theta} & d_{16}^{E,\theta} \\ d_{21}^{E,\theta} & d_{22}^{E,\theta} & d_{23}^{E,\theta} & d_{24}^{E,\theta} & d_{25}^{E,\theta} & d_{26}^{E,\theta} \\ d_{31}^{E,\theta} & d_{32}^{E,\theta} & d_{33}^{E,\theta} & d_{34}^{E,\theta} & d_{35}^{E,\theta} & d_{36}^{E,\theta} \end{bmatrix} . \begin{Bmatrix} T_1 \\ T_2 \\ T_3 \\ T_4 \\ T_5 \\ T_6 \end{Bmatrix} + \begin{bmatrix} \varepsilon_{11}^{T,\theta} & \varepsilon_{12}^{T,\theta} & \varepsilon_{13}^{T,\theta} \\ \varepsilon_{21}^{T,\theta} & \varepsilon_{22}^{T,\theta} & \varepsilon_{23}^{T,\theta} \\ \varepsilon_{31}^{T,\theta} & \varepsilon_{32}^{T,\theta} & \varepsilon_{33}^{T,\theta} \end{bmatrix} . \begin{Bmatrix} E_1 \\ E_2 \\ E_3 \end{Bmatrix} + \begin{Bmatrix} p_1^{T,E} \\ p_2^{T,E} \\ p_3^{T,E} \end{Bmatrix} . \Delta\theta \quad \textbf{(3.8)}$$

The coefficient p is the pyroelectric coefficient, defined as;

$$P_i^{E,T} = \left[\frac{\partial D_i}{\partial \theta}\right]_{E,T=const} = \left[\frac{c}{{}^oK.m^2}\right] \quad \textbf{(3.9)}$$

Coupling of both mechanical and electrical behavior

The piezoelectric coefficients, d_{ij}, are identical for both electrical and mechanical response. This means that piezoelectricity involves the interaction between the electrical and mechanical behavior of the medium.

Hence, it is possible to express the global response by a matrix that coupled both behaviors.

This matrix is called the elasto-piezo-dielectric matrix, and is indicated in equation (3.10).

$$
\begin{Bmatrix} S_1 \\ S_2 \\ S_3 \\ S_4 \\ S_5 \\ S_6 \\ D_1 \\ D_2 \\ D_3 \end{Bmatrix}
= \begin{bmatrix}
s_{11}^{E,\theta} & s_{12}^{E,\theta} & s_{13}^{E,\theta} & s_{14}^{E,\theta} & s_{15}^{E,\theta} & s_{16}^{E,\theta} & d_{11}^{E,\theta} & d_{12}^{E,\theta} & d_{13}^{E,\theta} \\
s_{21}^{E,\theta} & s_{22}^{E,\theta} & s_{23}^{E,\theta} & s_{24}^{E,\theta} & s_{25}^{E,\theta} & s_{26}^{E,\theta} & d_{21}^{E,\theta} & d_{22}^{E,\theta} & d_{23}^{E,\theta} \\
s_{31}^{E,\theta} & s_{32}^{E,\theta} & s_{33}^{E,\theta} & s_{34}^{E,\theta} & s_{35}^{E,\theta} & s_{36}^{E,\theta} & d_{31}^{E,\theta} & d_{32}^{E,\theta} & d_{33}^{E,\theta} \\
s_{41}^{E,\theta} & s_{42}^{E,\theta} & s_{43}^{E,\theta} & s_{44}^{E,\theta} & s_{45}^{E,\theta} & s_{46}^{E,\theta} & d_{41}^{E,\theta} & d_{42}^{E,\theta} & d_{43}^{E,\theta} \\
s_{51}^{E,\theta} & s_{52}^{E,\theta} & s_{53}^{E,\theta} & s_{54}^{E,\theta} & s_{55}^{E,\theta} & s_{56}^{E,\theta} & d_{51}^{E,\theta} & d_{52}^{E,\theta} & d_{53}^{E,\theta} \\
s_{61}^{E,\theta} & s_{62}^{E,\theta} & s_{63}^{E,\theta} & s_{64}^{E,\theta} & s_{65}^{E,\theta} & s_{66}^{E,\theta} & d_{61}^{E,\theta} & d_{62}^{E,\theta} & d_{63}^{E,\theta} \\
d_{11}^{E,\theta} & d_{12}^{E,\theta} & d_{13}^{E,\theta} & d_{14}^{E,\theta} & d_{15}^{E,\theta} & d_{16}^{E,\theta} & \varepsilon_{11}^{T,\theta} & \varepsilon_{12}^{T,\theta} & \varepsilon_{13}^{T,\theta} \\
d_{21}^{E,\theta} & d_{22}^{E,\theta} & d_{23}^{E,\theta} & d_{24}^{E,\theta} & d_{25}^{E,\theta} & d_{26}^{E,\theta} & \varepsilon_{21}^{T,\theta} & \varepsilon_{22}^{T,\theta} & \varepsilon_{23}^{T,\theta} \\
d_{31}^{E,\theta} & d_{32}^{E,\theta} & d_{33}^{E,\theta} & d_{34}^{E,\theta} & d_{35}^{E,\theta} & d_{36}^{E,\theta} & \varepsilon_{31}^{T,\theta} & \varepsilon_{32}^{T,\theta} & \varepsilon_{33}^{T,\theta}
\end{bmatrix} . \begin{Bmatrix} T_1 \\ T_2 \\ T_3 \\ T_4 \\ T_5 \\ T_6 \\ E_1 \\ E_2 \\ E_3 \end{Bmatrix} \quad \textbf{(3.10)}
$$

The previous matrix is so-called d-form constitutive equation and usually is represented in a compact form as shown equation (3.11) in Table 3.1. The choice of independent variables (one mechanical, T, and one electrical, E) is arbitrary. A given pair of piezoelectric matrix equations corresponds to a particular choice of independent variables. Equations (3.11) to (3.14) show other possible constitutive matrix-equations using different independent variables.

Table 3.3: The set of constitutive equations for a piezoelectric material.

Independent Variables	Type	Piezoelectric Relation	Form
[T], [E]	Extensive	$\begin{Bmatrix}[S]\\ [D]\end{Bmatrix} = \begin{bmatrix}[S^E] & [d]\\ [d] & [\varepsilon^T]\end{bmatrix} . \begin{Bmatrix}[T]\\ [E]\end{Bmatrix}$ **(3.11)**	d-form
[S], [D]	Intensive	$\begin{Bmatrix}[T]\\ [E]\end{Bmatrix} = \begin{bmatrix}[c^D] & [-h]\\ [-h] & [\beta^S]\end{bmatrix} . \begin{Bmatrix}[S]\\ [D]\end{Bmatrix}$ **(3.12)**	h-form
[T], [D]	Mixed	$\begin{Bmatrix}[S]\\ [E]\end{Bmatrix} = \begin{bmatrix}[s^D] & [-g]\\ [-g] & [\beta^T]\end{bmatrix} . \begin{Bmatrix}[S]\\ [D]\end{Bmatrix}$ **(3.13)**	g-form
[S], [E]	Mixed	$\begin{Bmatrix}[T]\\ [D]\end{Bmatrix} = \begin{bmatrix}[c^E] & [e]\\ [e] & [\varepsilon^S]\end{bmatrix} . \begin{Bmatrix}[T]\\ [E]\end{Bmatrix}$ **(3.14)**	e-form

As a particular case, if the material is non-piezoelectric, $d_{ij} = 0$, the electrical and mechanicalbehavior are no-coupled.

[E] and [D] (so called electric tensors) are first-order tensors (vectors); [S] and [T] (so-called mechanical tensors) are second-order tensors (matrix 3×3); [d],[g],[e] and [h] (the piezoelectric coefficients) are third-order tensors (matrix 6×3); $[\varepsilon]$, $[\beta]$ (the dielectric coefficients) are secondorder tensors (3×3 matrix), and [s],[c] (elastic coefficients) are four-order tensors (6×6 matrix).

In the above mentioned constitutive equations, thermal effect has not been considered and it must be included if pyroelectric materials are considered.

3.3.2 Interpretation of the elasto-piezo-dielectric coefficients

3.3.2.1 Piezoelectric coefficients

The piezoelectric coefficient dij is known as piezoelectric strain coefficient. Since the d coefficient is equivalent for the direct and the converse effect, it is possible to use two equivalent expressions to define it, as shown equation (3.15).

$$d_{ij}^{\theta} = \begin{cases} = \left[\dfrac{\partial S_j}{\partial E_i}\right]_{D,\theta=const} = {}^{m}\!/_{V} \quad Converse\ effect\ (Sensor) \\ = \left[\dfrac{\partial D_i}{\partial T_j}\right]_{S,\theta=const} = {}^{C}\!/_{V} \quad Direct\ effect\ (Actuator) \end{cases} \qquad \textbf{(3.15)}$$

Since piezoelectric material can be anisotropic, their physical constants (elasticity, permittivity and piezoelectric coefficients) are tensor quantities and relate to both the direction of the applied stress, electric field, etc., and to the directions perpendicular to these. For this reason the coefficients are generally given with two subscript indices which refer to the direction of the two related quantities (e.g. stress and strain for elasticity, displacement and electric field for permittivity). A superscript index is used to indicate a quantity that is kept constant. For piezoelectric coefficients, which refer an electric quantity and a mechanical quantity, the first subscript indicates the direction of the considered electrical quantity (displacement or electric field) and the second subscript indicates the direction of the considered mechanical quantity (stress or strain).

The next matrix indicated the structure off the d-matrix for three important cases of piezoelectric materials: the single crystal quartz, the ferroelectric ceramics PZT and the ferroelectric polymer PVDF.

Mono-crystal α-Quartz

$$d_{quartz} = \begin{bmatrix} d_{11} & -d_{11} & 0 & d_{14} & 0 & 0 \\ 0 & 0 & 0 & 0 & -d_{14} & -2d_{11} \\ 0 & 0 & 0 & 0 & 0 & 0 \end{bmatrix}$$

$$d_{11} = 2.3\ 10^{-12}\ C/N \qquad \textbf{(3.16)}$$

$$d_{14} = -0.7\ 10^{-12}\ C/N$$

$BaTiO_3$, PZT, PLZT, and other polycrystalline ferroelectrics.(Poling axis = 3)

$$d_{PZT} = \begin{bmatrix} 0 & 0 & 0 & 0 & d_{15} & 0 \\ 0 & 0 & 0 & d_{15} & 0 & 0 \\ d_{31} & d_{31} & d_{33} & 0 & 0 & 0 \end{bmatrix} \qquad \textbf{(3.17)}$$

PVDF (piezoelectric polymer)

$$d_{PVDF} = \begin{bmatrix} 0 & 0 & 0 & 0 & d_{15} & 0 \\ 0 & 0 & 0 & d_{24} & 0 & 0 \\ d_{31} & d_{32} & d_{33} & 0 & 0 & 0 \end{bmatrix} \qquad \textbf{(3.18)}$$

The rest of piezoelectric coefficients have an analogous definition, as is indicated in the next equations;

Piezoelectric voltage coefficient;

$$g_{ij}^{\theta} = \begin{cases} = \left[\dfrac{\partial S_j}{\partial E_i}\right]_{D,\theta=const} = \dfrac{m^2}{C} \ \ Converse\ effect \\ = \left[-\dfrac{\partial E_i}{\partial T_j}\right]_{S,\theta=const} = \dfrac{V.m}{N} \ \ Direct\ effect \end{cases} \qquad \textbf{(3.19)}$$

Piezoelectric stiffness coefficient;

$$h_{ij}^{\theta} = \begin{cases} = \left[\dfrac{\partial E_i}{\partial S_j}\right]_{D,\theta=const} = \dfrac{V}{m} \ \ Direct\ effect \\ = \left[-\dfrac{\partial T_j}{\partial D_i}\right]_{S,\theta=const} = \dfrac{N}{C} \ \ Converse\ effect \end{cases} \qquad \textbf{(3.20)}$$

Piezoelectric e coefficient

$$e_{ij}^{\theta} = \begin{cases} = \left[\dfrac{\partial D_i}{\partial S_j}\right]_{E,\theta=const} = \dfrac{C}{m^2} \ \ Direct\ effect \\ = \left[-\dfrac{\partial T_j}{\partial E_i}\right]_{S,\theta=const} = \dfrac{N/m}{V} \ \ Converse\ effect \end{cases} \qquad \textbf{(3.21)}$$

3.3.2.2 Elastic coefficients

In order to express the relation between the mechanical strain and the stress, two elastic coefficients can be considered: the compliance and the stiffness.

The compliance s of a material is defined as the strain produced per unit of applied stress. It can be measured at electric field constant or at electric charge constant as is indicated in the next equations.

Elastic compliance coefficient sij :

$$s_{ij}^{E,\theta} = \left[\frac{\partial S_i}{\partial T_j}\right]_{E,\theta=const} = \frac{m^2}{N}\ Compliance\ at\ E$$
$$= const\ or\ zero\ (short - circuit)$$
$$s_{ij}^{D,\theta} = \left[\frac{\partial S_i}{\partial T_j}\right]_{D,\theta=const} = \frac{m^2}{N}\ Compliance\ at\ D \quad \textbf{(3.22)}$$
$$= const\ or\ zero\ (open - circuit)$$

The first subscript refers to the direction of strain, the second to the direction of stress. For example: s_{23}^{E} is the compliance for a normal stress about axis 3 and accompanying strain in direction 2 under conditions of electric field constant (o zero).

Similarly it is defined the stiffness coefficient as:

Elastic stiffness coefficient c_{ij} :

$$c_{ij}^{E,\theta} = \left[\frac{\partial T_j}{\partial S_i}\right]_{E,\theta=const} = \frac{N}{m^2}\ Stiffness\ at\ E$$
$$= const\ or\ zero\ (short - circuit)$$
$$c_{ij}^{D,\theta} = \left[\frac{\partial T_j}{\partial S_i}\right]_{D,\theta=const} = \frac{N}{m^2}\ Stiffness\ at\ D \quad \textbf{(3.23)}$$
$$= const\ or\ zero\ (open - circuit)$$

3.3.2.3 Dielectric coefficients

The absolute permittivity (or dielectric constant) is defined as the dielectric displacement per unit of electric field. It is followed of two subscripts: the first subscript gives the direction of the dielectric displacement, the second gives the direction of the electric field. It can be measured at free displacement (T=0) or at blocking force (S=0) as is illustrated in equation (3.24).

$$\varepsilon_{ij}^{S,\theta} = \left[\frac{\partial D_i}{\partial E_j}\right]_{S,\theta=const} = \frac{F}{m}\ Permittivity\ at\ D$$

$$= const\ or\ zero\ (blocking\ force)$$

(3.24)

$$\varepsilon_{ij}^{T,\theta} = \left[\frac{\partial D_i}{\partial E_j}\right]_{T,\theta=const} = \frac{F}{m}\ Permittivity\ at\ T$$

$$= const\ or\ zero\ (free\ displacement)$$

The data handbook tables give values for the relative permittivity$\varepsilon/\varepsilon_0$, i.e. the ratio of absolute permittivity to the permittivity of free space (8.85×10^{-12}F/m).

It is also possible to define another dielectric coefficient as:

$$\beta_{ij}^{S,\theta} = \left[\frac{\partial E_j}{\partial D_i}\right]_{S,\theta=const} = \frac{m}{F}\ Impermittivity\ at\ D$$

$$= const\ or\ zero\ (blocking\ force)$$

(3.25)

$$\beta_{ij}^{T,\theta} = \left[\frac{\partial E_j}{\partial D_i}\right]_{T,\theta=const} = \frac{m}{F}\ Impermittivity\ at\ T$$

$$= const\ or\ zero\ (free\ displacement)$$

3.3.3 Linear theory limitations

It has been previously commented that different aspects limit the application of the linear theory of piezoelectricity.At the following each of them have been considered.

3.3.3.1 Electrostriction

In general the response of piezoelectric materials has a quadratic component which is superposed to the linear behavior. This component depends on a coefficient called electrostrictive coefficient. For piezoelectric materials this coefficient is usually lower than the linear piezoelectric coefficient but they can be very significant when the electric field is increased.

3.3.3.2 Depolarization

After its poling treatment a PZT ceramic will be permanently polarized, and care must therefore be taken in all subsequent handling to ensure that the ceramic is not depolarized, since this will result in partial or even total loss of its piezoelectric properties. The ceramic may be depolarized electrically, mechanically or thermally.

Electrical depolarization: Exposure to a strong electric field of opposite polarity to the poling field will depolarize the material. The field strength required for starting the depolarization depends, among other things, on the material grade, the time the material is subjected to the depolarizing field and the poling temperature.

Mechanical depolarization*:* Mechanical depolarization occurs when the mechanical stress on a piezoelectric element becomes high enough to disturb the orientation of the domains and hence destroy the alignments of the dipoles. The safety limits for mechanical stress vary considerably with material grade.

Thermal depolarization: If a piezoelectric element is heated to its Curie point, the domains become disordered and the element becomes completely depolarized. A piezoelectric element can therefore function for long period without marked depolarization only at temperatures well below the Curie point. A safe operating temperature would normally be about half way between 0ºC and the Curie point.

3.3.3.3 Frequency limitations

All the physical systems have an associate frequency natural of vibration. When the system is exposed to a periodic serial of impulses (such as electrics, mechanics, acoustics, etc) with a frequency in the vicinity of the natural frequency, the system will oscillate with very high amplitudes. In general a body mechanically exited will response with a mechanical resonance.

However, if the material is piezoelectric an electrical resonance can be achieved when the material is driven with a mechanical field. On the other hand, high mechanical deformations can be produced when the material is electrically driven. Hence, an electrical signal with a frequency very close to the mechanical natural frequency of the system will produce a resonance.

Figure 3.7 shows the typical frequency response of a piezoelectric disc. It displays the different resonance peaks. In general the linear response can be considered up to a half of the first resonance of the system. The resonance frequency will depend on the characteristics of the piezoelectric material and the mechanical and electrical conditions of environment.

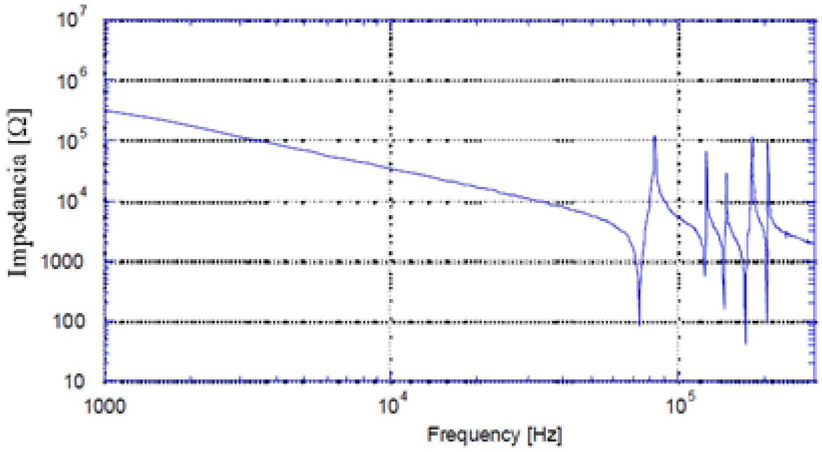

Figure 3.7: The impedance of a PZT disc as a function of frequency. [56]

3.3.3.4 Coupling factor

Piezoelectric materials couple electric and mechanic fields. Thus, it is possible to use this kind of materials introducing an electrical energy and obtaining a mechanical one, or vice versa. Then, it is necessary to have a coefficient for measuring the effectiveness with which electrical energy is converted into mechanical energy or the opposite case. This coefficient is the coupling factor k_{eff} and is defined at frequencies below the resonant frequency of the piezoelectric body as:

$$k_{eff}^2 = \frac{energy\ converted}{input\ energy\ applied\ to\ the\ material} \qquad \textbf{(3.26)}$$

In the direct piezoelectric effect, the coefficient k is defined as:

$$k_{eff}^2 = \frac{electrical\ energy}{mechanical\ energy\ driven\ to\ the\ material} \qquad \textbf{(3.27)}$$

As for the converse piezoelectric effect, k will be defined as:

$$k_{eff}^2 = \frac{mechanical\ energy\ generated}{electrical\ energy\ driven\ to\ the\ material} \qquad \textbf{(3.28)}$$

A study of the values of k_{eff} shows that for modern piezoelectric ceramics, up to 50% of the stored energy can be converted at low frequencies. The values of k_{eff}^2 quoted in tables, however, are usually theoretical maxim, based on precisely defined vibration modes of ideal (i.e. unrealistic) specimens of the material. In practical transducers, the coupling factors are usually lower.

The coupling coefficient k_{eff} describes energy conversion in all directions. When only conversions in specific directions are taken into account, the resulting coupling factor is indicated by subscripts. For instance, k_{33} is the coupling factor for longitudinal vibrations of a very long, very slender rod (in theory infinitely long, in practice, with a length/diameter ratio > 10) under the influence of a longitudinal electric field. k_{31} is the coupling factor for longitudinal vibrations of long rod under the influence of a transverse electric field, and k_{15} describe shear mode vibrations o a piezoelectric body. Special cases of the coupling factor are the planar coupling factor kp and the thickness coupling factor kt. The planar coupling factor kp of a thin disc represents the coupling between the electric field in direction 3 (parallel to the disc axis) and simultaneous mechanical effects in directions 1 and 2 (Figure 3.8) that result in radial vibrations. This is known as radial coupling.

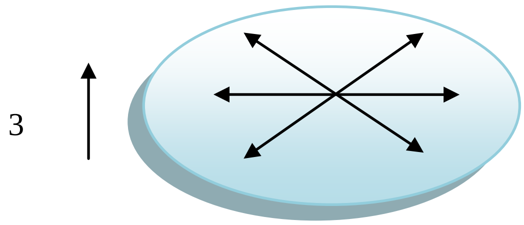

Figure 3.8: Planar oscillations of a thin disc of piezoelectric material

The thickness coupling factor k_t represents the coupling between an electric field in direction 3 and the mechanical vibrations in direction 3 of a thin, planar object of arbitrary contour (i.e. an object whose surface dimensions are large compared with its thickness).

The resonant frequency of the thickness mode of a thin planar object is far higher that of its transverse mode.

The coupling factor k_{eff} can be expressed as a quotient of energy densities.

$$k_{eff}^2 = \frac{\frac{1}{2}\varepsilon^T E^2 - \frac{1}{2}\varepsilon^S E^2}{\frac{1}{2}\varepsilon^T E^2} \qquad \textbf{(3.29)}$$

In the equation (2.29), the term $\frac{1}{2}\varepsilon^T E^2$ represents the total stored energy density for the freely deforming piezoelectric body (T=0). The term $\frac{1}{2}\varepsilon^S E^2$ represents the electrical energy density when the body is constrained (s=0). The difference between these two terms (numerator) equals the stored, converted, mechanical energy.

This energy can often be extracted and the unconverted energy can also be recovered.

Although a high k is desirable for efficient transduction, k2 should not be thought of as a measure of efficiency (this is defined as the ratio of the usefully converted power to the input power), since the unconverted energy is not necessarily lost (converted into heat) and can in many cases be recovered.

The real efficiency is the ratio of the converted useful energy to the energy taken up by the transducer, and a properly tuned and well-adjusted transducer operating in its resonance region can achieve efficiencies of well over 90%. Well outside its resonance region, however, its efficiency could be very low.

4. DYNAMIC BEHAVIOR OF BEAMS

4.1 Introduction

There are a number of beam theories that are used to present the kinematics of deformation. To descrie the various beam theories, the following coordinate system has been introduced. The x-coordinate is taken along the length of the beam, z-coordinate along the thickness (the height) of the beam, and the y-coordinate is taken along the width of the beam. In a general beam theory, all applied loads and geometry are such that displacements (u, v, w) along the coordinates (x, y, z) are only functions of the x and z coordinates. It is further assumed that the displacement v is identically zero.

The simplest beam theory is the Euler-Bernoulli Beam Theory (EBT), which is based on the displacement field.

Where w_0 is the transverse deflection of the point $(x, 0)$ of a point on the mid-plane (i.e. , $z = 0$) of the beam. The displacement field in Eq (4.1) implies that straight lines normal to the mid-plane after deformation, as shown in Figure 4.1a . These assumptions amount to neglecting both transverse shear and transverse normal strains.

$$u(x, z) = -z\frac{dw_0}{dx} \quad \textbf{(4.1)}$$

$$w(x, z) = -w_0(x) \quad \textbf{(4.2)}$$

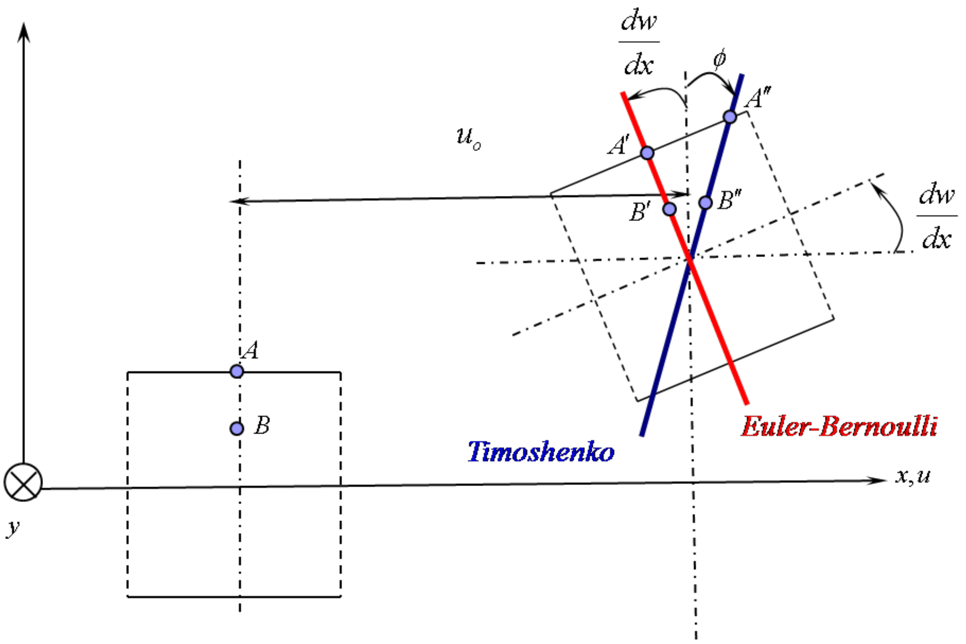

Figure 4.1: The deformation of a typical transverse normal line in EBT and TBT

Timoshenko Beam Theory (1921) is based on the displacement field

$$u(x,z) = -z\phi(x) \tag{4.3}$$

$$w(x,z) = -w_0(x) \tag{4.4}$$

Where ϕ denotes the rotation of the cross section (see Figure 4.1b). In the Timoshenko Beam Theory the normality assumpiton of the Euler-Bernoulli beam theory is relaxed and a constant state of transverse shear strain (and thus constant shear stress computed from the constitutive equation) with respect to the thickness coordinate is included. The Timoshenko beam theory requires shear correction factors to compensate for the error due to this constant shear stress assumption. As stated earlier, the shear correction factors depend not only on the material and geometric parameters but also on the loading and boundary conditions.

4.2 Euler-Bernoulli Beam Theory

The virtual strain energy δU of a beam is given by

$$\delta U = \int_0^L \int_A \sigma_{xx}\, \delta\varepsilon_{xx} dA dx \quad \textbf{(4.5)}$$

where δ is the variational symbol, A the cross-sectional area of uniform beam, L the length of the beam, σ_x the axial stress, and ε_x the normal strain. Note that the strain energy associated with the shearing is zero in the Euler-Bernoulli Beam Theory.
Using the linear strain-displacement relation (see Eq. (4.1))

$$\varepsilon_{xx} = \frac{\partial U}{\partial x} = -z\frac{\partial^2 w_0}{\partial x^2} \quad \textbf{(4.6)}$$

In Eq (4.5) it is obtained that;

$$\delta U = -\int_0^L M_x \frac{\partial^2 w_0}{\partial x^2} dx \quad \textbf{(4.7)}$$

where M_x is the bending moment

$$M_x = \int_A z\sigma_{xx}\, dA \quad \textbf{(4.8)}$$

Assuming that the transverse load *q(x)* acts at the centroidal axis of the beam and that are no other applied loads, the virtual potential energy of the load *q* is given by

$$\delta V = -\int_0^L q\, \delta w_0 dx \quad \textbf{(4.9)}$$

The principle of virtual displacements states that if a body is in equilibrium, then the total virtual work done, $\delta W = \delta U + \delta V$, is zero. Thus, it is obtained that;

$$\delta W = -\int_0^L \left(M_x \frac{\partial^2 w_0}{\partial x^2} + q\delta w_0 \right) dx = 0 \quad \textbf{(4.10)}$$

Integration by parts of the first term in Eq. (4.10) twice leads to

$$\int_0^L \left(-\frac{\partial^2 M_x}{\partial x^2} - q \right) \delta w_0 dx + \left[M_x \frac{d\delta w_0}{dx} - \frac{dM_x}{dx}\delta w_0 \right]_0^L = 0 \quad \textbf{(4.11)}$$

Since δw_0 is arbitrary in $(0 < x < L)$ the equilibrium equation is recovered as

$$-\frac{\partial^2 M_x}{\partial x^2} = q \quad for \quad (0 < x < L) \qquad \textbf{(4.12)}$$

It is useful to introduce the shear force Q_x and rewrite the equilibrium equation (4.12) in the following form

$$\frac{\partial^2 M_x}{\partial x^2} + Q_x = 0, -\frac{dQ_x}{dx} = q \qquad \textbf{(4.13)}$$

The form of the boundary conditions of the Euler-Bernoulli theory is provided by the boundary expression in Eq. (4.11). It is clear that either the displacement w_0 is known or the shear force $\frac{\partial^2 M_x}{\partial x^2} \equiv Q_x$ is specified at a point on the boundary. In addition, either the slope $\delta w_0/dx$ is specified or the bending moment M_x is known at a boundary point. Using Hooke's law, it can be written that;

$$\sigma_{xx} = E_x \varepsilon_{xx} = -E_x z \frac{\partial^2 w_0}{\partial x^2} \qquad \textbf{(4.14)}$$

where E_x is the modulus of elasticity. Thus,

$$M_x = \int_A z\sigma_{xx}\, dA = -D_x \frac{\partial^2 w_0}{\partial x^2} \qquad \textbf{(4.15)}$$

where $D_x = E_x I_y$ is the flexural rigidity of the beam and $I_y = \int_A z^2\, dA$ the second moment of area about y axis.

Some standard boundary conditions associated with the Euler- Bernoulli beam theory are given below:

Simple support: The transverse displacement w_0 is prescribed as zero and the transverse shear force $Q_x \equiv \frac{\partial^2 M_x}{\partial x^2}$ is unknown. In addition, the bending moment M_x should be specified while the slope $\frac{dw_0}{dx} = 0$ is not specified.

Clamped: The transverse deflection $w_0(L) = 0$ as well as the slope $\frac{dw_0}{dx}$ are specified to be zero. The shear force $Q_x$and bending moment M_x are unknown.

Free: The transverse deflection w_0 as well as the slope $\frac{dw_0}{dx}$ are not specified. The shear force $Q_x$and bending moment M_x should be specified.

4.3 Timoshenko Beam Theory

In view of the displacement field, the strain displacement relations are given by

$$\varepsilon_{xx} = \frac{\partial u(x,z)}{\partial x} = z\frac{\partial \phi(x)}{\partial x} \qquad \textbf{(4.16)}$$

$$\gamma_{xz} = \frac{\partial w(x,z)}{\partial x} + \frac{\partial u(x)}{\partial z} = \frac{\partial w(x,z)}{\partial x} - \phi(x) \qquad \textbf{(4.17)}$$

Note that the transverse shear strain is nonzero. Hence, the virtual strain energy δU includes the virtual energy associated with the shearing strain

$$\delta U = \int_0^L \int_A (\sigma_{xx}\,\delta\varepsilon_{xx} + \sigma_{xz}\delta\gamma_{xz})dAdx$$

$$= \int_0^L \int_A \left[\sigma_{xx} z\frac{\partial \delta\phi(x)}{\partial x} + \sigma_{xz}\left(\frac{\partial w(x,z)}{\partial x} - \phi(x)\right)\right] dAdx$$

$$= \int_0^L \left[M_x \frac{\partial \delta\phi(x)}{\partial x} + Q_x\left(\frac{\partial w(x,z)}{\partial x} - \phi(x)\right)\right] dx \qquad \textbf{(4.18)}$$

Here, σ_{xx} is the normal stress σ_{xz} the transverse shear stress, andM_x and $Q_x$are the bending moment and shear force, respectively

$$M_x = \int_A \sigma_{xx} z dA, \qquad Q_x = \int_A \sigma_{xz} dA \qquad \textbf{(4.19)}$$

As before, assuming that the transverse load $q(x)$ acts at the centroidal axis of the Timoshenko beam, the virtual potential energy of the transverse load q is given by

$$\delta V = -\int_0^L q(x)\,\delta w_0 dx \qquad \textbf{(4.20)}$$

Substituting the expressions for δU and δV, into δW = δU + δV, and carrying out integration by parts to relieve δw_0 and $\delta\phi$ of any differentiation, it is obtained that

$$0 = \int_0^L \left[M_x \frac{\partial \delta\phi(x)}{\partial x} + Q_x\left(\frac{\partial w(x,z)}{\partial x} - \phi(x)\right) - \delta w_0\right] dx$$

$$= \int_0^L \left[\left(-\frac{dM_x(x)}{dx} + Q_x \right) \delta\phi + \left(\frac{dQ_x}{dx} - \phi(x) \right) - \delta w_0 \right] dx + \left[M_x \delta\phi + Q_x \delta w_0 \right]_0^L \quad \textbf{(4.21)}$$

Setting the coefficients of δw_0 and $\delta\phi$ in $(0 < x < L)$ to zero, the following equilibrium equations are obtained

$$-\frac{dM_x(x)}{dx} + Q_x = 0, \frac{dQ_x}{dx} - \phi(x) = 0 \quad \textbf{(4.22)}$$

4.4 Vibration Analysis of Beams

4.4.1 Free vibration analysis

The natural frequencies of a simple beam model can be determined by considering free vibration motion equations. The free motion equation for isotropic beam can be seen in the Eq. (4.23). In this equation, E refers elasticity modulus, I inertial momemt, ρ is density, A the areo of section, t is time and, W(x,t) means the deflection depends on time and location.

$$EI \frac{\partial^4 W(x,t)}{\partial x^4} + \rho A \frac{\partial^2 W(x,t)}{\partial t^2} = 0 \quad \textbf{(4.23)}$$

With considering harmonic motion acception, the natural frequencies and mod shapes for a beam can be investigated in Eq. (4.24). Therefore, Eq. (4.25) is obtained from these convertion.

$$W(x,t) = \sum_n \emptyset_n(x) q_n(t) \quad \textbf{(4.24)}$$

$$\sum_n EI \frac{\partial^4 \emptyset_n(x)}{\partial x^4} q_n(t) + \sum_n \rho A \frac{\partial^2 q_n(t)}{\partial t^2} \emptyset_n(x) = 0 \quad \textbf{(4.25)}$$

Integration by parts of equation (4.25) gives the final equation which includes the natural frequencies of beam. Finally, the equation of natural frequencies can be written as Eq. (4.27) in which $\emptyset_{\boldsymbol{n}}$can be determined from the boundary conditions of the beam.

$$\ddot{q}_n(t) + \omega_n q_n(t) = 0 \tag{4.26}$$

$$\omega_n = \sqrt{\frac{EI}{\rho A}\frac{\int_0^L \frac{d^4\emptyset_n(x)}{dx^4}\emptyset_n(x)dx}{\int_0^L {\emptyset_n}^2(x)dx}} \tag{4.27}$$

4.4.2 Effects of piezoelectric patches

Adopting the Euler Bernoulli beam theory, the dynamic equation (4.28) is given by where EI is the flexural rigidity of the beam, ρ the density of the beam, A the cross sectional area of the beam, $W(x,t)$ the transverse displacement of the beam, t the time, f (t) the external force vector, and $M(x)$ induced moment provided by the piezoelectric actuators.

$$EI\frac{\partial^4 W(x,t)}{\partial x^4} + \rho A\frac{\partial^2 W(x,t)}{\partial t^2} + c\frac{\partial W(x,t)}{\partial t} = f(t) + \frac{\partial^2 M(x)}{\partial x^2} \tag{4.28}$$

$$M = \left[-b_a e_{31}\left(h + \frac{\delta}{2}\right)v_a - b_a C_{11} h\delta\left(h + \frac{\delta}{2}\right)\frac{\partial^2 W(x,t)}{\partial z^2}\right][H(z - z_{a2}) - H(z - z_{a1})] \tag{4.29}$$

Eq. (4.29) shows the moment definition, which b_a is the width of piezoelectric actuator, C_{11} is the transformed reduced elastic modulus measured at constant electrical potential, $e_{31}$the transformed reduced piezoelectric constant, va the electrical potential provided to the piezoelectric actuator, h the half thickness of the beam and $\delta$the thickness of piezoelectric actuator.

Substituting Eq. (4.29) into Eq. (4.28) and considering harmonic motion acception, the natural frequencies and mod shapes for a beam can be investigated in Eq. (4.24), the equation of motion of a beam with piezoelectric patches is obtained.

$$\begin{bmatrix} A_{11} & \cdots & A_{1N} \\ \vdots & \ddots & \vdots \\ A_{N1} & \cdots & A_{NN} \end{bmatrix} \begin{Bmatrix} q_1 \\ \vdots \\ q_N \end{Bmatrix} + \frac{c}{\rho A} \begin{bmatrix} B_{11} & \cdots & B_{1N} \\ \vdots & \ddots & \vdots \\ B_{N1} & \cdots & B_{NN} \end{bmatrix} \begin{Bmatrix} \dot{q_1} \\ \vdots \\ \dot{q_N} \end{Bmatrix}$$
$$+ \begin{bmatrix} B_{11} & \cdots & B_{1N} \\ \vdots & \ddots & \vdots \\ B_{N1} & \cdots & B_{NN} \end{bmatrix} \begin{Bmatrix} \ddot{q_1} \\ \vdots \\ \ddot{q_N} \end{Bmatrix} \tag{4.30}$$
$$= \begin{Bmatrix} F_1(t) \\ \vdots \\ F_N(t) \end{Bmatrix} + \begin{bmatrix} Ak_{11} & \cdots & Ak_{1N} \\ \vdots & \ddots & \vdots \\ Ak_{N1} & \cdots & Ak_{NN} \end{bmatrix} \begin{Bmatrix} q_1 \\ \vdots \\ q_N \end{Bmatrix} + \begin{Bmatrix} G_1 \\ \vdots \\ G_N \end{Bmatrix}$$

$$A_{MN} = \frac{EI}{\rho A} \frac{\int_0^L \frac{d^4 \emptyset_n}{dz^4} \emptyset_m dz}{\int_0^L {\emptyset_n}^2 dz} \tag{4.31}$$

$$B_{MN} = \frac{\int_0^L \emptyset_n \emptyset_m dz}{\int_0^L {\emptyset_n}^2 dz} \tag{4.32}$$

$$G_N = b_a e_{31} v_a \left(h + \frac{\delta}{2}\right) \frac{{\emptyset_m}' |_{z_{a2}}^{z_{a1}}}{\rho A \int_0^L {\emptyset_n}^2 dz} \tag{4.33}$$

$$\begin{aligned} Ak_{MN} = & -2 b_a e_{31} v_a \frac{\int_0^L \frac{d^2 \emptyset_n}{dz^2} \emptyset_m [H(z - z_{a2}) - H(z - z_{a1})] dz}{\rho A \int_0^L {\emptyset_n}^2 dz} \\ & - 2 b_a e_{31} v_a \frac{\frac{d\emptyset_n}{dz} |_{z_{a2}}^{z_{a1}} \emptyset_m}{\rho A \int_0^L {\emptyset_n}^2 dz} \\ & - 2 C_{11} b_a h \delta \left(h + 1 + \frac{\delta}{3h}\right) \frac{\frac{d^3 \emptyset_n}{dz^3} |_{z_{a2}}^{z_{a1}} \emptyset_m}{\rho A \int_0^L {\emptyset_n}^2 dz} \\ & - C_{11} b_a h \delta \frac{\int_0^L \frac{d^4 \emptyset_n}{dz^4} \emptyset_m [H(z - z_{a2}) - H(z - z_{a1})] dz}{\rho A \int_0^L {\emptyset_n}^2 dz} \end{aligned} \tag{4.34}$$

For a clamped-free beam which has mode two piezoelectric patch, which has dimensions 325x2x20 mm for beam and 25x1x20 mm for piezoelectric patches, and of which material characteristics can be seen in the Table 4.1 and Table 4.2 natural frequencies calculated as seen in Table 4.2.

Table 4.1: The characteristics for BM532 (PZT-5H) and aluminium

	BM532 (PZT-5H)	Aluminum Beam
E (N/m^2)	-	17.52
Density (kg/m^3)	7500	2716
Poisson ratio	-	0.32

Table 4.2: The material characteristics for BM532 (PZT-5H)

	BM532 (PZT-5H)
C_{11} (N/m^2)	12.6×10^{10}
C_{12} (N/m^2)	7.95×10^{10}
C_{13} (N/m^2)	8.41×10^{10}
C_{33} (N/m^2)	11.7×10^{10}
C_{44} (N/m^2)	2.33×10^{10}
E_{31} (C/m^2)	-6.5×10^{10}
E_{33} (C/m^2)	23.3×10^{10}
E_{15} (C/m^2)	17×10^{10}
ε_{11} (F/m)	1.503×10^{-8}
ε_{22} (F/m)	1.503×10^{-8}
ε_{33} (F/m)	1.3×10^{-8}

Table 4.3: The comparision of the frequencies of passive and smart beam

Natural frequencies(Hz)	Passive Beam	Smart BeamClamped-free beam with piezoelectric patches
f_1	15.30	17.52
f_2	95.89	105.48
f_3	268.58	284.92

5. SHAPE CONTROL OF BEAMS

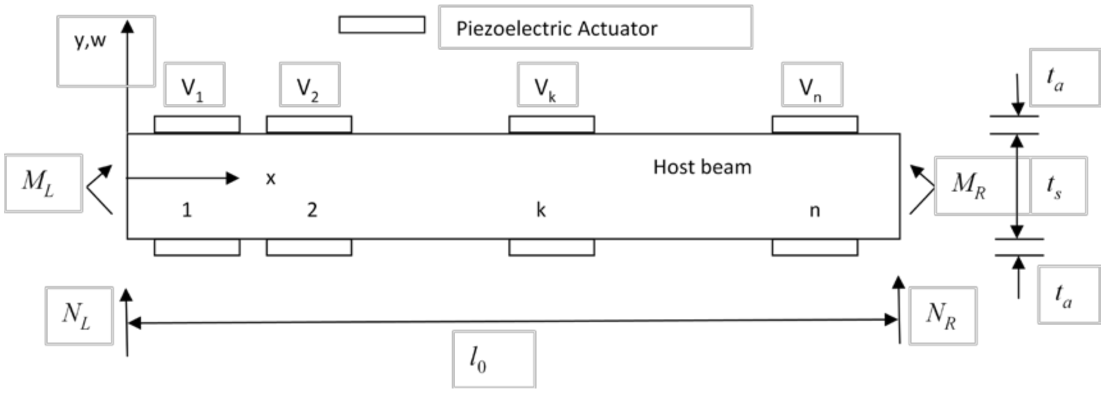

Figure 5.1: A beam with *n* patches of piezoelectric actuators bonded on it.

Figure 5.1 shows a beam with *n* patches of piezoelectric actuators bonded on it. Each pair of piezoelectric actuators consists of one actuator bonded on the top surface of the beam and the same type of actuator symmetrically bonded on the bottom surface of the beam. This symmetric distribution of piezoelectric actuators was commonly adopted in literature. The length, width, and thickness of the beam are l_0, *b*, and t_s , respectively. The width and thickness of each piezoelectric actuator are *b* and t_a , respectively. The left and right end of the *k*th pair of piezoelectric actuators are lk_1 and lk_2, far away from the left end of the beam. The voltage applied to each actuator of the *k*th pair of piezoelectric actuators is *Vk* . The two actuators of the *k*th pair of piezoelectric actuators are polarized so that a pure bending actuation effect can be produced by *Vk* , where *k* =1, 2, . . . , *n*. *Ys* and *Ya* are Young's modulus of the beam and the piezoelectric actuators, respectively. The piezoelectric strain constant of the piezoelectric actuators is d_{31}. N_L and M_L and N_R and M_R are the constrained forces and moments acting on the left and right ends of the beam, respectively.

5.1 Euler- Bernoulli Beam Theory Method

In the Euler- Bernoulli Beam Theory, as discussed above, it can be written such as If the excitation of the electric field in one of the piezoelectric patches is behaved as normal external excitation forces acting on the actuator, and simultaneously the actuator is regarded as a pure elastic body, the excitation forces act on the two ends of the actuator with the intensity of $d_{31}Y_aV_k$ / t_a and are in the axis x. Then the excitation of the voltage applied to kth pair of actuators behaves as two equal and opposite bending moments acting on the two ends of the pair of actuators. The bending moments M_{Bk} can be obtained by

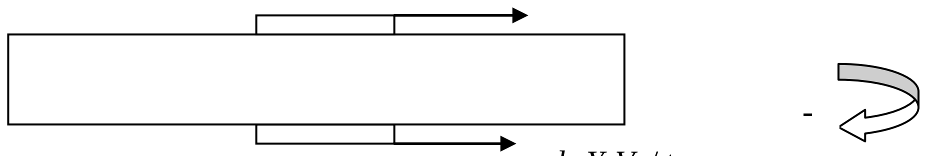

Figure 5.2: The definition of the problem; a beam with two piezoelectric patches

Bending moments can be written as

$$M_{Bk} = -d_{31}bY_a\,(V_k/t_a)t_a\frac{(t_a\ +\ t_s)}{2} - d_{31}bY_a\,(V_k/t_a)t_a\frac{(t_a\ +\ t_s)}{2} \quad \textbf{(5.1)}$$

$$M_{Bk}\ = -d_{31}bY_a\,(t_a\ +\ t_s)V_k \quad \textbf{(5.2)}$$

$$A(x) = \begin{cases} Y_SI_S & l_{(k-1)2} \le x \le l_{k1}\ and\ l_{n2} \le x \le l_0 \\ Y_SI_S + 2Y_aI_a & l_{k1} \le x \le l_{k2} \end{cases} \quad \textbf{(5.3)}$$

$$N_L = -N_R \quad \textbf{(5.4)}$$

$$M_L = M_R + N_Rl_0 \quad \textbf{(5.5)}$$

$$I_s = \frac{bt_s^3}{12} \quad \textbf{(5.6)}$$

$$I_s = \frac{bt_a(3t_s^2 + 6t_at_s + 4t_a^2)}{12} \quad \textbf{(5.7)}$$

$$M(x) = \begin{cases} M_R + N_R(l_0 - x) + M_e(x) & l_{(k-1)2} \le x \le l_{k1} \ and \ l_{n2} \le x \le \\ M_{Bk} + M_R + N_R(l_0 - x) + M_e(x) & l_{k1} \le x \le l \end{cases} \quad \textbf{(5.8)}$$

The moment relation with the shape function can be written as follows;

$$A(x)W''(x) = M(x) \quad \textbf{(5.9)}$$

Now, for Substituting Eqs. (5.2) and (5.3) into Eq. (5.9) and integrating it, we obtain

For $l_{(k-1)2} \le x \le l_{k1}$

$$Y_S I_S W''(x) = M_R + N_R(l_0 - x) + M_e(x)$$

$$\int Y_S I_S W''(x)\,dx = \int [M_R + N_R(l_0 - x) + M_e(x)]\,dx$$

$$\int G(x)\,dx = H(x) \quad \textbf{(5.10)}$$

$$\int M_e(x)\,dx = G(x) \quad \textbf{(5.11)}$$

$$Y_S I_S W'(x) = M_R x + N_R l_0 x - N_R \frac{x^2}{2} + G(x) + C_k$$

$$Y_S I_S W'(x) = -N_R \frac{x^2}{2} + [M_R + N_R l_0]x + G(x) + C_k \quad \textbf{(5.12)}$$

For $l_{n2} \le x \le l_0$ similarly,

$$Y_S I_S W''(x) = M_R + N_R(l_0 - x) + M_e(x)$$

$$\int Y_S I_S W''(x)\,dx = \int [M_R + N_R(l_0 - x) + M_e(x)]\,dx$$

$$Y_S I_S W'(x) = M_R x + N_R l_0 x - N_R \frac{x^2}{2} + G(x) + C_{n+1} \quad \textbf{(5.13)}$$

For $l_{k1} \le x \le l_{k2}$

$$[Y_S I_S + 2Y_a I_a]W''(x) = M_{Bk} + M_R + N_R(l_0 - x) + M_e(x)$$

Where $M_{Bk} = -d_{31} b Y_a (t_a + t_s) V_k$

$$\int [Y_S I_S + 2Y_a I_a] W''(x) dx$$
$$= \int [M_{Bk} + M_R + N_R(l_0 - x) + M_e(x)] dx$$
$$[Y_S I_S + 2Y_a I_a] W'(x)$$
$$= -N_R \frac{x^2}{2} + [M_{Bk} + M_R + N_R l_0] x + G(x) + D_k \quad \textbf{(5.14)}$$

For $l_{(k-1)2} \leq x \leq l_{k1}$

$$Y_S I_S W'(x) = -N_R \frac{x^2}{2} + [M_R + N_R l_0] x + G(x) + C_k \quad \textbf{(5.12)}$$

For $l_{n2} \leq x \leq l_0$

$$Y_S I_S W'(x) = -N_R \frac{x^2}{2} + [M_R + N_R l_0] x + G(x) + C_{n+1} \quad \textbf{(5.13)}$$

For $l_{k1} \leq x \leq l_{k2}$

$$[Y_S I_S + 2Y_a I_a] W'(x)$$
$$= -N_R \frac{x^2}{2} + [M_{Bk} + M_R + N_R l_0] x + G(x) + D_k \quad \textbf{(5.14)}$$

Integrating 5.12 5.13 5.14 wrt x;

For $l_{(k-1)2} \leq x \leq l_{k1}$

$$\int Y_S I_S W'(x) dx = \int \left[-N_R \frac{x^2}{2} + [M_R + N_R l_0] x + G(x) + C_k \right] dx$$

$$Y_S I_S W(x) = -N_R \frac{x^3}{6} + \frac{[M_R + N_R l_0] x^2}{2} + H(x) + C_k x + E_k \quad \textbf{(5.15)}$$

For case $l_{n2} \leq x \leq l_0$

$$\int Y_S I_S W'(x) dx = \int \left[-N_R \frac{x^2}{2} + [M_R + N_R l_0] x + G(x) + C_{n+1} \right] dx$$

And finally, for case $l_{k1} \leq x \leq l_{k2}$

$$Y_S I_S W(x) = -N_R \frac{x^3}{6} + \frac{[M_R + N_R l_0] x^2}{2} + H(x) + C_{n+1} x + E_{n+1} \quad \textbf{(5.16)}$$

$$\int [Y_S I_S + 2Y_a I_a] W'(x) dx = \int \left[-N_R \frac{x^2}{2} + [M_{Bk} + M_R + N_R l_0] x + G(x) + D_k \right] dx$$

$$[Y_S I_S + 2Y_a I_a] W(x) = -N_R \frac{x^3}{6} + \frac{[M_{Bk} + M_R + N_R l_0] x^2}{2} + H(x) + D_k x + F_k \quad \textbf{(5.17)}$$

Re-writing all equations for all conditions;

For $l_{(k-1)2} \leq x \leq l_{k1}$ the shape function can be called $W_1(x)$ instead of the general fuction $W(x)$,so following the equations may become easier.

$$Y_S I_S W_1(x) = -N_R \frac{x^3}{6} + \frac{[M_R + N_R l_0] x^2}{2} + H(x) + C_k x + E_k \quad \textbf{(5.18)}$$

Like as the specification above, for the boundary condition $l_{k1} \leq x \leq l_{k2}$, the general function $W(x)$ can be named as $W_2(x)$

$$[Y_S I_S + 2Y_a I_a] W_2(x) = -N_R \frac{x^3}{6} + \frac{[M_{Bk} + M_R + N_R l_0] x^2}{2} + H(x) + D_k x + F_k \quad \textbf{(5.19)}$$

And for $l_{n2} \leq x \leq l_0$, the shape function $W(x)$ can be entitled as $W_3(x)$ with the aim of tracing calculations.

$$Y_S I_S W_3(x) = -N_R \frac{x^3}{6} + \frac{[M_R + N_R l_0] x^2}{2} + H(x) + C_{n+1} x + E_{n+1} \quad \textbf{(5.20)}$$

C_k, C_{n+1}, D_k, E_k, E_{n+1}, F_k are the constants of integration and will be determined by the boundary conditions and continuity conditions of the deflection and slope of the beam together with N_R and M_R.

For clamped fixed end:

$$W|_{x=0} = 0 \quad \textbf{(5.21)}$$

$$\frac{\partial W}{\partial x}|_{x=0} = 0 \quad \textbf{(5.22)}$$

Derivation of equation 5.18 wrt x;

$$Y_S I_S W'(x) = -N_R \frac{x^2}{2} + [M_R + N_R l_0]x + G(x) + C_k$$

$$x = 0 \rightarrow \qquad W'(0) = 0$$

$$0 = G\ (0) + C_1$$

$$C_1 = -\ G\ (0) \quad \textbf{(5.23)}$$

Continuity relations can be shown as belows;

$$W'_1(l_{11}) = W'_2(l_{11}) \quad \textbf{(5.24)}$$

$$[Y_S I_S + 2Y_a I_a]\left[-N_R \tfrac{{l_{11}}^2}{2} + [M_R + N_R l_0]l_{11} + G(l_{11}) + C_1\right] = Y_S I_S \left[-N_R \tfrac{{l_{11}}^2}{2} + [M_{B1} + M_R + N_R l_0]l_{11} + G(l_{11}) + D_1\right] \quad \textbf{(5.25)}$$

$$W'_2(l_{12}) = W'_3(l_{12}) \quad \textbf{(5.26)}$$

$$[Y_S I_S + 2Y_a I_a]\ \left[-N_R \tfrac{{l_{12}}^2}{2} + [M_R + N_R l_0]l_{12} + G(l_{12}) + C_2\right] = Y_S I_S\ \left[-N_R \tfrac{{l_{12}}^2}{2} + [M_{B1} + M_R + N_R l_0]l_{12} + G(l_{12}) + D_1\right] \quad \textbf{(5.27)}$$

Substituting Eq. (5.27) – Eq. (5.25)

$$[Y_S I_S + 2Y_a I_a]\left[\frac{-N_R}{2}\left({l_{12}}^2 - {l_{11}}^2\right) + [M_R + N_R l_0](l_{12} - l_{11}) + G(l_{12}) - G(l_{11}) + C_2 - C_1\right] = Y_S I_S \left[\frac{-N_R}{2}\left({l_{12}}^2 - {l_{11}}^2\right) + [M_{B1} + M_R + N_R l_0](l_{12} - l_{11}) + G(l_{12}) - G(l_{11})\right] \quad \textbf{(5.28)}$$

Re-arranging the equation and dividing it the term $[Y_S I_S + 2Y_a I_a]$

$$C_2 = C_1 + \frac{Y_S I_S}{[Y_S I_S + 2Y_a I_a]}\left[\frac{-N_R}{2}\left({l_{12}}^2 - {l_{11}}^2\right) + [-M_R - N_R l_0](l_{12} - l_{11}) - [G(l_{12}) - G(l_{11})]\right] + \frac{2Y_a I_a}{[Y_S I_S + 2Y_a I_a]}[\lambda_1 M_{B1}](l_{12} - l_{11}) \quad \textbf{(5.29)}$$

As it can be seen in the Eq. (5.30), λ_1 has been described.

$$\lambda_1 = \frac{Y_S I_S}{2Y_a I_a} \quad \textbf{(5.30)}$$

Therefore,

$$\frac{2Y_a I_a}{[Y_S I_S + 2Y_a I_a]} = \frac{1}{1+\lambda_1} \quad \textbf{(5.31)}$$

Taking M_{B1} into the parenthesis

$$C_2 = C_1 + \frac{1}{1+\lambda_1}\left[\frac{-N_R}{2}\left({l_{12}}^2 - {l_{11}}^2\right) + [\lambda_1 M_{B1} - M_R - N_R l_0](l_{12} - l_{11}) - [G(l_{12}) - G(l_{11})]\right] \quad \textbf{(5.32)}$$

The Eq. (5.32) has been obtained for a beam with one piezoelectric patch. Generalizing Eq. (5.32) to solve the behaviour of a beam with n piezoelectric patches;

$$C_{k+1} = -G(0) + \frac{1}{1+\lambda_1}\sum_{i=1}^{k}\left[\frac{-N_R}{2}\left({l_{i2}}^2 - {l_{i1}}^2\right) + [\lambda_1 M_{Bi} - M_R - N_R l_0](l_{i2} - l_{i1}) - [G(l_{i2}) - G(l_{i1})]\right] \quad \textbf{(5.33)}$$

Taking the co-efficient D_1 from Eq. (5.27)

$$2Y_aI_a\left[-N_R\frac{{l_{12}}^2}{2}+[M_R+N_Rl_0]l_{12}+G(l_{12})\right]+[Y_SI_S+2Y_aI_a]C_2 = Y_SI_S\,M_{B1}l_{12}D_1 \tag{5.34}$$

Composing Eq. (5.34) again;

$$D_1=-M_{B1}l_{12}+\frac{1}{\lambda_1}\left[\left\{-N_R\left(l_0-\frac{{l_{12}}^2}{2}\right)+M_R\right\}l_{12}+G(l_{12})\right]+\frac{1+\lambda_1}{\lambda_1}C_2 \tag{5.35}$$

Generalization of Eq. (5.35);

$$D_k=-M_{Bk}l_{k2}+\frac{1}{\lambda_1}\left[\left\{-N_R\left(l_0-\frac{{l_{k2}}^2}{2}\right)+M_R\right\}l_{k2}+G(l_{k2})\right]+\frac{1+\lambda_1}{\lambda_1}C_{k+1} \tag{5.36}$$

Substituting Eq. (5.33) into the Eq. (5.36)

$$\begin{aligned}D_k=&-M_{Bk}l_{k2}+\frac{1}{\lambda_1}\left[\left\{-N_R\left(l_0-\frac{{l_{k2}}^2}{2}\right)+M_R\right\}l_{k2}+G(l_{k2})\right]\\&-\frac{1+\lambda_1}{\lambda_1}G(0)\\&+\frac{1}{\lambda_1}\sum_{i=1}^{k}\Bigg[\frac{-N_R}{2}\left({l_{i2}}^2-{l_{i1}}^2\right)+[\lambda_1M_{Bi}-M_R\\&-N_Rl_0](l_{i2}-l_{i1})-[G(l_{i2})-G(l_{i1})]\Bigg]\end{aligned} \tag{5.37}$$

For the boundary conditions of clamped free ended beam, as it can be seen in the equation (5.21), taking $x=0$ in the Eq. (5.18)

$$x=0\ \rightarrow\ E_1=-H(0) \tag{5.38}$$

And providing the continuity relations,

$$x=l_{11}\ \rightarrow\ W_1(l_{11})=W_2(l_{11}) \tag{5.39}$$

Again for a beam with one piezoelectric patch, (i.e. k=1)

$$[Y_S I_S + 2Y_a I_a]\left[-N_R \frac{{l_{11}}^3}{6} + \frac{[M_R + N_R l_0]{l_{11}}^2}{2} + H(l_{11}) + C_1 l_{11} + E_1\right] = Y_S I_S \left[-N_R \frac{{l_{11}}^3}{6} + \frac{[M_{B1} + M_R + N_R l_0]{l_{11}}^2}{2} + H(l_{11}) + D_1 l_{11} + F_1\right] \quad \textbf{(5.40)}$$

$$x = l_{12} \rightarrow\ W_2(l_{12}) = W_3(l_{12}) \quad \textbf{(5.41)}$$

$$[Y_S I_S + 2Y_a I_a]\left[-N_R \frac{{l_{12}}^3}{6} + \frac{[M_R + N_R l_0]{l_{12}}^2}{2} + H(l_{12}) + C_2 l_{12} + E_2\right] = Y_S I_S \left[-N_R \frac{{l_{12}}^3}{6} + \frac{[M_{B1} + M_R + N_R l_0]{l_{12}}^2}{2} + H(l_{12}) + D_1 l_{12} + F_1\right] \quad \textbf{(5.42)}$$

Substituting Eq. (5.42) to Eq. (5.40)

$$[Y_S I_S + 2Y_a I_a]\left[-N_R \frac{({l_{12}}^3 - {l_{11}}^3)}{6} + \frac{[M_R + N_R l_0]({l_{12}}^2 - {l_{11}}^2)}{2} + H(l_{12}) - H(l_{11}) + C_2 l_{12} - C_1 l_{11} + E_2 - E_1\right] = Y_S I_S \left[-N_R \frac{({l_{12}}^3 - {l_{11}}^3)}{6} + \frac{[M_{B1} + M_R + N_R l_0]({l_{12}}^2 - {l_{11}}^2)}{2} + H(l_{12}) - H(l_{11}) + D_1 (l_{12} - l_{11})\right] \quad \textbf{(5.43)}$$

Aligning above equation with arranging the terms with N_R to left hand side;

$$2Y_a I_a \left[-N_R \frac{({l_{12}}^3 - {l_{11}}^3)}{6} + \frac{[M_R + N_R l_0]({l_{12}}^2 - {l_{11}}^2)}{2} + H(l_{12}) - H(l_{11})\right] + [Y_S I_S + 2Y_a I_a]\{C_2 l_{12} - C_1 l_{11} + E_2 - E_1\} = \frac{Y_S I_S M_{B1}({l_{12}}^2 - {l_{11}}^2)}{2} + Y_S I_S D_1 (l_{12} - l_{11}) \quad \textbf{(5.44)}$$

Leaving the co-efficient E_2 alone in the right hand side;

$$\begin{aligned}[Y_S I_S + 2Y_a I_a]\, E_2 &= [Y_S I_S + 2Y_a I_a]\,\{-C_2 l_{12} + C_1 l_{11} + E_1\} \\ &+ \frac{Y_S I_S M_{B1}(l_{12}{}^2 - l_{11}{}^2)}{2} + Y_S I_S D_1 (l_{12} - l_{11}) \\ &- 2Y_a I_a \left[-N_R \frac{(l_{12}{}^3 - l_{11}{}^3)}{6} \right. \\ &\left. + \frac{[M_R + N_R l_0](l_{12}{}^2 - l_{11}{}^2)}{2} + H(l_{12}) - H(l_{11}) \right]\end{aligned} \quad \textbf{(5.45)}$$

Multiplying Eq. (5.45) with $\frac{1}{[Y_S I_S + 2Y_a I_a]}$ also considering following equation (5.46), the following equations (5.47) and (5.48) are obtained;

$$\frac{Y_S I_S}{[Y_S I_S + 2Y_a I_a]} = \frac{\lambda_1}{1 + \lambda_1} \quad \textbf{(5.46)}$$

$$\begin{aligned}E_2 = -C_2 l_{12} + C_1 l_{11} + E_1 + \frac{\lambda_1}{1 + \lambda_1} D_1 (l_{12} - l_{11}) \\ - \frac{1}{1 + \lambda_1} \left[-N_R \frac{(l_{12}{}^3 - l_{11}{}^3)}{6} \right. \\ + \frac{[-\lambda_1 M_{B1} + M_R + N_R l_0](l_{12}{}^2 - l_{11}{}^2)}{2} + H(l_{12}) \\ \left. - H(l_{11}) \right]\end{aligned} \quad \textbf{(5.47)}$$

$$\begin{aligned}D_1 = -M_{B1} l_{12} + \frac{1}{\lambda_1} \left[\left\{ -N_R \left(l_0 - \frac{l_{12}{}^2}{2} \right) + M_R \right\} l_{12} + G(l_{12}) \right] \\ - \frac{1 + \lambda_1}{\lambda_1} G(0) \\ + \frac{1}{\lambda_1} \left[\frac{-N_R}{2} \left(l_{12}{}^2 - l_{11}{}^2 \right) + [\lambda_1 M_{B1} - M_R \right. \\ \left. - N_R l_0](l_{12} - l_{11}) - [G(l_{12}) - G(l_{11})] \right]\end{aligned} \quad \textbf{(5.48)}$$

Multiply the Eq. (5.48) with $\frac{\lambda_1}{1+\lambda_1}(l_{12} - l_{11})$

$$\frac{\lambda_1}{1+\lambda_1} D_1(l_{12} - l_{11}) = -(l_{12} - l_{11})G(0) - M_{B1}\frac{\lambda_1}{1+\lambda_1}(l_{12} - l_{11})l_{12} + \frac{1}{1+\lambda_1}\left[\left\{-N_R\left(l_0 - \frac{{l_{12}}^2}{2}\right) + M_R\right\} l_{12} + G(l_{12})\right](l_{12} - l_{11}) + \frac{1}{1+\lambda_1}\left[\frac{-N_R}{2}\left({l_{12}}^2 - {l_{11}}^2\right) + [\lambda_1 M_{B1} - M_R - N_R l_0](l_{12} - l_{11}) - [G(l_{12}) - G(l_{11})]\right](l_{12} - l_{11}) \quad \textbf{(5.49)}$$

$$C_2 l_{12} = -G(0)l_{12} + \frac{1}{1+\lambda_1}\left\{\left[\frac{-N_R}{2}\left({l_{12}}^2 - {l_{11}}^2\right) + [\lambda_1 M_{B1} - M_R - N_R l_0](l_{12} - l_{11}) - [G(l_{12}) - G(l_{11})]\right]\right\} \quad \textbf{(5.50)}$$

To substitute all co-efficient for obtaining E_2 in the Eq. (5.47);

$$E_2 = \frac{1}{1+\lambda_1}\left[N_R\frac{({l_{12}}^3 - {l_{11}}^3)}{6} + \frac{[\lambda_1 M_{B1} - M_R - N_R l_0]({l_{12}}^2 - {l_{11}}^2)}{2} + H(l_{12}) - H(l_{11})\right] + G(0)l_{12} - \frac{1}{1+\lambda_1}\left[\frac{-N_R}{2}\left({l_{12}}^2 - {l_{11}}^2\right) + [\lambda_1 M_{B1} - M_R - N_R l_0](l_{12} - l_{11}) + [G(l_{12})l_{12} - G(l_{11})l_{12}]\right] = -(l_{12} - l_{11})G(0) - M_{B1}\frac{\lambda_1}{1+\lambda_1}(l_{12} - l_{11})l_{12} + \frac{1}{1+\lambda_1}\left[\left\{-N_R\left(l_0 - \frac{{l_{12}}^2}{2}\right) + M_R\right\} l_{12} + G(l_{12})\right](l_{12} - l_{11}) + \frac{1}{1+\lambda_1}\left[\frac{-N_R}{2}\left({l_{12}}^2 - {l_{11}}^2\right) + [\lambda_1 M_{B1} - M_R - N_R l_0](l_{12} - l_{11}) - [G(l_{12}) - G(l_{11})]\right](l_{12} - l_{11})C_1 - G(0)l_{11} - H(0) \quad \textbf{(5.51)}$$

Rewrite Eq. (5.51)

$$E_2 = \frac{1}{1+\lambda_1}\left\{N_R \frac{({l_{12}}^3 + 2{l_{11}}^3 - 2l_{11}{l_{12}}^2)}{6} - \frac{{l_{12}}^3}{2} + \frac{l_{11}{l_{12}}^2)}{2} G(l_{12})l_{12} - G(l_{11})l_{12} + [\lambda_1 M_{B1} - M_R - N_R l_0]\frac{({l_{11}}^2 - {l_{12}}^2)}{2} - H(l_{12}) + H(l_{11})\right\} - H(0)$$

$$E_2 = \frac{1}{1+\lambda_1}\left\{N_R \frac{({l_{11}}^3 - {l_{12}}^3)}{6} + [\lambda_1 M_{B1} - M_R - N_R l_0]\frac{({l_{11}}^2 - {l_{12}}^2)}{2} + G(l_{12})l_{12} - G(l_{11})l_{12} - H(l_{12}) + H(l_{11})\right\} - H(0) \quad \textbf{(5.52)}$$

With the aim of attaining F_1, to consider the equations (5.41) and (5.42)

$$x = l_{12} \rightarrow W_2(l_{12}) = W_3(l_{12}) \quad \textbf{(5.41)}$$

$$[Y_S I_S + 2Y_a I_a]\left[-N_R \frac{{l_{12}}^3}{6} + \frac{[M_R + N_R l_0]{l_{12}}^2}{2} + H(l_{12}) + C_2 l_{12} + E_2\right] = Y_S I_S\left[-N_R \frac{{l_{12}}^3}{6} + \frac{[M_{B1} + M_R + N_R l_0]{l_{12}}^2}{2} + H(l_{12}) + D_1 l_{12} + F_1\right] \quad \textbf{(5.42)}$$

$$\frac{1}{\lambda_1}\left[-N_R \frac{{l_{12}}^3}{6} + \frac{[-\lambda_1 M_{B1} + M_R + N_R l_0]{l_{12}}^2}{2} + H(l_{12})\right] + \left(\frac{1}{1+\lambda_1}\right) C_2 l_{12} + \left(1 + \frac{1}{\lambda_1}\right) E_2 - D_1 l_{12} = F_1 \quad \textbf{(5.43)}$$

For evaluating F_1following equations are calculated.

$$
\begin{aligned}
\left(1+\frac{1}{\lambda_1}\right)E_2 = &\left(-\frac{1+\lambda_1}{\lambda_1}H(0)\right) \\
&+\frac{1}{\lambda_1}\Bigg\{[-\lambda_1\, M_{B1}+M_R+N_R l_0]\frac{({l_{12}}^2-{l_{11}}^2)}{2} \\
&-N_R\frac{({l_{12}}^3-{l_{11}}^3)}{6}+G(l_{12})l_{12}-\ G(l_{11})l_{11} \\
&-[H(l_{12})-H(l_{11})]\Bigg\}
\end{aligned}
\qquad \textbf{(5.54)}
$$

$$
\begin{aligned}
D_1 l_{12} = &-\left(\frac{1}{1+\lambda_1}l_{12}\right)G(0)-M_{B1}{l_{12}}^2 \\
&+\frac{1}{\lambda_1}\left[\left\{N_R\left(l_0-\frac{l_{12}}{2}\right)+M_R\right\}{l_{12}}^2+G(l_{12})l_{12}\right] \\
&+\frac{1}{\lambda_1}\Bigg[\frac{N_R}{2}\left({l_{12}}^3-{l_{11}}^2 l_{12}\right)+[\lambda_1\, M_{B1}-M_R \\
&-N_R l_0]\left({l_{12}}^2-l_{12}l_{11}\right)-[G(l_{12})l_{12}-\ G(l_{11})l_{12}]\Bigg]
\end{aligned}
\qquad \textbf{(5.55)}
$$

$$
\begin{aligned}
F_1 = &\frac{1}{\lambda_1}\left[-N_R\frac{{l_{12}}^3}{6}+\frac{[-\lambda_1\, M_{B1}+M_R+N_R l_0]{l_{12}}^2}{2}+H(l_{12})\right] \\
&+\left(-\left(\frac{1}{1+\lambda_1}\right)G(0)l_{12}\right) \\
&+\frac{1}{\lambda_1}\Bigg\{\Bigg[\frac{-N_R}{2}\left({l_{12}}^3-{l_{11}}^2 l_{12}\right)+[\lambda_1\, M_{B1}-M_R \\
&-N_R l_0]\left({l_{12}}^2-l_{12}l_{11}\right)\Bigg]-[G(l_{12})l_{12}-\ G(l_{11})l_{12}]\Bigg\} \\
&+\left(-\frac{1+\lambda_1}{\lambda_1}H(0)\right) \\
&+\frac{1}{\lambda_1}\Bigg\{[-\lambda_1\, M_{B1}+M_R+N_R l_0]\frac{({l_{12}}^2-{l_{11}}^2)}{2} \\
&-N_R\frac{({l_{12}}^3-{l_{11}}^3)}{6}+G(l_{12})l_{12}-\ G(l_{11})l_{11} \\
&-[H(l_{12})-H(l_{11})]\Bigg\}+\left(\frac{1}{1+\lambda_1}l_{12}\right)G(0) \\
&+M_{B1}{l_{12}}^2 \\
&-\frac{1}{\lambda_1}\left[\left\{N_R\left(l_0-\frac{l_{12}}{2}\right)+M_R\right\}{l_{12}}^2+G(l_{12})l_{12}\right] \\
&-\frac{1}{\lambda_1}\Bigg[\frac{N_R}{2}\left({l_{12}}^3-{l_{11}}^2 l_{12}\right)+[\lambda_1\, M_{B1}-M_R \\
&-N_R l_0]\left({l_{12}}^2-l_{12}l_{11}\right)-[G(l_{12})l_{12}-\ G(l_{11})l_{12}]\Bigg]
\end{aligned}
\qquad \textbf{(5.56)}
$$

Arranging the coefficients in the Eq. (5.56)

$$F_1 = \frac{1}{\lambda_1}\left[N_R\left(\frac{{l_{11}}^3 - {l_{12}}^3}{3}\right) + \frac{[\lambda_1 M_{B1} - M_R - N_R l_0]({l_{12}}^2 - {l_{11}}^2)}{2}\right] + \frac{1}{\lambda_1}\{H(l_{12}) - [G(l_{12})l_{12} - G(l_{11})l_{12}] + [G(l_{12})l_{12} - G(l_{11})l_{11}] - [H(l_{12}) - H(l_{11})] - G(l_{11})l_{12}\} + \left(-\frac{1+\lambda_1}{\lambda_1}H(0)\right) \quad \textbf{(5.57)}$$

For simply supported:

$$x = 0 \to W = 0 \; so \; E_1 = -H(0) \quad \textbf{(5.58)}$$

$$x = 0 \to W = 0 \; so \; E_1 = -H(0) \quad \textbf{(5.59)}$$

$$x = l_0 \; W = 0 \quad \textbf{(5.60)}$$

$$0 = -N_R\frac{{l_0}^3}{6} + \frac{[M_R + N_R l_0]{l_0}^2}{2} + H(l_0) + C_2 l_0 + E_2$$

$$W_1(l_{11}) = W_2(l_{11}) \quad \textbf{(5.61)}$$

$$[Y_S I_S + 2Y_a I_a]\left[-N_R\frac{{l_{11}}^3}{6} + \frac{[M_R + N_R l_0]{l_{11}}^2}{2} + H(l_{11}) + C_1 l_{11} + E_1\right] = Y_S I_S\left[-N_R\frac{{l_{11}}^3}{6} + \frac{[M_{B1} + M_R + N_R l_0]{l_{11}}^2}{2} + H(l_{11}) + D_1 l_{11} + F_1\right]$$

$$W_2(l_{12}) = W_3(l_{12}) \quad \textbf{(5.62)}$$

$$[Y_S I_S + 2Y_a I_a]\left[-N_R\frac{{l_{12}}^3}{6} + \frac{[M_R + N_R l_0]{l_{12}}^2}{2} + H(l_{12}) + C_2 l_{12} + E_2\right] = Y_S I_S\left[-N_R\frac{{l_{12}}^3}{6} + \frac{[M_{B1} + M_R + N_R l_0]{l_{12}}^2}{2} + H(l_{12}) + D_1 l_{12} + F_1\right]$$

The continuity relations can be seen in the following;

$$W'_1(l_{11}) = W'_2(l_{11}) \tag{5.58}$$

$$W'_2(l_{12}) = W'_3(l_{12}) \tag{5.63}$$

$$[Y_S I_S + 2Y_a I_a]\left[-N_R \frac{{l_{11}}^2}{2} + [M_R + N_R l_0]l_{11} + G(l_{11}) + C_1\right] =$$

$$Y_S I_S\left[-N_R \frac{{l_{11}}^2}{2} + [M_{B1} + M_R + N_R l_0]l_{11} + G(l_{11}) + D_1\right]$$

$$W'_2(l_{12}) = W'_3(l_{12}) \tag{5.64}$$

$$[Y_S I_S + 2Y_a I_a]\left[-N_R \frac{{l_{12}}^2}{2} + [M_R + N_R l_0]l_{12} + G(l_{12}) + C_2\right] = Y_S I_S\left[-N_R \frac{{l_{12}}^2}{2} + [M_{B1} + M_R + N_R l_0]l_{12} + G(l_{12}) + D_1\right]$$

To simplify the equations taking $M_R = 0$ and $N_R = 0$ is suitable. The following equations are obtained as a result of these boundary conditions.

$$E_1 = -H(0) \tag{5.65}$$

$$0 = H(l_0) + C_2 l_0 + E_2 \tag{5.66}$$

$$[Y_S I_S + 2Y_a I_a][H(l_{11}) + C_1 l_{11} + E_1] = Y_S I_S\left[M_{B1}\ \frac{{l_{11}}^2}{2} + H(l_{11}) + D_1 l_{11} + F_1\right] \tag{5.67}$$

$$[Y_S I_S + 2Y_a I_a][H(l_{12}) + C_2 l_{12} + E_2] = Y_S I_S\left[M_{B1}\ \frac{{l_{12}}^2}{2} + H(l_{12}) + D_1 l_{12} + F_1\right] \tag{5.68}$$

$$[Y_S I_S + 2Y_a I_a][+G(l_{11}) + C_1] = Y_S I_S\ [M_{B1} l_{11} + G(l_{11}) + D_1] \tag{5.69}$$

$$[Y_S I_S + 2Y_a I_a][+G(l_{12}) + C_1] = Y_S I_S \, [M_{B1} l_{12} + G(l_{12}) + D_1] \quad \textbf{(5.70)}$$

Re-arranging Eq. (5.65);

$$E_2 = -H(l_0) - C_2 l_0 \quad \textbf{(5.71)}$$

Substituting Eq. (5.66) into Eq. (5.68) , new state of Eq. (5.68)

$$[Y_S I_S + 2Y_a I_a][H(l_{12}) + C_2 l_{12} - H(l_0) - C_2 l_0] = Y_S I_S \left[M_{B1} \frac{{l_{12}}^2}{2} + H(l_{12}) + D_1 l_{12} + F_1\right] \quad \textbf{(5.72)}$$

Extracting Eq. (5.67) from Eq. (5.72)

$$[Y_S I_S + 2Y_a I_a][H(l_{12}) - H(l_{11}) + C_2(l_{12} - l_0) - C_1 l_{11} - H(l_0) + H(0)] = Y_S I_S \left[M_{B1} \frac{{l_{12}}^2 - {l_{11}}^2}{2} + H(l_{12}) - H(l_{11}) + D_1(l_{12} - l_0)\right] \quad \textbf{(5.73)}$$

$$2Y_a I_a[H(l_{12}) - H(l_{11})] + [Y_S I_S + 2Y_a I_a][C_2(l_{12} - l_0) - C_1 l_{11} - H(l_0) + H(0)] - Y_S I_S M_{B1}\left(\frac{{l_{12}}^2 - {l_{11}}^2}{2}\right) = Y_S I_S D_1(l_{12} - l_0) \quad \textbf{(5.74)}$$

For obtaining C_1 from the Eq. (5.69)

$$[Y_S I_S + 2Y_a I_a][+G(l_{11}) + C_1] = Y_S I_S \, [M_{B1} l_{11} + G(l_{11}) + D_1] \quad \textbf{(5.75)}$$

$$C_1 = \frac{\lambda_1}{1 + \lambda_1}[M_{B1} l_{11} + D_1] - \frac{1}{1 + \lambda_1} \, G(l_{11}) \quad \textbf{(5.76)}$$

Same calculation for C_2 from the Eq. (5.70)

$$C_2 = \frac{\lambda_1}{1 + \lambda_1}[M_{B1} l_{12} + D_1] - \frac{1}{1 + \lambda_1} \, G(l_{12}) \quad \textbf{(5.77)}$$

Dividing Eq. (5.74) to $Y_S I_S$

$$\frac{1}{\lambda_1}[H(l_{12}) - H(l_{11})] + \frac{1+\lambda_1}{\lambda_1}[C_2(l_{12} - l_0) - C_1 l_{11} - H(l_0) + H(0)] - M_{B1}\left(\frac{{l_{12}}^2 - {l_{11}}^2}{2}\right) = D_1(l_{12} - l_0) \quad \textbf{(5.78)}$$

Subsitute Eq. (5.76) and Eq. (5.77) into Eq. (5.78)

$$D_1(l_{12} - l_0) = \frac{1}{\lambda_1}[H(l_{12}) - H(l_{11})] + \frac{1+\lambda_1}{\lambda_1}\left[\left(\frac{\lambda_1}{1+\lambda_1}[M_{B1}l_{12} + D_1] - \frac{1}{1+\lambda_1}\ G(l_{12})\right)(l_{12} - l_0) - \left(\frac{\lambda_1}{1+\lambda_1}[M_{B1}l_{11} + D_1] - \frac{1}{1+\lambda_1}\ G(l_{11})\right)l_{11} - H(l_0) + H(0)\right] - M_{B1}\left(\frac{{l_{12}}^2 - {l_{11}}^2}{2}\right) \quad \textbf{(5.79)}$$

Settiing out the Eq. (5.79)

$$D_1 = \frac{1}{l_0}\left(1 + \frac{1}{\lambda_1}\right)[H(0) - H(l_0)] + \frac{1}{l_0\lambda_1}[H(l_{12}) - H(l_{11}) - [G(l_{12})l_{12} - G(l_{11})l_{11}]] + \frac{1}{\lambda_1}\ G(l_{12}) - M_{B1}l_{12} + \frac{M_{B1}}{l_0}\left(\frac{{l_{12}}^2 - {l_{11}}^2}{2}\right) \quad \textbf{(5.80)}$$

Now, D_1 has been calculated and if it replaces into the Eq. (5.76)

$$C_1 = \frac{\lambda_1}{1+\lambda_1}\left[M_{B1}l_{11} + \frac{1}{l_0}\left(1+\frac{1}{\lambda_1}\right)[H(0) - H(l_0)] \right.$$
$$+ \frac{1}{l_0\lambda_1}[H(l_{12}) - H(l_{11}) - [G(l_{12})l_{12} - G(l_{11})l_{11}]]$$
$$\left. + \frac{1}{\lambda_1}\ G(l_{12}) - M_{B1}l_{12} + \frac{M_{B1}}{l_0}\left(\frac{{l_{12}}^2 - {l_{11}}^2}{2}\right)\right] \qquad \textbf{(5.81)}$$
$$- \frac{1}{1+\lambda_1}\ G(l_{11})$$

Arranging the Eq. (5.81)

$$C_1 = \frac{1}{l_0}[H(0) - H(l_0)]$$
$$+ \frac{1}{(1+\lambda_1)l_0}[H(l_{12}) - H(l_{11}) - [G(l_{12})l_{12}$$
$$- G(l_{11})l_{11}]] + \frac{1}{(1+\lambda_1)}[G(l_{12}) - G(l_{11})] \qquad \textbf{(5.81)}$$
$$+ \frac{\lambda_1}{1+\lambda_1}M_{B1}(l_{11} - l_{12}) + \frac{\lambda_1}{1+\lambda_1}\frac{M_{B1}}{l_0}\left(\frac{{l_{12}}^2 - {l_{11}}^2}{2}\right)$$

Remembering Eq. (5.77) for t he coefficient C_2

$$C_2 = \frac{\lambda_1}{1+\lambda_1}[M_{B1}l_{12} + D_1] - \frac{1}{1+\lambda_1}\ G(l_{12}) \qquad \textbf{(5.77)}$$

Writing C_2 into Eq. (5.77);

$$C_2 = \frac{\lambda_1}{1+\lambda_1}\left[M_{B1}l_{12} \right.$$
$$+ \frac{1}{l_0}\left(1+\frac{1}{\lambda_1}\right)[H(0) - H(l_0)]\frac{1}{\lambda_1\, l_0}[H(l_{12}) - H(l_{11})$$
$$- [G(l_{12})l_{12} - G(l_{11})l_{11}]] + \frac{1}{\lambda_1}G(l_{12}) - M_{B1}l_{12} \qquad \textbf{(5.78)}$$
$$\left. + \frac{M_{B1}}{l_0}\left(\frac{{l_{12}}^2 - {l_{11}}^2}{2}\right) - \frac{1}{1+\lambda_1}G(l_{12})\right]$$

$$C_2 = \frac{1}{l_0}[H(0) - H(l_0)] + \frac{1}{(1+\lambda_1)l_0}[H(l_{12}) - H(l_{11}) - [G(l_{12})l_{12} - G(l_{11})l_{11}]] + \frac{\lambda_1}{1+\lambda_1}\frac{M_{B1}}{l_0}\left(\frac{{l_{12}}^2 - {l_{11}}^2}{2}\right) \tag{5.78}$$

E_2 from Eq. (5.66);

$$E_2 = -H(l_0) - C_2 l_0 \tag{5.79}$$

Writing C_2 into Eq. (5.79) and adjusting the Eq. (5.80);

$$E_2 = -H(0) - \frac{1}{(1+\lambda_1)}[H(l_{12}) - H(l_{11}) - [G(l_{12})l_{12} - G(l_{11})l_{11}]] - \frac{\lambda_1 M_{B1}}{1+\lambda_1}\left(\frac{{l_{12}}^2 - {l_{11}}^2}{2}\right) \tag{5.80}$$

Considering the Eq. (5.67) for F_1 and E_1, C_1, D_1 into Eq. (5.81)

$$\frac{[Y_S I_S + 2Y_a I_a]}{Y_S I_S}\Bigg[H(l_{11}) + \Bigg\{\frac{1}{l_0}[H(0) - H(l_0)] + \frac{1}{(1+\lambda_1)l_0}\big[H(l_{12}) - H(l_{11}) - [G(l_{12})l_{12} - G(l_{11})l_{11}]\big] + \frac{1}{(1+\lambda_1)}[G(l_{12}) - G(l_{11})] + \frac{\lambda_1}{1+\lambda_1}M_{B1}(l_{11} - l_{12}) + \frac{\lambda_1}{1+\lambda_1}\frac{M_{B1}}{l_0}\left(\frac{{l_{12}}^2 - {l_{11}}^2}{2}\right)\Bigg\} l_{11} - H(0)\Bigg] = \Bigg[M_{B1}\frac{{l_{11}}^2}{2} + H(l_{11}) + \Bigg\{\frac{1}{l_0}\left(1 + \frac{1}{\lambda_1}\right)[H(0) - H(l_0)] + \frac{1}{l_0\lambda_1}\big[H(l_{12}) - H(l_{11}) - [G(l_{12})l_{12} - G(l_{11})l_{11}]\big] + \frac{1}{\lambda_1}G(l_{12}) - M_{B1}l_{12} + \frac{M_{B1}}{l_0}\left(\frac{{l_{12}}^2 - {l_{11}}^2}{2}\right)\Bigg\} l_{11} + F_1\Bigg] \quad \textbf{(5.82)}$$

$$F_{1=}\frac{M_{B1}{l_{11}}^2}{2} + \frac{1}{\lambda_1}H(l_{11}) - \frac{1}{\lambda_1}G(l_{11})l_{11} - \frac{1}{(1+\lambda_1)}H(0) \quad \textbf{(5.83)}$$

For a beam with the boundary conditions of simply supported; $G(x) = 0$, $H(x) = 0$ are considered.

$$E_{1=}0 \quad \textbf{(5.84)}$$

$$C_1 = \frac{\lambda_1}{1+\lambda_1}M_{B1}(l_{11} - l_{12}) + \frac{\lambda_1}{1+\lambda_1}\frac{M_{B1}}{l_0}\left(\frac{{l_{12}}^2 - {l_{11}}^2}{2}\right) \quad \textbf{(5.85)}$$

$$C_2 = \frac{\lambda_1}{1+\lambda_1}\frac{M_{B1}}{l_0}\left(\frac{{l_{12}}^2 - {l_{11}}^2}{2}\right) \quad \textbf{(5.86)}$$

$$E_2 = -\frac{\lambda_1 M_{B1}}{1+\lambda_1}\left(\frac{{l_{12}}^2 - {l_{11}}^2}{2}\right) \quad \textbf{(5.87)}$$

$$D_1 = -M_{B1} l_{12} + \frac{M_{B1}}{l_0}\left(\frac{{l_{12}}^2 - {l_{11}}^2}{2}\right) \qquad \textbf{(5.88)}$$

$$F_{1=} \frac{M_{B1} {l_{11}}^2}{2} \qquad \textbf{(5.89)}$$

Similarly, taking $G(x) = 0$, $H(x) = 0$ are zero for clamped free beam;

$$F_1 = M_{B1} \frac{({l_{12}}^2 - {l_{11}}^2)}{2} \qquad \textbf{(5.90)}$$

$$E_2 = \frac{\lambda_1 M_{B1}}{1+\lambda_1} \frac{({l_{11}}^2 - {l_{12}}^2)}{2} \qquad \textbf{(5.91)}$$

$$E_1 = 0 \qquad \textbf{(5.92)}$$

$$D_1 = -M_{B1} l_{12} + M_{B1}(l_{12} - l_{11}) \qquad \textbf{(5.93)}$$

$$C_2 = \frac{\lambda_1 M_{B1}(l_{12} - l_{11})}{1+\lambda_1} \qquad \textbf{(5.94)}$$

$$C_1 = 0 \qquad \textbf{(5.95)}$$

Finally, the general shape functions for a beam with clamped free boundary conditions;

$$W_1 = \frac{1}{Y_S I_S}(C_1 x + E_1) \qquad \textbf{(5.96)}$$

$$W_2 = \frac{1}{[Y_S I_S + 2 Y_a I_a]}\left(\frac{M_{B1}}{2} x^2 + D_1 x + F_1\right) \qquad \textbf{(5.97)}$$

$$W_3 = \frac{1}{Y_S I_S}(C_2 x + E_2) \qquad \textbf{(5.98)}$$

The shape functions for a beam with clamped free boundary conditions;

$$W_1 = 0 \qquad \textbf{(5.99)}$$

Describe λ_2 as following and re-arrange the equation ;

$$\frac{1}{[Y_S I_S + 2 Y_a I_a]} = \frac{1}{\lambda_2}$$

$$W_2 = \frac{1}{[Y_S I_S + 2Y_a I_a]}\left(\frac{M_{B1}}{2}x^2 + \left(-M_{B1}l_{12} + M_{B1}(l_{12} - l_{11})\right)x + M_{B1}\frac{({l_{12}}^2 - {l_{11}}^2)}{2}\right) \quad \textbf{(5.100)}$$

$$W_2 = \frac{M_{B1}}{2\lambda_2}(x - l_{11})^2$$

$$W_3 = \frac{1}{Y_S I_S}(C_2 x + E_2) \quad \textbf{(5.101)}$$

$$W_3 = \frac{M_{B1}}{\lambda_2}(l_{12} - l_{11})\left(x - \frac{l_{12} + l_{11})}{2}\right)$$

The shape functions for a beam with simply supported boundary conditions;

$$W_1 = \frac{1}{Y_S I_S}\left(\frac{\lambda_1}{1+\lambda_1}M_{B1}(l_{11} - l_{12}) + \frac{\lambda_1}{1+\lambda_1}\frac{M_{B1}}{l_0}\left(\frac{{l_{12}}^2 - {l_{11}}^2}{2}\right)\right)x \quad \textbf{(5.102)}$$

$$W_1 = \frac{1}{\lambda_2}M_{B1}\left((l_{11} - l_{12}) + \left(\frac{{l_{12}}^2 - {l_{11}}^2}{2l_0}\right)\right)x$$

$$W_2 = \frac{1}{[Y_S I_S + 2Y_a I_a]}\left(\frac{M_{B1}}{2}x^2 + \left(-M_{B1}l_{12} + \frac{M_{B1}}{l_0}\left(\frac{{l_{12}}^2 - {l_{11}}^2}{2}\right)\right)x + \frac{M_{B1}{l_{11}}^2}{2}\right) \quad \textbf{(5.103)}$$

$$W_3 = \frac{1}{\lambda_2}M_{B1}\left(\frac{{l_{12}}^2 - {l_{11}}^2}{2}\left(\frac{x}{l_0} - 1\right)\right) \quad \textbf{(5.104)}$$

Table 5.1: The shape functions for different boundary conditions

Simply supported	Clamped Free
$W_1 = \frac{1}{\lambda_2} M_{B1} \left((l_{11} - l_{12}) + \left(\frac{{l_{12}}^2 - {l_{11}}^2}{2l_0} \right) \right) x$	$W_1 = 0$
$W_2 = \frac{M_{B1}}{2\lambda_2} \left(x^2 + \left(-l_{12} + \left(\frac{{l_{12}}^2 - {l_{11}}^2}{l_0} \right) \right) x + {l_{11}}^2 \right)$	$W_2 = \frac{M_{B1}}{2\lambda_2} (x - l_{11})^2$
$W_3 = \frac{1}{\lambda_2} M_{B1} \left(\frac{{l_{12}}^2 - {l_{11}}^2}{2} \left(\frac{x}{l_0} - 1 \right) \right)$	$W_3 = \frac{M_{B1}}{\lambda_2} (l_{12} - l_{11}) \left(x - \frac{l_{12} + l_{11}}{2} \right)$

5.2 Timoshenko Beam Theory Method

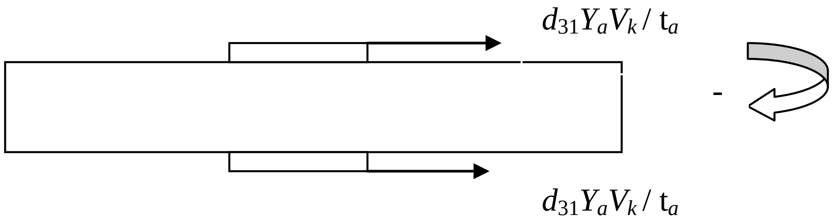

Figure 5.3: The definition of the problem; a beam with two piezoelectric patches

As discussed in last section, the bending moment is calculated like followings;

$$M_{Bk} = -d_{31} b Y_a (t_a + t_s) V_k \quad \textbf{(5.2)}$$

$$A(x) = \begin{cases} Y_S I_S & l_{(k-1)2} \leq x \leq l_{k1} \text{ and } l_{n2} \leq x \leq l_0 \\ Y_S I_S + 2 Y_a I_a & l_{k1} \leq x \leq l_{k2} \end{cases} \quad \textbf{(5.3)}$$

$$N_L = -N_R \quad \textbf{(5.4)}$$

$$M_L = M_R + N_R l_0 \quad \textbf{(5.5)}$$

$$I_s = \frac{bt_s^3}{12} \qquad \textbf{(5.6)}$$

$$I_s = \frac{bt_a(3t_s^2 + 6t_a t_s + 4t_a^2)}{12} \qquad \textbf{(5.7)}$$

$$M(x) = \begin{cases} M_R + N_R(l_0 - x) + M_e(x) & l_{(k-1)2} \leq x \leq l_{k1} \; and \; l_{n2} \leq x \leq \\ M_{Bk} + M_R + N_R(l_0 - x) + M_e(x) & l_{k1} \leq x \leq l \end{cases} \qquad \textbf{(5.8)}$$

Moreover, Timoshenko Beam Theory gives the moment equation which can be seen in the Eq. (5.104)

$$M(x) = D_{xx}\frac{d\phi^T}{dx} \qquad \textbf{(5.104)}$$

where;

$$D_{xx} = E_x I_y \qquad \textbf{(5.105)}$$

$$\frac{d\phi^T}{dx} = \frac{M(x)}{A(x)} \qquad \textbf{(5.106)}$$

$$\frac{d\phi^T}{dx} = \frac{M_R + N_R(l_0 - x) + M_e(x)}{Y_S I_S} \quad for \quad l_{(k-1)2} \leq x \leq l_{k1} \; and \; l_{n2} \leq x \leq l_0 \qquad \textbf{(5.107)}$$

$$\frac{d\phi^T}{dx} = \frac{M_{Bk} + M_R + N_R(l_0 - x) + M_e(x)}{Y_S I_S + 2Y_a I_a} \quad for \quad l_{k1} \leq x \leq l_{k2} \qquad \textbf{(5.108)}$$

$$\phi = \frac{1}{Y_S I_S}\left[M_R x + N_R x(l_0 - \frac{x}{2}) + G(x) + C_k\right] \quad for \quad l_{(k-1)2} \leq x \leq l_{k1} \qquad \textbf{(5.109)}$$

$$\phi = \frac{1}{Y_S I_S + 2Y_a I_a}\left[M_{Bk} x + M_R x + N_R x(l_0 - \frac{x}{2}) + G(x) + D_k\right] \; for \; l_{k1} \leq x \leq l_{k2} \qquad \textbf{(5.110)}$$

$$\phi = \frac{1}{Y_S I_S}\left[M_R x + N_R x(l_0 - \frac{x}{2}) + G(x) + C_{k+1}\right] \; for \; l_{n2} \leq x \leq l_0 \qquad \textbf{(5.111)}$$

$$Q_x = N_R \tag{5.112}$$

$$Q_x = N_R = K_s G_{xz} A \left(\frac{dw^T}{dx} - \phi \right) \tag{5.113}$$

$$\frac{dw^T}{dx} = \frac{N_R}{K_s A_{xz}} + \phi \tag{5.114}$$

$$\frac{dw^T}{dx} = \frac{N_R}{K_s A_{xz}} + \frac{1}{Y_S I_S} \left[M_R x + N_R x (l_0 - \frac{x}{2}) + G(x) + C_k \right] \quad for \quad l_{(k-1)2} \leq x \leq l_{k1} \tag{5.115}$$

$$\frac{dw^T}{dx} = \frac{N_R}{K_s A_{xz}} + \frac{1}{Y_S I_S + 2 Y_a I_a} \left[M_{Bk} x + M_R x + N_R x (l_0 - \frac{x}{2}) + G(x) + D_k \right] for \; l_{k1} \leq x \leq l_{k2} \tag{5.116}$$

$$\frac{dw^T}{dx} = \frac{N_R}{K_s A_{xz}} + \frac{1}{Y_S I_S} \left[M_R x + N_R x (l_0 - \frac{x}{2}) + G(x) + C_{k+1} \right] for \; l_{n2} \leq x \leq l_0 \tag{5.117}$$

For $l_{(k-1)2} \leq x \leq l_{k1}$

$$W(x) = \frac{N_R x}{K_s A_{xz}} + \frac{1}{Y_S I_S} \left[-N_R \frac{x^3}{6} + \frac{[M_R + N_R l_0] x^2}{2} + H(x) + C_k x \right] + E_k \tag{5.118}$$

For $l_{k1} \leq x \leq l_{k2}$

$$W(x) = \frac{N_R x}{K_s A_{xz}} + \frac{1}{[Y_S I_S + 2 Y_a I_a]} \left[-N_R \frac{x^3}{6} + \frac{[M_{Bk} + M_R + N_R l_0] x^2}{2} + H(x) + D_k x \right] + F_k \tag{5.119}$$

For $l_{n2} \leq x \leq l_0$

$$W(x) = \frac{N_R x}{K_s A_{xz}} + \frac{1}{Y_S I_S} \left[-N_R \frac{x^3}{6} + \frac{[M_R + N_R l_0] x^2}{2} + H(x) + C_{n+1} x \right] + E_{n+1} \tag{5.120}$$

C_k, C_{n+1}, D_k, E_k, E_{n+1}, F_k are the constants of integration and will be determined by the boundary conditions and continuity conditions of the deflection and slope of the beam together with N_R and M_R

$k = 1$ only for 1 patch

$$W_1 = \frac{N_R x}{K_s A_{xz}} + \frac{1}{Y_S I_S}\left[-N_R \frac{x^3}{6} + \frac{[M_R + N_R l_0]x^2}{2} + H(x) + C_1 x\right] + E_1 \quad \textbf{(5.121)}$$

$$W_2 = \frac{N_R x}{K_s A_{xz}} + \frac{1}{[Y_S I_S + 2Y_a I_a]}\left[-N_R \frac{x^3}{6} + \frac{[M_{Bk} + M_R + N_R l_0]x^2}{2} + H(x) + D_1 x\right] + F_1 \quad \textbf{(5.122)}$$

$$W_3 = \frac{N_R x}{K_s A_{xz}} + \frac{1}{Y_S I_S}\left[-N_R \frac{x^3}{6} + \frac{[M_R + N_R l_0]x^2}{2} + H(x) + C_2 x\right] + E_2 \quad \textbf{(5.123)}$$

$$\phi_1 = \frac{1}{Y_S I_S}\left[M_R x + N_R x(l_0 - \frac{x}{2}) + G(x) + C_1\right] \quad \textbf{(5.124)}$$

$$\phi_2 = \frac{1}{Y_S I_S + 2Y_a I_a}\left[M_{Bk} x + M_R x + N_R x(l_0 - \frac{x}{2}) + G(x) + D_1\right] \quad \textbf{(5.125)}$$

$$\phi_3 = \frac{1}{Y_S I_S}\left[M_R x + N_R x(l_0 - \frac{x}{2}) + G(x) + C_2\right] \quad \textbf{(5.126)}$$

The boundary conditions for a beam with clamped-free ended;

$$x = 0 \ \phi_1 = 0 \ C_1 = -G(0) \quad \textbf{(5.127)}$$

$$x = 0 \ \ W_1 = 0 \ E_1 = \frac{-H(0)}{Y_S I_S} \quad \textbf{(5.128)}$$

$$W_1(l_{11}) = W_2(l_{11}) \quad \textbf{(5.128)}$$

$$\frac{N_R l_{11}}{K_s A_{xz}} + \frac{1}{Y_S I_S}\left[-N_R \frac{{l_{11}}^3}{6} + \frac{[M_R + N_R l_0]{l_{11}}^2}{2} + H(l_{11}) + C_1 l_{11}\right] + E_1 = \frac{N_R l_{11}}{K_s A_{xz}} + \frac{1}{[Y_S I_S + 2Y_a I_a]}\left[-N_R \frac{{l_{11}}^3}{6} + \frac{[M_{B1} + M_R + N_R l_0]{l_{11}}^2}{2} + H(l_{11}) + D_1 l_{11}\right] + F_1 \quad \textbf{(5.129)}$$

Dividing the Eq. (5.129) to $\frac{N_R l_{11}}{K_s A_{xz}}$

$$\frac{1}{Y_S I_S}\left[-N_R\frac{{l_{11}}^3}{6}+\frac{[M_R+N_R l_0]{l_{11}}^2}{2}+H(l_{11})+C_1 l_{11}\right]+E_1$$
$$=\frac{1}{[Y_S I_S+2Y_a I_a]}\left[-N_R\frac{{l_{11}}^3}{6}+\frac{[M_{B1}+M_R+N_R l_0]{l_{11}}^2}{2}+H(l_{11})+D_1 l_{11}\right]+F_1 \quad \textbf{(5.130)}$$

$$W_2(l_{12})=W_3(l_{12}) \quad \textbf{(5.131)}$$

$$\frac{N_R l_{12}}{K_s A_{xz}}+\frac{1}{Y_S I_S}\left[-N_R\frac{{l_{12}}^3}{6}+\frac{[M_R+N_R l_0]{l_{12}}^2}{2}+H(l_{12})+C_2 l_{12}\right]+E_2$$
$$=\frac{N_R l_{12}}{K_s A_{xz}}+\frac{1}{[Y_S I_S+2Y_a I_a]}\left[-N_R\frac{{l_{12}}^3}{6}+\frac{[M_{B1}+M_R+N_R l_0]{l_{12}}^2}{2}+H(l_{12})+D_1 l_{12}\right]+F_1 \quad \textbf{(5.132)}$$

Dividing the Eq. (5.132) to $\frac{N_R l_{12}}{K_s A_{xz}}$

$$\frac{1}{Y_S I_S}\left[-N_R\frac{{l_{12}}^3}{6}+\frac{[M_R+N_R l_0]{l_{12}}^2}{2}+H(l_{12})+C_2 l_{12}\right]+E_2$$
$$=\frac{1}{[Y_S I_S+2Y_a I_a]}\left[-N_R\frac{{l_{12}}^3}{6}+\frac{[M_{B1}+M_R+N_R l_0]{l_{12}}^2}{2}+H(l_{12})+D_1 l_{12}\right]+F_1 \quad \textbf{(5.133)}$$

$$x=l_{11} \quad \phi_1(l_{11})=\phi_2(l_{11}) \quad \textbf{(5.134)}$$

$$\frac{1}{Y_S I_S}\left[M_R l_{11}+N_R x(l_0-\frac{l_{11}}{2})+G(l_{11})+C_1\right]$$
$$=\frac{1}{Y_S I_S+2Y_a I_a}\left[M_{B1} l_{11}+M_R l_{11}+N_R x(l_0-\frac{l_{11}}{2})+G(l_{11})+D_1\right] \quad \textbf{(5.135)}$$

$$\phi_2(l_{12})=\phi_3(l_{12}) \quad \textbf{(5.136)}$$

$$\frac{1}{Y_S I_S + 2Y_a I_a}\left[M_{B1} l_{12} + M_R x + N_R x(l_0 - \frac{x}{2}) + G(x) + D_1\right] = \frac{1}{Y_S I_S}\left[M_R x + N_R x(l_0 - \frac{x}{2}) + G(x) + C_2\right] \quad \textbf{(5.137)}$$

$$C_1 = -G(0) \quad \textbf{(5.138)}$$

$$E_1 = \frac{-H(0)}{Y_S I_S} \quad \textbf{(5.139)}$$

$$\frac{1}{Y_S I_S}\left[-N_R \frac{{l_{11}}^3}{6} + \frac{[M_R + N_R l_0]{l_{11}}^2}{2} + H(l_{11}) + C_1 l_{11}\right] + E_1 = \frac{1}{[Y_S I_S + 2Y_a I_a]}\left[-N_R \frac{{l_{11}}^3}{6} + \frac{[M_{B1} + M_R + N_R l_0]{l_{11}}^2}{2} + H(l_{11}) + D_1 l_{11}\right] + F_1 \quad \textbf{(5.140)}$$

$$\frac{1}{Y_S I_S}\left[-N_R \frac{{l_{12}}^3}{6} + \frac{[M_R + N_R l_0]{l_{12}}^2}{2} + H(l_{12}) + C_2 l_{12}\right] + E_2 = \frac{1}{[Y_S I_S + 2Y_a I_a]}\left[-N_R \frac{{l_{12}}^3}{6} + \frac{[M_{B1} + M_R + N_R l_0]{l_{12}}^2}{2} + H(l_{12}) + D_1 l_{12}\right] + F_1 \quad \textbf{(5.141)}$$

$$\frac{1}{Y_S I_S}\left[M_R l_{11} + N_R x(l_0 - \frac{l_{11}}{2}) + G(l_{11}) + C_1\right] = \frac{1}{Y_S I_S + 2Y_a I_a}\left[M_{B1} l_{11} + M_R l_{11} + N_R x(l_0 - \frac{l_{11}}{2}) + G(l_{11}) + D_1\right] \quad \textbf{(5.142)}$$

$$\frac{1}{Y_S I_S + 2Y_a I_a}\left[M_{B1} l_{12} + M_R l_{12} + N_R l_{12}(l_0 - \frac{l_{12}}{2}) + G(l_{12}) + D_1\right] = \frac{1}{Y_S I_S}\left[M_R l_{12} + N_R l_{12}(l_0 - \frac{l_{12}}{2}) + G(l_{12}) + C_2\right] \quad \textbf{(5.143)}$$

Writing C_1 from the Eq. (5.138) into the Eq. (5.143)

$$\frac{1}{Y_S I_S}\left[M_R l_{11} + N_R x(l_0 - \frac{l_{11}}{2}) + G(l_{11}) - G(0)\right]$$

$$= \frac{1}{Y_S I_S + 2Y_a I_a}\left[M_{B1} l_{11} + M_R l_{11} + N_R x(l_0 - \frac{l_{11}}{2}) + G(l_{11}) + D_1\right] \quad \textbf{(5.144)}$$

Re-arranging above equation step by step;

$$[Y_S I_S + 2Y_a I_a]\left[M_R l_{11} + N_R x(l_0 - \frac{l_{11}}{2}) + G(l_{11}) - G(0)\right]$$

$$= Y_S I_S\left[M_{B1} l_{11} + M_R l_{11} + N_R x(l_0 - \frac{l_{11}}{2}) + G(l_{11}) + D_1\right]$$

$$2Y_a I_a\left[M_R l_{11} + N_R x(l_0 - \frac{l_{11}}{2}) + G(l_{11})\right] - [Y_S I_S + 2Y_a I_a]G(0) - Y_S I_S M_{B1} l_{11} = Y_S I_S D_1 \quad \textbf{(5.145)}$$

Dividing Eq. (5.145) to $Y_S I_S$

$$D_1 = \frac{1}{\lambda_1}\left[M_R l_{11} + N_R x(l_0 - \frac{l_{11}}{2}) + G(l_{11})\right] - \frac{\lambda_1 + 1}{\lambda_1} G(0) - M_{B1} l_{11} \quad \textbf{(5.146)}$$

Generalizing the Eq. (5.146) for k=1,2,..,n

$$D_k = \sum_{k=1}^{n} \frac{1}{\lambda_1}\left[M_R l_{k1} + N_R x(l_0 - \frac{l_{k1}}{2}) + G(l_{k1})\right] - \frac{\lambda_1 + 1}{\lambda_1} G(0) - M_{B1} l_{k1}$$

$$D_k = -\left(1 + \frac{1}{\lambda_1}\right) G(0) + \sum_{k=1}^{n} -M_{B1} l_{k1} + \frac{1}{\lambda_1}\left[M_R l_{k1} + N_R x(l_0 - \frac{l_{k1}}{2}) + G(l_{k1})\right] \quad \textbf{(5.147)}$$

Writing D_1 into the Eq. (5.143)

$$\frac{1}{Y_S I_S + 2Y_a I_a}\Big[M_{B1} l_{12} + M_R l_{12} + N_R l_{12}(l_0 - \frac{l_{12}}{2}) + G(l_{12}) + \frac{1}{\lambda_1}\Big[M_R l_{11} + N_R x(l_0 - \frac{l_{11}}{2}) + G(l_{11})\Big] - \frac{\lambda_1 + 1}{\lambda_1} G(0) - M_{B1} l_{11}\Big] = \frac{1}{Y_S I_S}\Big[M_R l_{12} + N_R l_{12}(l_0 - \frac{l_{12}}{2}) + G(l_{12}) + C_2\Big] \tag{5.148}$$

$$Y_S I_S \Big\{-\frac{Y_S I_S + 2Y_a I_a}{Y_S I_S} G(0) + M_{B1} l_{12} - M_{B1} l_{11} + M_R l_{12} + N_R l_{12}(l_0 - \frac{l_{12}}{2}) + G(l_{12}) + \frac{2Y_a I_a}{Y_S I_S}\Big[M_R l_{11} + N_R x(l_0 - \frac{l_{11}}{2}) + G(l_{11})\Big]\Big\} = Y_S I_S + 2Y_a I_a \Big[M_R l_{12} + N_R l_{12}(l_0 - \frac{l_{12}}{2}) + G(l_{12}) + C_2\Big]$$

$$C_2 = -G(0) - M_R l_{12} - N_R l_{12}(l_0 - \frac{l_{12}}{2}) - G(l_{12}) + \frac{\lambda_1}{\lambda_1 + 1}\Big\{M_{B1}(l_{12} - l_{11}) + M_R\left(l_{12} - \frac{l_{11}}{\lambda_1}\right) + N_R\left[l_{12}\left(l_0 - \frac{l_{12}}{2}\right) + \frac{l_{11}}{\lambda_1}\left(l_0 - \frac{l_{11}}{2}\right)\right] + G(l_{12}) + \frac{G(l_{11})}{\lambda_1}\Big\} \tag{5.149}$$

Generalizing Eq. (5.149) for n patches;

$$\frac{1}{Y_S I_S}\left[-N_R \frac{{l_{11}}^3}{6} + \frac{[M_R + N_R l_0]{l_{11}}^2}{2} + H(l_{11}) - G(0) l_{11}\right] + \frac{-H(0)}{Y_S I_S} = \frac{1}{[Y_S I_S + 2Y_a I_a]}\Big[-N_R \frac{{l_{11}}^3}{6} + \frac{[M_{B1} + M_R + N_R l_0]{l_{11}}^2}{2} + H(l_{11}) + \Big(\frac{1}{\lambda_1}\Big[M_R l_{11} + N_R x(l_0 - \frac{l_{11}}{2}) + G(l_{11})\Big] - \frac{\lambda_1 + 1}{\lambda_1} G(0) - M_{B1} l_{11}\Big) l_{11}\Big] + F_1 \tag{5.151}$$

For finding F_1 ,replace C_1, E_1, D_1 into Eq. (5.140);

$$F_1 = \frac{1}{Y_S I_S}\left[-N_R \frac{{l_{11}}^3}{6} + \frac{[M_R+N_R l_0]{l_{11}}^2}{2} + H(l_{11}) - G(0) l_{11}\right] + \frac{-H(0)}{Y_S I_S} - \frac{1}{[Y_S I_S + 2Y_a I_a]}\left[-N_R \frac{{l_{11}}^3}{6} + \frac{[M_{B1} + M_R+N_R l_0]{l_{11}}^2}{2} + H(l_{11}) + \left(\frac{1}{\lambda_1}\left[M_R l_{11} + N_R x(l_0 - \frac{l_{11}}{2}) + G(l_{11})\right] - \frac{\lambda_1 + 1}{\lambda_1} G(0) - M_{B1} l_{11}\right) l_{11}\right] \quad \textbf{(5.152)}$$

$$F_1 = \frac{1}{Y_S I_S}\left[-N_R \frac{{l_{11}}^3}{6} + \frac{[M_R+N_R l_0]{l_{11}}^2}{2} + H(l_{11}) - H(0)\right] - \frac{1}{[Y_S I_S + 2Y_a I_a]}\left[\frac{M_{B1}{l_{11}}^2}{2} - \frac{M_R {l_{11}}^2}{2}\left(1 + \frac{1}{\lambda_1}\right) - N_R\left(\frac{{l_{11}}^3}{2\lambda_1} - \frac{l_0 {l_{11}}^2}{2} + \frac{{l_{11}}^3}{6} - \frac{l_0 {l_{11}}^2}{\lambda_1}\right) + H(l_{11}) + G(l_{11})\frac{l_{11}}{\lambda_1}\right] \quad \textbf{(5.153)}$$

$$F_k = \sum_{k=1}^{n}\left\{\frac{1}{Y_S I_S}\left[-N_R \frac{{l_{k1}}^3}{6} + \frac{[M_R+N_R l_0]{l_{k1}}^2}{2} + H(l_{k1}) - H(0)\right] - \frac{1}{[Y_S I_S + 2Y_a I_a]}\left[\frac{M_{Bk}{l_{k1}}^2}{2} - \frac{M_R {l_{k1}}^2}{2}\left(1 + \frac{1}{\lambda_1}\right) - N_R\left(\frac{{l_{k1}}^3}{2\lambda_1} - \frac{l_0 {l_{k1}}^2}{2} + \frac{{l_{k1}}^3}{6} - \frac{l_0 {l_{k1}}^2}{\lambda_1}\right) + H(l_{k1}) + G(l_{k1})\frac{l_{k1}}{\lambda_1}\right]\right\} \quad \textbf{(5.154)}$$

$$
\begin{aligned}
&\frac{1}{Y_S I_S}\left[-N_R\frac{{l_{12}}^3}{6}+\frac{[M_R+N_R l_0]{l_{12}}^2}{2}+H(l_{12})\right.\\
&\qquad+\left(-G(0)-M_R l_{12}-N_R l_{12}(l_0-\frac{l_{12}}{2})-G(l_{12})\right.\\
&\qquad+\frac{\lambda_1}{\lambda_1+1}\left\{M_{B1}(l_{12}-l_{11})+M_R\left(l_{12}-\frac{l_{11}}{\lambda_1}\right)\right.\\
&\qquad+N_R\left[l_{12}\left(l_0-\frac{l_{12}}{2}\right)+\frac{l_{11}}{\lambda_1}\left(l_0-\frac{l_{11}}{2}\right)\right]+G(l_{12})\\
&\qquad\left.\left.\left.+\frac{G(l_{11})}{\lambda_1}\right\}\right)l_{12}\right]+E_2\\
&\qquad=\frac{1}{[Y_S I_S+2Y_a I_a]}\left[-N_R\frac{{l_{12}}^3}{6}+\frac{[M_{B1}+M_R+N_R l_0]{l_{12}}^2}{2}\right.\\
&\qquad+H(l_{12})\\
&\qquad+\left(\frac{1}{\lambda_1}\left[M_R l_{11}+N_R x(l_0-\frac{l_{11}}{2})+G(l_{11})\right]\right.\\
&\qquad\left.\left.-\frac{\lambda_1+1}{\lambda_1}G(0)-M_{B1}l_{11}\right)l_{12}\right]\\
&\qquad+\frac{1}{Y_S I_S}\left[-N_R\frac{{l_{11}}^3}{6}+\frac{[M_R+N_R l_0]{l_{11}}^2}{2}+H(l_{11})-H(0)\right]\\
&\qquad-\frac{1}{[Y_S I_S+2Y_a I_a]}\left[\frac{M_{B1}{l_{11}}^2}{2}-\frac{M_R{l_{11}}^2}{2}\left(1+\frac{1}{\lambda_1}\right)\right.\\
&\qquad-N_R\left(\frac{{l_{11}}^3}{2\lambda_1}-\frac{l_0{l_{11}}^2}{2}+\frac{{l_{11}}^3}{6}-\frac{l_0{l_{11}}^2}{\lambda_1}\right)+H(l_{11})\\
&\qquad\left.+G(l_{11})\frac{l_{11}}{\lambda_1}\right]
\end{aligned}
\qquad \textbf{(5.155)}
$$

$$
\begin{aligned}
E_2 = \frac{1}{[Y_S I_S + 2Y_a I_a]} \Bigg[& -N_R \frac{{l_{12}}^3}{6} + \frac{[M_{B1} + M_R + N_R l_0]{l_{12}}^2}{2} + H(l_{12}) \\
& + \left(\frac{1}{\lambda_1} \left[M_R l_{11} + N_R x(l_0 - \frac{l_{11}}{2}) + G(l_{11}) \right] \right. \\
& \left. - \frac{\lambda_1 + 1}{\lambda_1} G(0) - M_{B1} l_{11} \right) l_{12} \Bigg] \\
& + \frac{1}{Y_S I_S} \left[-N_R \frac{{l_{11}}^3}{6} + \frac{[M_R + N_R l_0]{l_{11}}^2}{2} + H(l_{11}) - H(0) \right] \\
& - \frac{1}{[Y_S I_S + 2Y_a I_a]} \Bigg[\frac{M_{B1}{l_{11}}^2}{2} - \frac{M_R {l_{11}}^2}{2} \left(1 + \frac{1}{\lambda_1} \right) \\
& - N_R \left(\frac{{l_{11}}^3}{2\lambda_1} - \frac{l_0 {l_{11}}^2}{2} + \frac{{l_{11}}^3}{6} - \frac{l_0 {l_{11}}^2}{\lambda_1} \right) + H(l_{11}) \\
& + G(l_{11}) \frac{l_{11}}{\lambda_1} \Bigg] \\
& - \frac{1}{Y_S I_S} \Bigg[-N_R \frac{{l_{12}}^3}{6} + \frac{[M_R + N_R l_0]{l_{12}}^2}{2} + H(l_{12}) \\
& + \Bigg(-G(0) - M_R l_{12} - N_R l_{12}(l_0 - \frac{l_{12}}{2}) - G(l_{12}) \\
& + \frac{\lambda_1}{\lambda_1 + 1} \Bigg\{ M_{B1}(l_{12} - l_{11}) + M_R \left(l_{12} - \frac{l_{11}}{\lambda_1} \right) \\
& + N_R \left[l_{12} \left(l_0 - \frac{l_{12}}{2} \right) + \frac{l_{11}}{\lambda_1} \left(l_0 - \frac{l_{11}}{2} \right) \right] + G(l_{12}) \\
& + \frac{G(l_{11})}{\lambda_1} \Bigg\} \Bigg) l_{12} \Bigg]
\end{aligned}
$$

$$
\begin{aligned}
E_2 = \frac{1}{[Y_S I_S + 2Y_a I_a]} \Bigg\{ \Bigg[& -N_R \frac{{l_{12}}^3}{6} + \frac{[M_{B1} + M_R + N_R l_0]{l_{12}}^2}{2} + H(l_{12}) \\
& + \left(\frac{1}{\lambda_1} \left[M_R l_{11} + N_R x(l_0 - \frac{l_{11}}{2}) + G(l_{11}) \right] \right. \\
& \left. - \frac{\lambda_1 + 1}{\lambda_1} G(0) - M_{B1} l_{11} \right) l_{12} \Bigg] \\
& - \left[\frac{M_{B1}{l_{11}}^2}{2} - \frac{M_R {l_{11}}^2}{2} \left(1 + \frac{1}{\lambda_1} \right) \right. \\
& - N_R \left(\frac{{l_{11}}^3}{2\lambda_1} - \frac{l_0 {l_{11}}^2}{2} + \frac{{l_{11}}^3}{6} - \frac{l_0 {l_{11}}^2}{\lambda_1} \right) + H(l_{11}) \\
& \left. + G(l_{11}) \frac{l_{11}}{\lambda_1} \right] \Bigg\} \\
& + \frac{1}{Y_S I_S} \Bigg\{ \Bigg[-N_R \frac{{l_{11}}^3}{6} + \frac{[M_R + N_R l_0]{l_{11}}^2}{2} + H(l_{11}) \\
& - H(0) \Bigg] \\
& - \Bigg[-N_R \frac{{l_{12}}^3}{6} + \frac{[M_R + N_R l_0]{l_{12}}^2}{2} + H(l_{12}) \\
& + \Bigg(-G(0) - M_R l_{12} - N_R l_{12}(l_0 - \frac{l_{12}}{2}) - G(l_{12}) \\
& + \frac{\lambda_1}{\lambda_1 + 1} \Bigg\{ M_{B1}(l_{12} - l_{11}) + M_R \left(l_{12} - \frac{l_{11}}{\lambda_1} \right) \\
& + N_R \left[l_{12} \left(l_0 - \frac{l_{12}}{2} \right) + \frac{l_{11}}{\lambda_1} \left(l_0 - \frac{l_{11}}{2} \right) \right] + G(l_{12}) \\
& + \frac{G(l_{11})}{\lambda_1} \Bigg\} \Bigg) l_{12} \Bigg] \Bigg\}
\end{aligned}
\quad \textbf{(5.156)}
$$

For a beam with one patch; assume that all functions came from integrating basic equations are zero; $G(x) = 0, H(x) = 0$

$$D_1 = -M_{B1} l_{11} \quad \textbf{(5.157)}$$

$$C_2 = \frac{\lambda_1}{\lambda_1 + 1} M_{B1}(l_{12} - l_{11}) \quad \textbf{(5.158)}$$

$$C_1 = 0 \quad \textbf{(5.159)}$$

$$E_1 = 0 \quad \textbf{(5.160)}$$

$$E_2 = \frac{M_{B1}}{\lambda_2} \left(\frac{-{l_{12}}^2 - {l_{11}}^2}{2} \right) \quad \textbf{(5.161)}$$

$$F_1 = \frac{-M_{B1}}{\lambda_2}\frac{{l_{11}}^2}{2} \quad \textbf{(5.162)}$$

Considering Timoshenko Beam Theory , the shape functions for a beam with one piezoelectric patch and having clamped free boundary condition are as followings;

$$W_1 = 0 \quad \textbf{(5.163)}$$

$$W_2 = \frac{M_{B1}}{2\lambda_2}(x - l_{11})^2 \quad \textbf{(5.164)}$$

$$W_3 = \frac{M_{B1}}{\lambda_2}\left(x(l_{12} - l_{11}) + \frac{{l_{12}}^2 + {l_{11}}^2}{2}\right) \quad \textbf{(5.165)}$$

5.3 Numerical Results

The goal of this research is to do vibration analysis and shape control of a beam with Piezoelectric Patches which are exposed to different boundary conditions. Firstly, the dynamic analysis of a beam with piezoelectric patches, equation of motion is obtained and then solved. Natural frequencies are calculated and compared with literature. Then shape analysis and control of a beam with piezoelectric patches are examined with considering both Euler Bernoulli Beam Theory (EBT) and Timoshenko Beam Theory (TBT). In the determination of structural models, all solutions are performed analytically to a beam subjected to different boundary conditions. The numerical analysis of natural frequencies of a beam with piezoelectric patches and shape analysis of beams with piezoelectric patches with using both EBT and TBT.

Furthermore, how the piezoelectric patches can impose the shape of a beam is shown by the obtained solutions. Figure 5.4 shows the relative longtidunal distance to normalized deflection for both simply supported and clamped free beam with piezoelectric patches. These shape functions have been found with good agreement in the literature. [50]. With these results, the deflections of a beam with piezoelectric patches of which are exposed to diffrent boundary conditions can be easily investigated.

Moreover, Figure 5.5 can be the resource for understanding the effectcs of voltage on a clamped-free beam with piezoelectric patches. It is seen in this figure that the effects of actuator voltage on transverse deflection of a cantilevered beam which have piezoelectric patches. The increased voltage makes the transverse deflection raise.

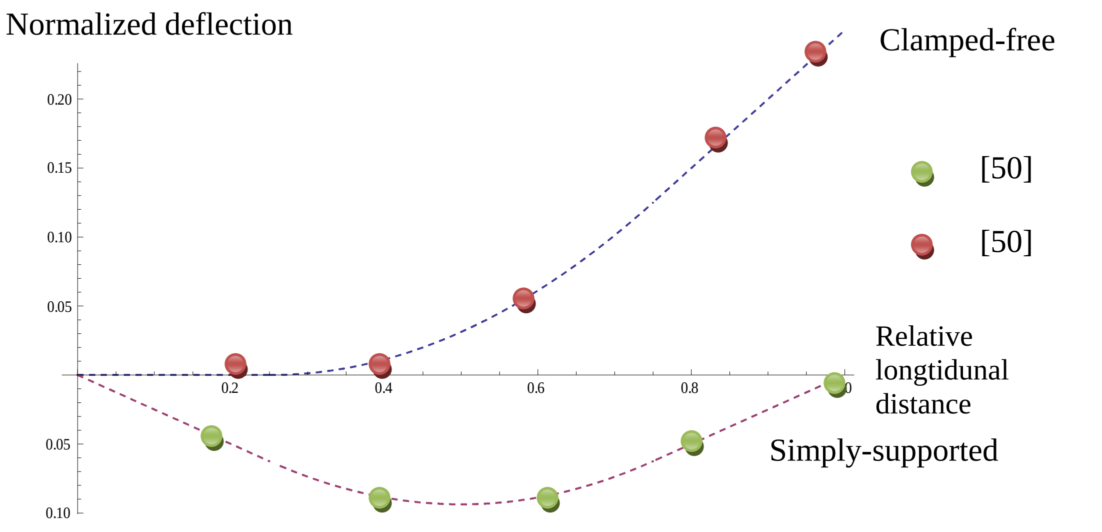

Figure 5.4: The deflections of the beam for different boundary conditions

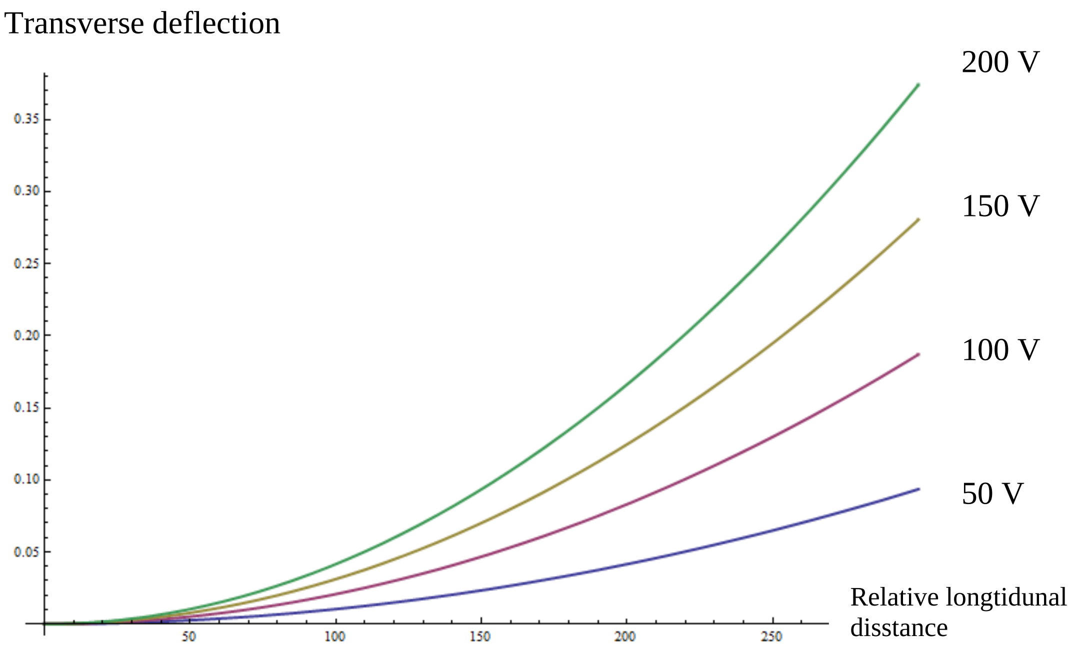

Figure 5.5 : The effects of different voltages on transverse deflection for cantilevered beam

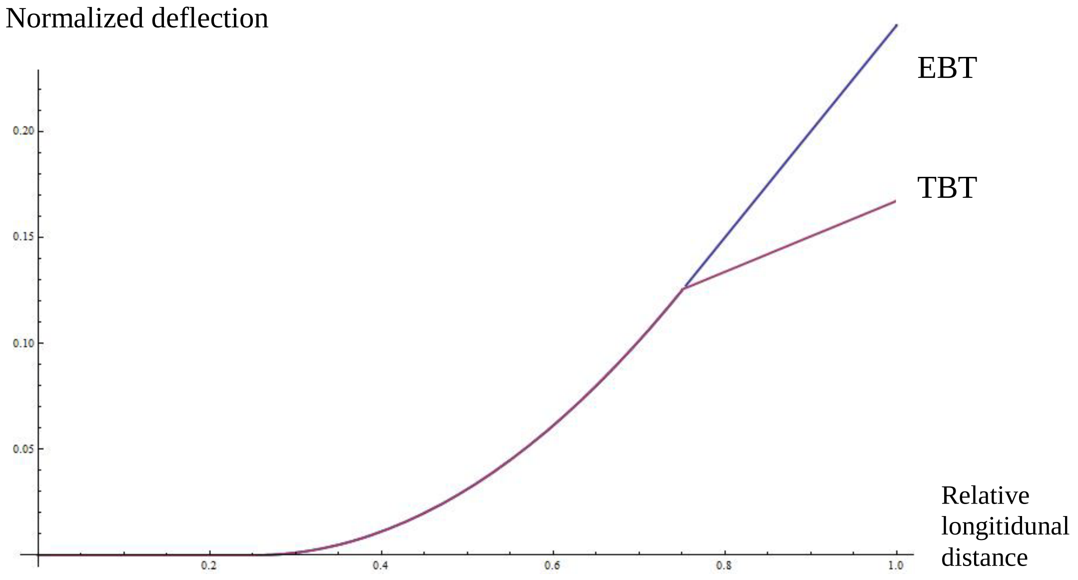

Figure 5.6 : The comparison of EBT and TBT for cantilevered beam

In this thesis, the shape functions for a beam with piezoelectric patches are obtained for different boundary conditions. This study has been performed by using two different methods, which are Euler-Bernoulli beam theory and Timoshenko beam theory. The shape functions for a cantilevered beam with piezoelectric patches are obtained both Euler-Bernoulli beam theory and Timoshenko beam theory, also. Furthermore, Figure 5.6 shows the comparison of these two obtained beam theory for a clamed-free beam with piezoelectric patches. It seems in this figure that, these functions behave in same manner until the end of the beam. Only a small amount of difference is attained about the ending of the beam.

6. CONCLUSIONS

In this study, Euler Bernoulli Beam Theory (EBT) and Timoshenko Beam Theory (TBT) are explained in detail and shape analysis and control of a beam with piezoelectric patches are examined with considering both Euler Bernoulli Beam Theory (EBT) and Timoshenko Beam Theory (TBT). In the determination of structural models, all solutions are performed analytically to a beam subjected to different boundary conditions. The numerical analysis of natural frequencies of a beam with piezoelectric patches and shape analysis of beams with piezoelectric patches with using both EBT and TBT are demonstrated.

Finally, the effects of not only different voltage but also piezoelectric patch position on frequency and on shape functions of beam are interrogated and also compared with literature and found to be in good agreement. With a view to control the shape of beam in a good manner and obtaining better results, the errors are minimized.

The comparision between Euler-Bernoulli beam theory and Timoshenko beam theory is performed for a beam with piezoelectric patches of which has been exposed to clamped-free boundary conditions. Also the effects of different voltage of a cantilevered beam is studied. The shape funtions are found for both Euler-Bernoulli beam theory and Timoshenko beam theory.

REFERENCES

[1] **Gandhi, M.V., *and* Thompson, B.S.,** 1992. Smart materials and structures**,** Chapman and Hall, London, 310.

[2] **Lnman, D.J., and Cudney, H.H.,** 2000. Structural and machine design using piezoceramic materials final report to NASA Langley Research Center, NASA Grant Number NAG-l-1998.

[3] **Crawley, E. F., and de Luis, J., 1987.** Use of piezoelectric actuators as elements of intelligent structures, *AIAA Journal*, **25** (10), 1373-1385.

[4] **H. Abramovich, H. and Livshits, A., 1993.** Dynamic behavior of cross-ply laminated beams with piezoelectric layers, *Composite Structures,* **25** (1-4), 371-379.

[5] **Waisman, H., and Abramovich, H., 2002.** Active stiffening of laminated composite beams using piezoelectric actuators, *Composite Structures,* **58** (1), 109-120.

[6] **Yocum, M. and Abramovich, H., 2002.** Static behavior of piezoelectric actuated beams, *Computers and Structures,* **80** (23), 1797-1808.

[7] **Waisman, H. and Abramovich, H., 2002.** Variation of natural frequencies of beams using the active stiffening effect, *Composites Part B: Engineering,* **33** (6), 415-424.

[8] **Azulay L.E., and Abramovich, H., 2006.** Active damping of piezo-composite beams, *Composite Structures,* **74** (4), 458-466.

[9] **Abramovich, H., 1998.** Deflection control of laminated composite beams with piezoceramic layers — closed form solutions, *Composite Structures,* **43** (3), 217-231.

[10] **Fridman, Y. and Abramovich, H., 2008.** Enhanced structural behavior of flexible laminated composite beams, *Composite Structures,* **82** (1), 140-154.

[11] **Nir, A. and Abramovich, H., 2010.** Design, analysis and testing of a smart fin, *Composite Structures,* **92** (4), 863-872.

[12] **Frampton,K.D., Clark, R.L., Dowell, E.H., 1996.** Active Control of Panel Flutter with Piezoelectric Transducers, *Journal of Aircraft,* **33** (4), 768-774.

[13] **Lim,Y., Vasundara V Varadan, V.V., K Varadan, V.K., 1997.** Closed loop finite element modeling of active structural damping in the frequency domain, *Smart Materials and Structures,* **6** (2), 161-168.

[14] **Tzou H. S. and Ye R., 1996.** Pyroelectric and thermal strain effects of piezoelectric (pvdf and pzt) devices, *Mechanical Systems and Signal Processing,* **10** (4), 459-469.

[15] **Brennan M. J., Elliott S. J., Pinnington R. J., 1995.** Strategies for the active control of flexural vibration on a beam, *Journal of Sound and Vibration,* **186** (4), 657-688.

[16] **Steven R H., and Prechtl E.F., 1996.** Development of a piezoelectric servoflap for helicopter rotor control, *Smart Materials and Strucurest.* **5**, 26-34.

[17] **Lai, Z.,; Huang, J., Mai, C., 1995.** Shape and placement of piezoelectric sensors for panel flutter limit-cycle suppression, *AIAA Journal,* **34** (4), 855-857.

[18] **Zhang, N., and Kirpitchenko, I., 2002.** Modelling dynamics of a continuous structure with a piezoelectric sensor actuator for passive structural control, *Journal of Sound and Vibration,* **249** (2), 251-261.

[19] **Lee, Y.S., and Elliott, S.J., 2001.** Active position control of a flexible smart beam using internal model control. *Journal of Sound and Vibration,* **242** (5), 767-791.

[20] **M. Sunar, M., Hyder, S. J. , Yilbas, B. S., 2001**. Robust design of piezoelectric actuators for structural control, *Computer Methods in Applied Mechanics and Engineering,* **190** (46-47), 6257-6270.

[21] **Yaman, Y., Çalışkan, T., Nalbantoğlu, V., Waechter, D., Prasad, E. 2001.** Active vibration control of a smart beam, *Canada-US CaSmart Workshop Smart Materials and Structures proceedingds,* Montreal Quebec Canada, 137-147.

[22] **Sloss, J. M., Bruch, J. C., Adali, S., Sadek, S., 2001.** Piezoelectric patch control using an integral equation approach, *Thin-Walled Structures,* **39** (1), 45-63.

[23] **Li, Y., Onoda,J., Minesugi, K., 2002.** Simultaneous optimization piezoelectric actuator placement and feedback for vibration suppression, *Acta Astronautica,* **50** (6), 335-341

[24] **Wang, Q., Wang, C. M., 2001. A** controllability index for optimal design of piezoelectric actuators in vibration control of beam structures, *Journal of Sound and Vibration*, **242**, 507-518

[25] **Park, C. H., 2003.** Dynamics modelling of beams with shunted piezoelectric elements**,** *Journal of Sound and Vibration,* **268** (1), 115-129.

[26] **Singh, S.P., Pruthi, H.P., Agarwal, V. P., 2003.** Efficient modal control strategies for active control of vibrations, *Journal of Sound and Vibration,* **262** (3), 563-575.

[27] **Wang,Q., Quek, S. T., 2002.** Enhancing flutter and buckling capacity of column by piezoelectric layers, *International Journal of Solids and Structures,* **39** (16), 4167-4180.

[28] **Moon, S.H., Hwang, J.S., 2005.** Panel flutter suppression with an optimal controller based on the nonlinear model using piezoelectric materials, *Composite Structures,* **68** (3), 371-379.

[29] **Song, G., Zhou, X., Binienda, W., 2004.** Thermal deformation compensation of a composite beam using piezoelectric actuators, *Smart Materials and Structures,* **13** (1), 30-37.

[30] **Tsai, M.S., Wang, K.W., 1999**. On the structural damping characteristics of active piezoelectric actuators with passive shunt, *Journal of Sound and Vibration,* **221**, 1–22.

[31] **Dadfarnia,M., Jalili, N., Liu, Z., Dawson, D.M., 2004.** An observer-based piezoelectric control of flexible cartesian robot arms: theory and experiment, *Control Engineering Practice,* **12** (8), 1041-1053.

[32] **Lin, J., Nien, M.H., 2005.** Adaptive control of a composite cantilever beam with piezoelectric damping-modal actuators/sensors, *Composite Structures,* **70** (2), 170-176.

[33] **Suleman,A., Costa, A.P., 2004.** Adaptive control of an aeroelastic flight vehicle using piezoelectric actuators, *Composite Structures*, **82** (17-19), 1303-1314.

[34] **Han,J., Tani, J., Qiu,J., 2006.** Active flutter suppression of a lifting surface using piezoelectric actuation and modern control theory, *Journal of Sound and Vibration,* **291** (3-5), 706-722.

[35] **Shih, H., Watkins, J., Tzou, H., 2005.** Displacement control of a beam using photostrictive optical actuators, *Journal of Intelligent Material Systems and Structures,* **16** (4), 355-359.

[36] **Kapuria, S., Alam, N., 2006.** Efficient layerwise finite element model for dynamic analysis of laminated piezoelectric beams, Computer Methods in Applied Mechanics and Engineering, **195** (19-22), 2742-2760.

[37] **Moon, S.H., Hwang, J.S., 2005.** Panel flutter suppression with an optimal controller based on the nonlinear model using piezoelectric materials, *Composite Structures,* **68** (3), 371-379.

[38] **Lin, J., Liu, W., 2006.** Experimental evaluation of a piezoelectric vibration absorber using a simplified fuzzy controller in a cantilever beam, *Journal of Sound and Vibration,* **296** (3), 567-582.

[39] **Nyungen, C.H., Pietrzko, S.J., 2006.** FE analysis of a PZT-actuated adaptive beam with vibration damping using a parallel *R-L* shunt circuit, *Journal Finite Elements in Analysis and Design,* **42** (14), 1120-1134.

[40] **Moon, S.H., 2006.** Finite element analysis and design of control system with feedback output using piezoelectric sensor/actuator for panel flutter suppression, *Finite Elements in Analysis and Design,* **42** (12), 1071-1078.

[41] **Raja, S., Pashilkar, A.A., Sreedeep, R., Kamesh, J.V., 2006.** Flutter control of a composite plate with piezoelectric multilayered actuators, *Aerospace Science and Technology,* **10** (5), 435-441.

[42] **Maurini, C., Porfiri, M., Pouget, J. 2006.** Numerical methods for modal analysis of stepped piezoelectric beams, *Journal of Sound and Vibration,* **298** (4-5), 918-933.

[43] **Bhadbhade, V., Jalili, N., Mahmoodi, S.M. 2008.** A novel piezoelectrically actuated flexural/torsional vibrating beam gyroscope, *Journal of Sound and Vibration,* **311** (3-5), 1305-1324.

[44] **Z. Kıral, L. Malgaca, M. Akdağ, 2008.** Active Control of Residual Vibrations of a Cantilever Smart Beam, *Turkish Journal of Engineering and Environmental Sciences, TUBİTAK,* **32**, 51-57.

[45] **Wang, J., Shepard, W.S., Cunefare, K. A., Williams, K. A., 2007.** Actuation of a discontinuous structure with piezoelectric actuators, *Journal of Sound and Vibration*, **309** (3-5), 677-694.

[46] **Qiu, Z., Han, J., Zhang, X., Wang, Y., Zhen, W., 2009.** Active vibration control of a flexible beam using a non-collocated acceleration sensor and piezoelectric patch actuator, *Journal of Sound and Vibration,* **326** (3-5), 438-455.

[47] **Mahieddine, A., and Ouali, M., 2010.** Finite element formulation of a beam with piezoelectric patch, *Journal of Computers*, **5** (3), 401-409.,

[48] ***Zhang, J., He, L., Wang, E., 2010.*** Active vibration control of piezoelectric intelligent structures, *Journal of Computers*, **5** (3) , 401-409.

[49] **Donthireddy, P., and Chandrashekhara, K., 1996.** Modeling and shape control of composite beams with embedded piezoelectric actuators, *Composite Structures*, **35** (2), 237-244.
[50] **Wang, C.M., Ang, K.K., Ajit, A., 1999.** Shape control of laminated cantilevered beams with piezoelectric actuators, *Journal of Intelligent Material Systems and Structures, **10** (2),* 164-175.
[51] **Yang, S., Ngoi, B., 2000.** Shape Control of Beams by Piezoelectric Actuators, *AIAA Journal*, **38** (12), 2292-2298 .
[52] **Shen, M.H., 1995.** A new modeling technique for piezoelectrically actuated beams, *Composite Structures*, **57** (3), 361-366.
[53] **Punhani, A., 2008.** Shape and vibration control of smart laminated plates, The Ohio State University.
[54] **Riley,M.J., 2005.** Investigation into feasibility of implementing piezoelectric patches for sensing and actuation of structural components, Dalhousie universtity
[55] **Çalışkan, T., 2002.** Piezoelectric ceramics and their applications in smart aerospace structures, METU
[56] **Carazo, V., 2000.** Novel piezoelectric transducers for high voltage measurements, Universitat politecnica de Catalunya
[57] **Moheimani,S.O., 2006.** Piezoelectric Transducers for Vibration Control and Damping, University of Newcastle
[58] Piezoelectric Materials Synthesis, http://cnx.org/content/m25441/1.2/_
[59] **Kawai, H., (1969).** The piezoelectricity of poly(vinylidene fluoride) , *Jpn. J. Appl. Phys*, **8**, 975-976.
[60] **Safari, A., 1994.** Development of piezoelectric composites for transducers, *J. Phys. III France*, **4**, 1129-1149
[61] 176-1987 - IEEE Standard on Piezoelectricity

APPENDICES

APPENDIX A.1 : Mathematica Codes for Figure 5.

```
M_B=100;
lambda2=1;
L_0=12;
L_1=L_0/4;
L_2=3*L_0/4;
W2 Euler
Plot[( M_B/(2*lambda2))*(x-L_1)^2,{x,L_0/4,3*L_0/4}]
(*W2 Timoshenko*)
Plot[(- M_B/(2*lambda2))*(x-L_1)^2,{x,0,1}]
W3 Euler
Plot[( M_B/lambda2)*(L_2-L_1)*(x-(L_1+L_2)/2),{x,3*L_0/4,}];
W1Euler=Plot[( M_B/lambda2)*(L_2-L_1)*(((L_1+L_2)/(2*L_0))-1)*x,{x,0,0.25}];

W2Euler=Plot[( M_B/(2*lambda2))*(x^2 +(((L_2^2-L_1^2)/L_0) -2 L_2)*x
+L_1^2),{x,0.25,0.75}];

W3Euler=Plot[( M_B/2*lambda2)*(L_2^2-L_1^2)*(x/L_0-1),{x,3/4,1}];
Plot[Piecewise[{{0,x<0.25},{( 1/(2*1))*(x-0.25)^2,x<0.75},{( 1/1)*(0.75-
0.25)*(x-(0.25+0.75)/2),x>0.75}}],{x,0,1}];Plot[Piecewise[{{x*(0.75-0.25)
(((0.75+0.25)/(2*1))-1),x<0.25},{( 1/(2*1))*((x^2) +(((0.75^2-0.25^2)/1) -
2*0.75)*x +0.25^2),0.25<x<0.75},{( 1/2*1)*(0.75^2-0.25^2)*(x-
1),x>0.75}}],{x,0,1}];

Plot[{Sin[x],Sin[2 x],Sin[3 x]},{x,0,2 Pi}];
Table[Plot[{Piecewise[{{0,x<0.25},{( 1/(2*1))*(x-0.25)^2,x<0.75},{(
1/1)*(0.75-0.25)*(x-(0.25+0.75)/2),x>0.75}}],Piecewise[{{x*(0.75-0.25)
(((0.75+0.25)/(2*1))-1),xlambda0.25},{( 1/(2*1))*((x^2) +(((0.75^2-0.25^2)/1)
-2*0.75)*x +0.25^2),0.25<x<0.75},{( 1/2*1)*(0.75^2-0.25^2)*(x-
1),x>0.75}}]},
Table[Plot[Sin[x],{x,0,2
Pi},PlotStyle□ps],{ps,{Red,Thick,Dashed,Directive[Red,Thick]}}];
```

CURRICULUM VITAE

Candidate's full name: **H. Tuğba Tan**

Place and date of birth: **Üsküdar, 1985**

Permanent Address: **9 Rue Pasteur 92120 Montrouge, France**

Universities and

Colleges Attended:

1999 - 2003	Pertevniyal High School
2003 - 2008	Istanbul Technical University, Istanbul, TURKEY Bachelor of Science, Physics Engineering
2010 - 2011	Institut Polytechnique des Sciences Avancées, Paris, France, Exchange Student, Aéronautique.

Publications:

- Kacar,A., **Tan, H.T.,** Kaya, M.O., 2011. Free vibration analysis of beams on variable winkler elastic foundation by using differential transform method, Mathematical and Computational Applications, 16 (3), 773-783
- **Tan, H.T.,** Kaya, M.O., 2011. Shape Control and Vibration Analysis of a Beam with Piezoelectric Patches, IFASD (*International Forum of Aeroelasticity and Structural Dynamics),* 26-30 june 2011 Paris (Accepted)